12

U. S. NAVAL AIR ENGINEERING CENTER

LAKEHURST, NEW JERSEY

GROUND SUPPORT EQUIPMENT DEPARTMENT

NAEC-GSED-98 MARCH 1976

FINAL TECHNICAL REPORT

AIRCRAFT SYSTEM ONE-SIXTH SCALE MODEL STUDIES

COANDA/REFRACTION NOISE SUPPRESSION CONCEPT
ADVANCED DEVELOPMENT

AIRTASK A3405343/051C/4W4569001 & 5W4569001

NAVAL AIR ENGINEERING CENTER

LAKEHURST, NEW JERSEY 08733

GROUND SUPPORT EQUIPMENT DEPARTMENT

NAEC GSED 98 MARCH 1976

FINAL TECHNICAL REPORT

AIRCRAFT SYSTEM ONE-SIXTH SCALE MODEL STUDIES

COANDA/REFRACTION NOISE SUPPRESSION CONCEPT
ADVANCED DEVELOPMENT

AIRTASK A3405343 051C 4W4569001 & 5W4569001

PREPARED BY R. E. Ballard

The Boeing Company
Wichita Division
Wichita, Kansas 67210

REVIEWED BY _____

D. D. CROCE
Project Engineer

APPROVED BY _____

W. J. COX
Department Superintendent

Unclassified

REPORT DOCUMENTATION PAGE

READ INSTRUCTIONS BEFORE COMPLETING FORM

1 REPORT NUMBER: NAEC GSED 98	2 GOVT ACCESSION NO	3 RECIPIENT'S CATALOG NUMBER
4 TITLE (and Subtitle): Aircraft System One Sixth Scale Model Studies, Coanda Refraction Noise Suppression Concept, Advanced Development,		5 TYPE OF REPORT & PERIOD COVERED: Final Technical Report, August 1974 – January 1976,
		6 PERFORMING ORG REPORT NUMBER: D3 9903-1
7 AUTHOR(s): R. E. Ballard		8 CONTRACT OR GRANT NUMBER(s): N00156-74-C-1710
9 PERFORMING ORGANIZATION NAME AND ADDRESS: The Boeing Company, Wichita Division, Wichita, Kansas 67210		10 PROGRAM ELEMENT, PROJECT, TASK AREA & WORK UNIT NUMBERS: A.T A3405343/051C/ 4W4569001 & 5W4569001
11 CONTROLLING OFFICE NAME AND ADDRESS: Naval Air Systems Command (AIR 340E & AIR 53431B) Washington, D.C. 20361		12 REPORT DATE: March 1976
		13 NUMBER OF PAGES: 116
14 MONITORING AGENCY NAME & ADDRESS (if different from Controlling Office): Naval Air Engineering Center, Ground Support Equipment Dept. (92623), Lakehurst, N. J. 08733		15 SECURITY CLASS (of this report): Unclassified
		15a DECLASSIFICATION/DOWNGRADING SCHEDULE: N/A

16 DISTRIBUTION STATEMENT (of this Report): Approved for public release: distribution unlimited

DISTRIBUTION STATEMENT A
Approved for public release;
Distribution Unlimited

17 DISTRIBUTION STATEMENT (of the abstract entered in Block 20, if different from Report): Approved for public release; distribution unlimited.

18 SUPPLEMENTARY NOTES:

19 KEY WORDS (Continue on reverse side if necessary and identify by block number): Aerodynamics, acoustics, thermodynamics, Coanda jet deflection, acoustic refraction, ground run up noise suppression, jet engine exhaust noise, aircraft acoustical enclosures, aircraft run up suppressors.

20 ABSTRACT (Continue on reverse side if necessary and identify by block number):

The proven Coanda/refraction concept is applied to the Navy requirement for effective exhaust noise suppression of aircraft (installed engines) ground run up tests. The technical approach is comprised of analytic studies and one-sixth scale model tests using simulated sources for single and twin-engine aircraft. The results of previous exploratory studies, using simulated static sources, are applied to the more complex situation with the engine tailpipe centerline displaced horizontally, vertically, longitudinally and angularly from the model suppressor inlet. Test runs at

DD FORM 1 JAN 73 1473 EDITION OF 1 NOV 65 IS OBSOLETE

Unclassified
SECURITY CLASSIFICATION OF THIS PAGE (When Data Entered)

varied simulated engine power settings and varied model geometric orientations were conducted to determine the effects on jet attachment to the Coanda surface and on cooling air eduction. The extensive recorded test data were analyzed to identify aero/thermodynamic trends related to suppressor internal components, ejector geometry and material cooling properties. Results present operational limits and configurations for further development as exhaust systems for aircraft test enclosures and aircraft run up suppressors.

TABLE OF CONTENTS

TABLE OF CONTENTS (CONT'D)

LIST OF FIGURES

LIST OF FIGURES (CONT'D)

LIST OF FIGURES (CONT'D)

LIST OF FIGURES (CONT'D)

LIST OF FIGURES (CONT'D)

LIST OF TABLES

1.0 SUMMARY

A one-sixth scale model program was conducted concurrently with the full-scale demonstrator program (Reference 1 Final Report). This model testing was directed toward developing and evaluating Coanda noise suppressor configurations and their ability to suppress engine noise while the engine is installed in an airframe. The initial studies consisted of three model tests but were subsequently expanded to include two additional test configurations.

To adapt the Coanda system to in-airframe usage considerations must be given to:

- Initial aircraft tailpipe vertical and horizontal misalignment relative to the suppressor inlet
- Fore and aft positioning of engine exhaust relative to the suppressor inlet
- Adaptation to twin-engine aircraft (such as the F-4 and F-14) and any adverse effects on attachment and cooling of the turning of twin flows
- Accommodation of coannular airflows (such as TF30-P-408 and TF41 engines) and size extrapolation of current suppressors to accommodate coannular airflows simulating the scaled engine airflow range of 470 to 600 lbs/sec. (It should be noted that the current full-scale Coanda noise suppressor configuration was designed to handle airflows to 300 lbs/sec.)

Model testing was accomplished in the Boeing-Wichita Acoustic Arena facility described later in Section 2.0. The same program rationale was maintained that was utilized for the previous (References 2 and 3) scale-model programs, that is, the tests were primarily aerothermodynamic with limited acoustic evaluation. Each of the five model tests in this program are summarized in the following paragraphs.

Single Engine Tailpipe Misalignment Test

The first model test in this series evaluated the effects of airplane tailpipe movement and initial misalignment on Coanda flow attachment and system cooling. The inlet to the first ejector was sized large enough to capture the flow from the engine exhaust with a misalignment of engine centerline to ejector centerline of six inches (full scale) in any direction. To accommodate the misalignment, it was necessary to increase the ejector area ratios (ejector exit area/primary nozzle area) and the last ejector aspect ratio (exit width/exit height) as compared to previous models. A schematic of the model setup is shown on Figure 5 in Paragraph 3.2. Tests were run with the nozzle displaced one inch (model scale) in the horizontal and vertical directions with and without the adapter section installed. Metal surface temperatures, internal static pressures, and flow attachment data (obtained from the Coanda exit pressure and temperature rake) were recorded plus ambient conditions and exhaust nozzle flow parameters.

REFERENCES

1. "Test Cell Experimental Program - Coanda Refraction Noise Suppression Concept - Advanced Development," Final Technical Report for Navy Contract N00156-74-C-1710, Navy Document Number NAEC-GSED-97, The Boeing Company, Wichita, Kansas, March 1976.

2. Ballard, R. E., Brees, D. W., and Sawdy, D. T., "Feasibility and Initial Model Studies of a Coanda Refraction Type Noise Suppressor System," The Boeing Company, Wichita, Kansas, D3-9068, January 1973.

3. Ballard, R. E., and Armstrong, D. L., "Configuration Scale Model Studies of a Coanda Refraction Type Noise Suppressor System," The Boeing Company, Wichita, Kansas, D3-9258, October 1973.

Preceding Page BLANK

The results of the single-engine misalignment test indicate that the Coanda suppressor system may be adapted to in-airframe ground runups and account for initial aircraft misalignment and tailpipe movement relative to the suppressor inlet. The transition ejector set used was not optimal. However, the data and subsequent analysis indicate that increasing the first ejector inlet area to capture the misaligned flow need not create any cooling problems. Misalignments that could reasonably be expected in service can be tolerated in all directions without seriously affecting flow attachment.

Coannular Flow Test

A second model test was run to determine the effects on Coanda flow attachment of the coannular flow produced by fan engines such as the TF41 and TF30-P-408 (nonafterburning). These tests evaluated the effects on jet deflection of exhaust flow with a nigh velocity annulus of cooler gas surrounding the hot exhaust primary core. A bypass ratio of approximately 1.0 was used. These scale-model tests provided data and operational trends that may be extrapolated to full-scale operation of long duct, coannular flow, turbofan engines, and to engines with airflows higher than 300 lbs/sec.

Figure 28 in Paragraph 4.2 is a schematic of the coannular flow test setup. A dual flow system with the center flow heated to the TF30-P-408 primary conditions was provided. Existing model hardware from previous tests, Reference 3, was used for the ejector set and Coanda surface. (These model components were the ones used to define the demonstration full-scale test article.) The test included misalignment configurations similar to those accomplished in the preceding pure turbojet flow simulation test. Similar data were recorded with the exception that, in this test, two sets of exhaust nozzle flow parameters were required: the primary jet and the cooler annulus of fan airflow.

The results of the coannular flow model test indicate no adverse effects on flow attachment at any power level due to the cooler fan air surrounding the primary flow, and with the presence of the fan air there are no system cooling problems. These tests provide assurance of the feasibility of turning the low bypass ratio flows of engines like the TF41 and TF30-P-408; however, feasibility with higher bypass ratio turbofan jets such as the TF34 (6 to 1 bypass ratio) were not evaluated.

Initial Twin-Engine Test

The third model test was the initial step in developing a Coanda flow turning system for twin-engine aircraft with closely spaced engines. The object of the test was to observe: (1) the effects of concurrent jet deflection of two distinct power jet sheets in the same deflection chamber, (2) any adverse boundary conditions between two distinct energy levels of dynamic gases which might prevent deflection, and (3) to determine if a divider wall is required between the two flows.

Figure 36 in Paragraph 5.2 is a schematic of the initial twin-engine model test setup. A new model was fabricated for this test consisting of three ejectors with removable internal splitters and a "double wide" Coanda deflection surface with a removable splitter. Facility changes were required to provide the second nozzle flow with an exit centerline simulating the distance between aircraft (F-4, F-111, and F-15) engines. Only one side of the twin system was instrumented for metal surface temperatures, internal static pressures, and flow attachment data (Coanda exit pressure and temperature rake). The other side was run at idle conditions and system symmetry assumed for the case of interchanged power settings. (It should be noted that current airplane ground test limitations restrict the second engine to idle power while the first engine is at any power up to afterburning.) Ambient conditions and the two exhaust nozzle flow parameters were also recorded. Test conditions were run with nozzle to ejector inlet misalignments (offsets) in the vertical and horizontal direction for configurations with and without the ejector splitters, and with and without the Coanda surface splitter.

The results of the initial twin-engine test indicate the feasibility of turning the two engine flows using the Coanda concept. The results also show that the Coanda surface splitter is necessary but that ejector splitters are of no particular benefit for flow turning. This test configuration pointed out the need to revise the ejector configuration to

permit secondary (cooling) air entrainment to the area between the two engine flows. This was subsequently accomplished and was tested during the fifth series of model tests.

Single-Engine Tailpipe/Suppressor Translation Test

The purpose of the fourth test series was to determine the effect, on flow attachment and system cooling, of varying the distance between the engine exhaust nozzle and suppressor inlet. Engine installations such as on the F-4 aircraft where the engine exhaust is relatively far forward of the aft stabilizer necessitated this study. Additionally, in the case of an engine test cell installation, the distance from the engine tailpipe to the ejector inlet varies because the location of the engine thrust trailer in the cell is fixed and the various engines differ in length and in their fore and aft positioning on the thrust trailer.

The same test hardware used in the first (misalignment) test was used for this translation test even though the first test results indicated that ejector set to be inefficient for cooling. This was done to eliminate the cost of building a new model since relative cooling performance could be determined. A schematic of the translation test setup is shown on Figure 56 in Paragraph 6.2.

The results of the translation test indicate no problem with flow attachment or cooling due to increasing the translation distance between the nozzle exit and the suppressor (i.e., ejector) inlet. On the contrary, the flow attachment seems to be improved with greater translation distances, probably because the mixing which occurs prior to entering the suppressor provides a more uniform flow at the ejector/transition exit. With increased translation distance, the ejector inlet size has to be increased because of the expansion of the exhaust flow. If, however, the translation distance is too great, the exhaust entrains more secondary air (prior to the ejector inlet) than the ejector is capable of pumping, and results in back flow unless the ejector area is increased.

Twin-Engine Misalignment Test

The fifth and last model test series was a misalignment test of a twin-engine model that was different from the initial twin-engine suppressor model of the third test series. The difference was primarily in the transition ejectors. This ejector set was designed to allow more secondary entrainment between the two engine flows than in the previous model used in the initial twin-engine test. This model was also designed with a dual five-ejector transition section. The first two ejectors were cylindrical and could be removed. The five ejectors were used to study the feasibility of extending the transition section out in front of the suppressor to capture the flow from aircraft, such as the F-4, which have the engine exhaust forward of the airplane empennage. The purpose of the test was to evaluate the effects of concurrent jet deflection of two distinct jet flows, as well as to determine any adverse effects on flow attachment and system cooling of angular and offset misalignments to the exhaust nozzle.

Figure 84 in Paragraph 7.2 is a schematic of the test setup. The transition consisted of a double set of five ejectors. The ejectors exit onto a "double width" Coanda surface with a removable center splitter. One side of the twin system was instrumented for metal surface temperatures, internal static pressures, and flow attachment data (Coanda exit pressure and temperature rake). The other side was operated at idle conditions and system symmetry was assumed. Ambient conditions and the two exhaust nozzle flow parameters were also recorded. The test was conducted with one engine at afterburning, full military, and idle while the other was at idle power setting. Test conditions were run with five, four and three ejectors on each side. Nozzle to ejector inlet offset and vertical angular misalignments were tested with the three ejector dual transition.

The results of the twin-engine misalignment test indicate that no severe problems would be encountered in adapting the Coanda suppressor system to a twin-engine aircraft. This model demonstrated that, with a carefully developed ejector transition section, the high Coanda splitter and surface temperatures measured during the initial twin-engine test (discussed previously in this summary) can be reduced to within the desired 1000° goal. The model test also demonstrated that offset and angular misalignments encountered by poor initial aircraft positioning and aircraft tailpipe motion during engine runup do not appreciably affect suppressor operation.

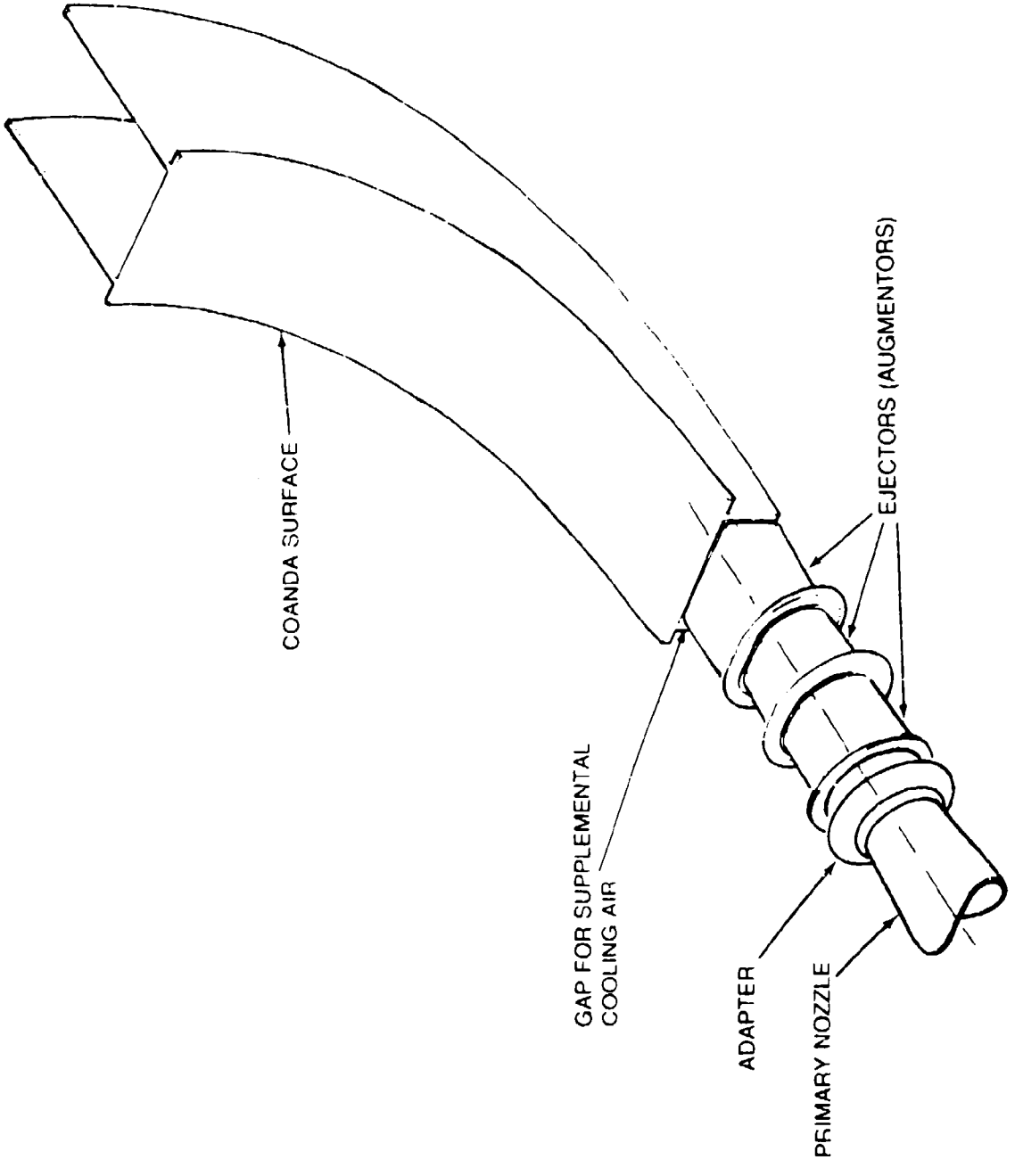

Figure 1. Coanda surface and ejectors.

2.0 INTRODUCTION

The objective of the one-sixth scale model test program was to perform preliminary investigations adapting the Coanda refraction exhaust noise suppressor concept to engines in-airframe ground runup applications. Some of the aspects which must be considered for in-airframe applications include allowance for motion of the aircraft engine tailpipe during operation, fore and aft positioning relative to the suppressor inlet, adaptation to twin engine aircraft (such as the F-4 and F-14) and size extrapolation of current suppressors to accommodate coannular airflows simulating the scaled engine airflow range of 470 to 600 lbs/sec. The current full scale configuration (described in Reference 1) is designed to handle airflows to 300 lbs sec. An outline of the method of investigating these aspects by scale model testing is given below. The same program rationale was maintained that was utilized for the previous scale model programs, References 2 and 3, that is, the tests were primarily aerothermodynamic in nature, with limited acoustic evaluations. These tests were run independently, but concurrently with the full scale test program. These model tests, as well as the full scale test, were funded by the Reference 4 Navy contract. The initial studies consisted of three model tests but were subsequently expanded to include two additional test configurations.

These model tests were designated as Task V of the Reference 5 Program Plan Document and were accomplished during the period of October, 1974 through December, 1975. A schematic of the flow transitioning and flow deflecting components of the Coanda refraction noise suppressor system is shown on Figure 1.

The first configuration that was tested evaluated the effects on Coanda flow attachment and ejector and Coanda cooling of vertical and horizontal offset (misalignments) between the exhaust nozzle and suppressor inlet centerlines. These offsets were to simulate initial misalignment of the aircraft tailpipe and suppressor inlet as well as any engine tailpipe movement during runup. These effects were evaluated with and without the adapter plate between the nozzle and ejector inlet. The set of transition ejectors were revised from previous configurations (reported in References 2 and 3) to enlarge the first ejector inlet enough to capture the flow when misaligned. Offsets of one-inch (model scale) were tested which is equivalent to six inches full scale.

A second model test series was run to determine the effects on Coanda flow attachment of the coannular flow produced in fan engines such as the TF41 and TF30-P-408 (nonafterburning). These tests evaluated the effects on jet deflection of exhaust flow with a high velocity annulus of cooler air surrounding the hot exhaust primary core flow. Since previous test conditions simulated only pure turbojet engines, these tests were to provide data and operational trends that may be extrapolated to full scale operation of long duct turbofan engines. The method used was to provide a dual flow system with a hot inner core, sized to one-sixth scale of a TF41 or TF30-P-408 engine. Existing model hardware from previous testing was used. The results of these tests were used to determine a method of extrapolating the current suppressor size to that necessary to accommodate engine airflows up to 600 lbs sec. (It should be noted that the current full scale Coanda noise suppressor configuration was designed to handle airflows to 300 lbs sec.)

The third series of model tests was conducted as the initial step in developing a Coanda noise suppressor system for twin-engine aircraft ground runup application. The object of those tests was to determine: (1) the effects of concurrent jet deflection of two jet sheets, of distinctly differing power, in the same deflection chamber; (2) any adverse boundary conditions between two distinct energy levels of dynamic gases which might prevent deflection;

REFERENCES

4 Contract N00156-74-C-1710, "Coanda Refraction Noise Suppressor System," Naval Air Engineering Center and The Boeing Company, July 1974

5. Ballard, R. E. and Burton, L. L., "Navy Coanda Refraction Ground Noise Suppressor Program Plan," The Boeing Company, Wichita, Kansas D3-9574-1, August 1975

and (3) to determine if a divider wall is required between the two chambers. These tests required a new model with "double width" ejectors and Coanda surface each with removable center splitters. Test simulation was conducted alternately with one engine at afterburning and the other at idle; with one engine at full military and the other at idle; and with both engines at idle power settings. The tests were repeated with and without a center surface boundary (splitter) installed in the ejectors and Coanda surface. The results of this test were used to influence the model configuration for the twin-engine misalignment test (fifth test series).

The purpose of the fourth model test series was to determine the effect on flow attachment as the distance varies between the engine exhaust and suppressor inlet. Engines installed in aircraft with the exhaust plane forward of the stabilizers (such as the F-4 aircraft) made it necessary to study the effects of translation of the engine exhaust from the suppressor inlet. Existing model hardware from the single engine misalignment test (first test series) was used. The distance from exhaust nozzle to suppressor inlet was increased up to the point at which the inlet size would not capture the expanding flow. The effects of offset misalignments at the increased translation distances were also evaluated.

The fifth and last model test series of this development contract was a misalignment test of a twin-engine model configuration. A different model configuration than that used for the third test series was fabricated with the capability of offset and angular (in the vertical plane) misalignments to the exhaust nozzle. The purpose of this test was to study a different model configuration (than in the initial twin-engine test) for any adverse effects of concurrent jet deflection of two distinct jet flows, as well as to determine if offset and angular misalignments create any adverse effects on flow attachment and system cooling. The model consisted of a double set of five transition ejectors which exited into a double width Coanda surface with a removable center splitter. The first two ejectors were removable to allow testing with three, four, and five ejectors. The test was conducted by alternately simulating one engine at afterburing and the other at idle; one engine at full military and the other at idle; and both engines at idle power settings.

The model testing was accomplished in the Boeing-Wichita Acoustic Arena facility shown on Figure 2. The Arena wall is 16 feet high, inclined at an angle of 30 degrees to the vertical and is 100 feet in diameter at the base. The burner (hot gas generator) is a two stage configuration. The first stage is a J47 jet engine burner can and spray nozzles, capable of reaching gas temperatures of 1500°F at the 15-pound per second maximum airflow rate. The second, or afterburning stage consists of a central fuel spray nozzle and eight radial spray bars and a flame holder. This stage is water jacketed and can boost the jet exhaust temperature to 3000°F. The primary airflow source has a 300 psia line pressure. A secondary airflow source is available with a 60 psia line pressure with a maximum flow rate of 40 pounds per second of cold air to simulate fan flows. All necessary revisions to the facility for the tests outlined above are subsequently described in the following sections in which that particular test is discussed.

A pictorial block diagram of the Acoustic Arena data acquisition system is shown on Figure 3. The burner and airflow controls are housed in a small building next to the Arena with a window for visual observation of the model. The control instrumentation is shown in the upper right of Figure 3. The data acquisition instrumentation, computer, and printer are housed at a remote site and are shown at the lower center of Figure 3.

The Arena data acquisition system is built around the Varian 620/L Mini-Computer, which is a general purpose digital computer. The central processing unit of the computer has a 12K memory system. The input/output system provides the interface between the computer electronic system and the electromechanical devices that input data to the computer or output the computed results. The Beehive CRT (cathode ray tube) terminal enables control of the computer, and, the printer lists the data. The Tri-Data model 4036 provides program loading or storage of data on magnetic tape. The multiplexer allows each channel to be sampled sequentially or randomly, as required. The A/D converter converts the analog signal to a digital voltage level. A pressure scanner valve allows all the total pressures to be measured by the same ± 15 psid transducer. Ambient pressure was measured by a 15 psia transducer. A second pressure scanner valve and a ± 5 psid transducer were used to measure static pressures. Statham pressure transducers were used.

Temperature measurements were taken through four temperature scanners. Thermocouples were Iron-Constantan and Cromel-Alumel. Pace, and Research Incorporated reference junctions were used.

For both temperatures and pressures, signal processing was accomplished by use of a B & F Instruments, Inc. signal conditioner and a Dynamics amplifier. The conditioned signal was connected to a monitor panel which permitted manual monitoring capability as well as calibration monitoring.

The fuel flow was measured by a 1 gpm turbine type flow transducer in the primary fuel line and a 5 gpm turbine type flow transducer in the afterburner fuel line. The signal was conditioned by a Cox signal conditioner and the signal sent to the monitor panel. The flow rates were also displayed on digital voltmeters in the test control room. The monitor panel inputs were paralleled to the multiplexer input panel where further monitoring was possible. The signals then went into the multiplexer for processing.

Although no acoustic data were recorded during the testing described in this document a discussion of the acoustic data acquisition sysytem is provided for reference information. The accustic instrumentation system begins with the Bruel & Kjaer Models 4135 and 4136 microphone buttons. These are coupled to General Radio Model 560-P42 preamplifiers. A microphone scanner selects the proper channel for input to the autogain amplifier for signal processing. The General Radio Model 1925 Real Time Analyzer integrates the signal and the computer interfaces the signal to the computer input.

Two computer programs were used for data acquisition. One program was used for performance data and the other for acoustic data, when recorded.

The acoustics program allows manual selection of the microphone data to be recorded. When the data from each microphone are analyzed, the computer signals the microphone scanner to advance one position. Data are taken sequentially. The analyzed acoustic data are printed in tabular form and plots of SPL versus frequency in one-third octave bands. Computations of OASPL and PNL converted to full scale equivalent distances are also provided.

The performance program provided automatic data acquisition. Once the program was started, all parameters were sampled and the scanners automatically controlled by the computer. The raw performance data in the form of digital voltages were converted to engineering units and calculation performed in the CPU. The data were then listed in tabulated form.

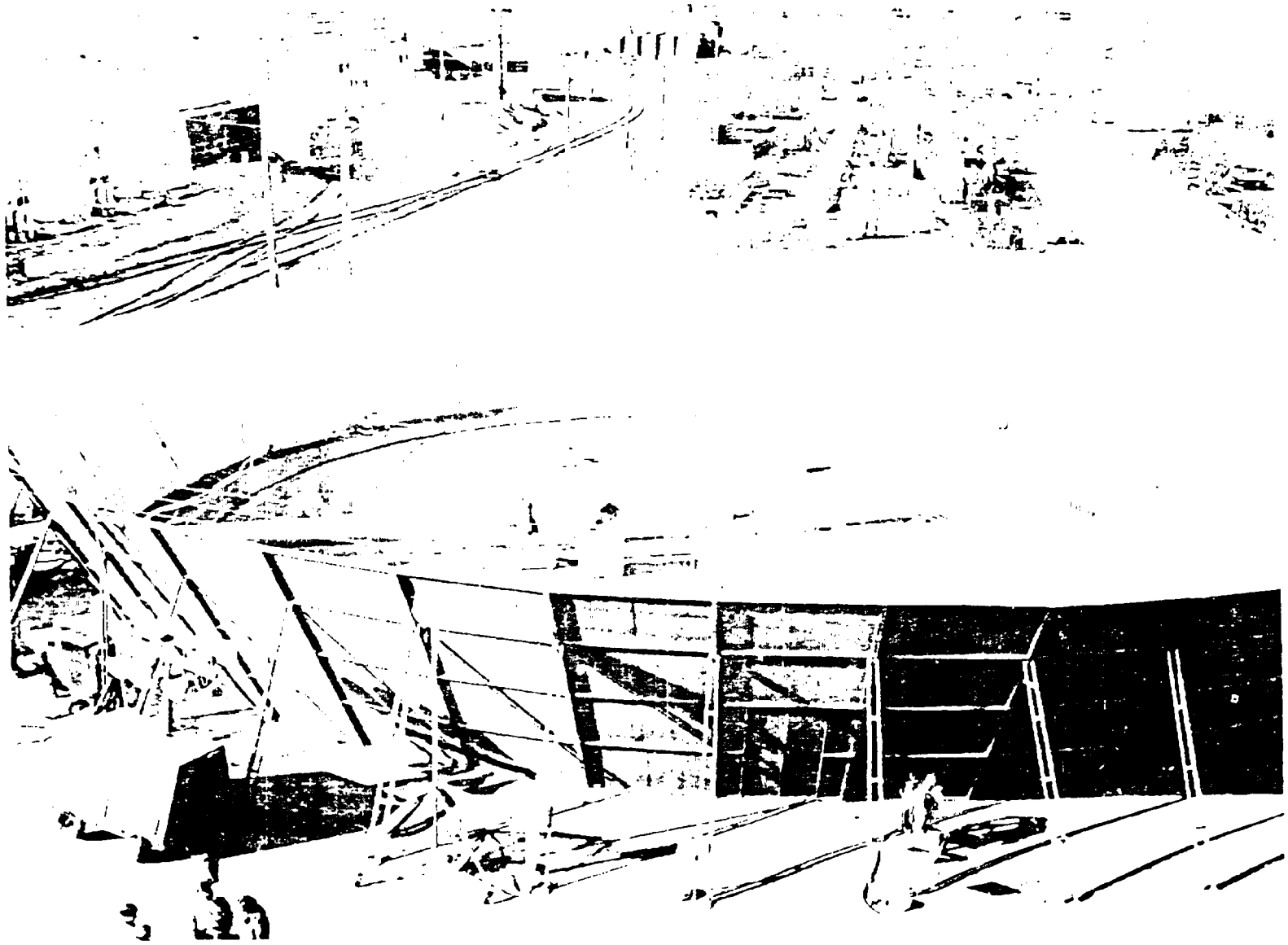

Figure 2. Acoustic Arena model scale test facility

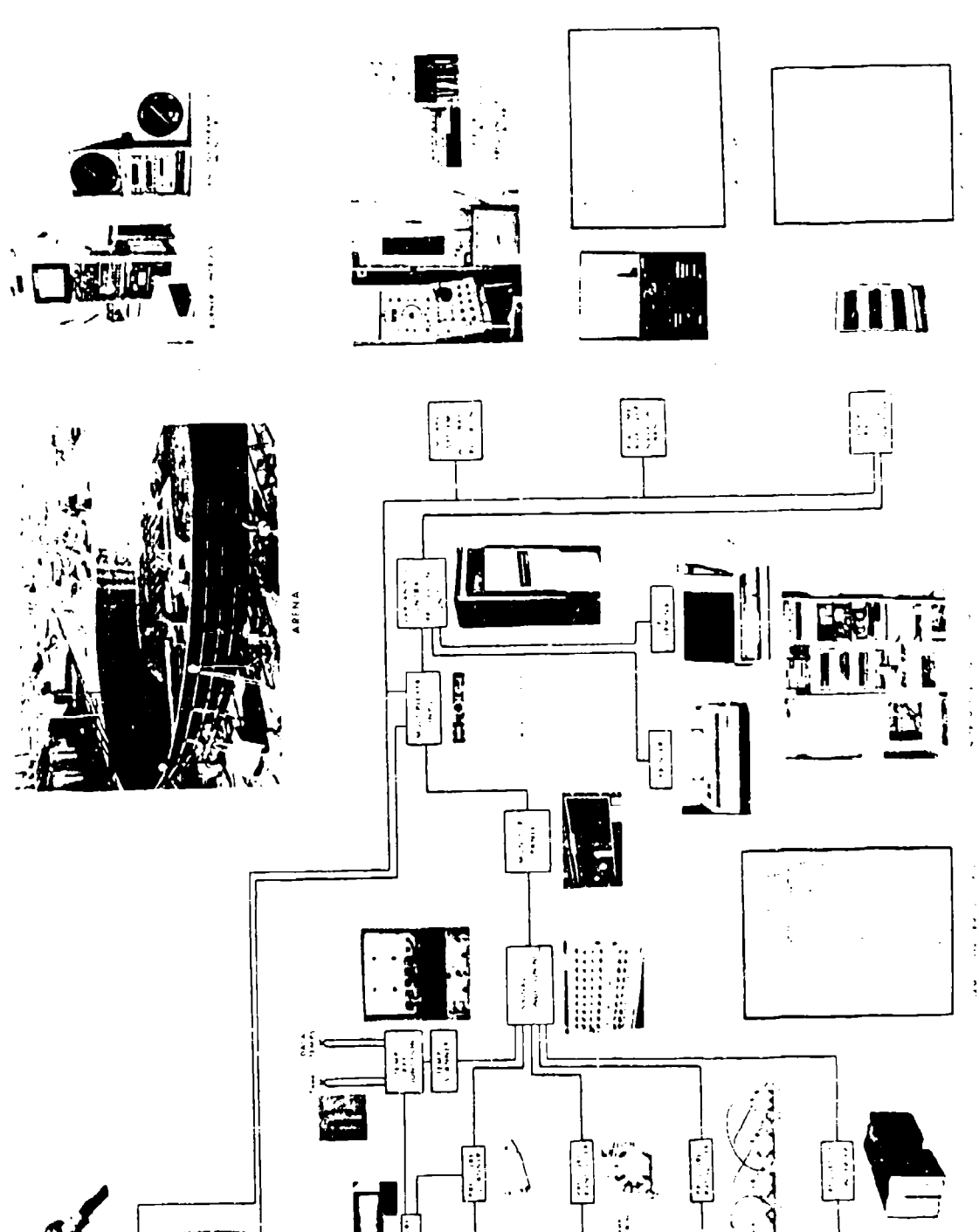

Figure 3. Acoustic Arena data acquisition system

3.0 SINGLE ENGINE TAILPIPE MISALIGNMENT TEST

3.1 Objectives

One problem that arises from the use of ground runup noise suppressors on in-airframe applications that is not present for test cell suppressor application is the alignment of the engine exhaust and the suppressor inlet. In test cell noise suppressors, the engine is rigidly constrained on a test trailer or stand which positions the exhaust centerline on the exhaust suppressor centerline. With the engine in-airframe, however, the aircraft is usually constrained by the wheels and/or tail hook which allow some tailpipe movement due to changes in engine power settings. Another possibility for sizable alignment variation is the initial positioning of the aircraft relative to the suppressor. Stringent initial aircraft alignment requirements create time consuming problems for the suppressor operators and are therefore undesirable.

The single engine tailpipe misalignment test was the initial step in ascertaining acceptable alignment criteria for in-airframe applications of the Coanda ground runup noise suppressor. The objective of the test was to evaluate the effects on Coanda flow attachment and ejector and Coanda cooling of vertical and horizontal offset misalignments between the exhaust nozzle and suppressor inlet centerlines. The inlet to the first ejector was sized large enough to capture the flow from the engine exhaust with a misalignment of engine to suppressor centerlines of six inches (full scale) in any direction. The six-inch dimension was supplied as a maximum requirement by the Navy Technical Manager for this program.

A secondary objective of this test was to determine the effect the adapter plate in front of the ejectors (see Figure 1) has on the flow attachment and cooling with misalignments. The purpose of the adapter plate was to inhibit flow entrainment next to the exhaust nozzle, thus assuring no pressure "suck down" at the nozzle as well as providing an acoustic barrier for noise emitting from the ejector inlet. The fact that this adapter has an opening that closely fits the exhaust flow diameter creates a problem for in-airframe application. Allowance for tailpipe movement and initial aircraft misalignment would require that the adapter float with the aircraft tailpipe. The complexity of such an adapter makes it desirability questionable. Previous Boeing-Wichita IR&D testing has indicated that the nozzle static pressure depression due to the presence of the ejector inlet decreases rapidly at a short distance between engine exhaust and suppressor inlet. Therefore, if the adapter does not prove to be of appreciable acoustic or aerothermodynamic benefit, it may be deleted. Acoustic measurements were planned during this test to determine the acoustic benefit, if any, of the adapter. It became apparent, however, that it would be difficult to isolate the inlet emitted noise from the exhaust noise without enclosing the Coanda and ejectors. Therefore, it was decided to determine the inlet adapter acoustic effectivity during the full scale tests reported in Reference 1.

3.2 Model Description and Test Apparatus

The one-sixth scale model used in this test was designed with the inlet of the first ejector large enough to capture the flow from the engine exhaust with a misalignment of the engine and ejector centerline of one inch (six inches full scale) in any direction. To accommodate the misalignment, it was necessary to increase the ejector area ratios and the last ejector aspect ratio (exit width/exit height) as compared to previous models. Each of the three ejectors was convergent in area progression (inlet area larger than exit area). The Coanda surface had the same curvature developed by previous model tests for the full scale demonstration, however, it was a little wider due to the larger aspect ratio of the third ejector exit. Dimensional drawings of the ejectors, adapter, and Coanda surface are shown on Figure 4. The first ejector has an inlet area of 63.6 in^2 and an exit area of 49.5 in^2 which results in an exit area ratio (ejector exit area/primary nozzle area) of 1.65, based on the afterburning nozzle area. The second ejector has an inlet area of 54.7 in^2, an exit area of 52.5 in^2 which is an exit area ratio of 1.75. The third ejector has an inlet area of 57.6 in^2, an exit area of 55.5 in^2, and exit area ratio of 1.85. The primary nozzles used (not shown) are 4.31 inches and 6.18 inches in diameter (14.60 in^2 and 30.00 in^2 area) for military rated thrust and afterburning, respectively. These nozzles simulate the exit area of a TF30-P-12A engine at military rated thrust and afterburning.

A schematic of the model setup with adapter is shown on Figure 5. Static pressures are provided at the nozzle lip to

measure the pressure changes that may affect engine operating conditions. Static pressure ports are provided on the internal wall of the ejectors to determine the ejector pumping characteristics and along the Coanda surface centerline to measure the extent of the pressure gradient that produces the flow turning. Thermocouples are provided on the ejectors and Coanda surface to measure the metal surface temperatures so that the effects of configuration changes on system cooling may be determined. A total pressure and total temperature rake is provided at the Coanda surface exit to obtain exit flow conditions (Mach number, velocity, etc.) and to determine the extent of flow attachment

Figure 6 is a photograph of the model setup in the Acoustic Arena Test Facility and Figure 7 is a close-up of the new large inlet ejector and exhaust nozzle. The existing Coanea support frame from previous model tests (Reference 2) was used. The ejectors are positioned such that the exit plane of one coincides with the inlet plane of the next. The exhaust nozzle to ejector inlet spacing was 2.0 inches without the adapter and 1.59 inches with the adapter (adapter was half way between nozzle and ejector inlet)

3.3 Test Plan

Table 1 presents the test configurations that were run for evaluating single engine tailpipe misalignment. Also listed are the data that were recorded for each configuration. The location of the pressure and temperature instrumentation on the model is shown on Figure 5. The configuration numbers are listed on all data shown later in this report as an aid in identification. It should be noted in the column of Table 1 that describes the misalignment direction that the model is moved rather than the exhaust nozzle. This was necessary because of the stationary attachment of the burner and nozzle system to the facility floor. When the configuration is described as "Model 1-inch down" the exhaust nozzle centerline is one inch above the ejector model centerline, and for "Model 1-inch up" the nozzle centerline is one inch below the ejector model centerline. All ambient conditions such as termperature, pressure, relative humidity, wind velocity, etc., were recorded along with the data shown in Table 1.

The flow conditions listed in Table 1 are simulated TF30-P-12A engine conditions and are defined in Table 2.

3.4 Test Results and Conclusions

3.4.1 Coanda Flow Turning Data

The effect of misalignment in each direction without the adapter installed on mixing and flow attachment at military rated thrust conditions is presented in the Coanda exit velocity profiles of Figure 8. These data indicate a slight improvement in flow attachment when the primary exhaust is misaligned below the ejector centerline such that the flow impinges on the ejector lower surface. The attachment was slightly reduced with misalignment to the side as indicated by the peak velocity being farther from the Coanda surface, however, a slight decrease in attachment is not altogether detrimental since it causes a decrease in peak velocity, probably from enhanced mixing.

The Coanda exit velocity profiles for aligned and misaligned configurations with the adapter plate installed (see Figure 5) at military rated thrust conditions are presented on Figure 9. These data indicate a considerable improvement in flow attachment for the configuration with misalignment to the side due to the presence of the adapter. This improvement is also indicated by the Coanda surface static pressures presented on Figure 10 and Figure 11 for the configurations without and with adapters, respectively. Without the adapter and with misalignment to the side, the surface static pressure approaches ambient faster at the last 20° of flow turning (70° to 90°) than the other configurations which indicates impending flow separation. On Figure 11, with the adapter installed, this trend is not observed. The exit velocity profiles of Figure 9 also indicate improved attachment (peak velocity closer to Coanda surface) for the aligned and flow toward upper ejector surface configurations with the adapter. The improvement in attachment for these configurations is not reflected in the Coanda surface static pressures (Figures 10 and 11), therefore, the higher exit velocities could be caused by a reduction in the mixing with the adapter installed.

The Coanda exit velocity profiles for aligned and misaligned configurations at afterburning power with and without

the adapter are presented on Figures 12 and 13, respectively. These data indicate very good flow attachment with no apparent change due to misalignments at one inch (equivalent to six inches full scale) in any direction. The data also indicate no significant change in flow attachment or mixing due to the adapter plate.

Figures 14 and 15 present the Coanda surface static pressures for the aligned and misaligned configurations at afterburning power with and without the adapter, respectively. These data also verify excellent flow attachment and that the misalignments and or adapter plate create no significant changes to flow attachment at afterburning conditions. The high static pressures (approximately ambient) at the entrance to the Coanda surface are the result of the gap between the last ejector upper surface and the Coanda surface. The purpose of that gap is to allow entrainment of additional secondary air for cooling the surface.

3.4.2 System Cooling Data

Figures 16 and 17 present the Coanda surface temperatures for the aligned and misaligned model configurations at afterburning power with and without the adapter, respectively. The peak temperatures reached on the Coanda surface indicate that the ejector set used to transition the primary flow is not efficient at providing a cooling film for the Coanda surface. Peak temperatures were at least 400 degrees more than those reached on the model, described in Paragraph 3.2 and in Reference 3, which was used to develop the full scale demonstrator unit. The new ejector set was designed with a larger aspect ratio (exit width:exit height) than the previous model, and included an enlarged first ejector inlet to capture the misaligned flow. These changes made it necessary to enlarge the ejector area ratios (ejector area:primary flow area). The higher Coanda surface termperatures were not attributed to these changes but rather that all three ejectors were made slightly convergent in flow area progression instead of constant area. The ejector theory upon which the analysis for this program is based indicated that convergent area progression ejectors have reduced entrainment capability relative to constant area ejectors. This reduced pumping capability due to the convergent area progression was to be compensated for by the increased area ratio, mentioned above, which increases ejector pumping. However, the area ratio increase did not sufficiently increase the entrainment enough to overcome the effects of the convergence. In addition to the area increase, the ejectors should have been lengthened to further increase pumping capability. This deficiency illustrates the necessity for detailed computer analysis prior to fabrication to ensure cooling capabilities within the 1000°F design goal. In Figures 16 and 17, the configuration with the primary flow misaligned toward the upper surfaces of the ejectors (i.e., ejector centerline below nozzle centerline) has a lower peak Coanda surface temperature (by 150 degrees). This lower temperature is the result of the higher velocity flow past the upper surface causing more entrainment of secondary air at the upper surface of the second and third ejector entrance and the gap between the third ejector exit and the entrance to the Coanda surface. This is also shown by the ejector upper surface temperatures and static pressures for that configuration.

Figures 18 through 21 present the ejector surface temperatures and internal static pressures for the aligned and misaligned model configurations at afterburning power without the adapter plate installed. These data also indicate a less efficient cooling than in previous models. The upper and lower surfaces (no data measured on lower surface) are expected to be the hottest due to the impingement of the expanding flow caused by the oval shape of the ejector exit. The aft recorded temperatures should also be the hottest as the entrained secondary flow from the ejector inlet mixes out. These data indicate that the first ejector is the only one with a significant change in temperature due to misalignments. The internal static pressure data are an indication of the entrainment of secondary airflow. A value of the ratio of internal static to ambient pressure below 1.00 at the ejector inlet indicates secondary air entrainment at that area of the ejector inlet. A value above 1.00 indicates a lack of entrainment at that position.

Figures 22 through 25 present the ejector surface temperatures and internal static pressures for the aligned and misaligned model configurations at afterburning power with the adapter plate installed. The most significant difference in these data with the adapter and the previous data without the adapter is seen in the internal static pressures, especially at the first ejector inlet. The adapter plate tends to equalize the inlet static pressure indicating more uniform entrainment around the inlet, whereas, without the adapter, there was a large change in static pressure at the inlet on the side toward which the primary flow was misaligned. The ejector surface temperatures were not significantly affected by the presence of the adapter plate.

3.4.3 Conclusions

The following conclusions may be made from the results of the single engine misalignment test:

- The Coanda suppressor system may be adapted to in-airframe ground runups and account for initial aircraft misalignment and tailpipe movement relative to the suppressor inlet
- The transition ejector set used was not optimum and pointed out the need for detailed analysis to develop a better design.
- The data and subsequent analysis indicate that increasing the first ejector inlet diameter to capture the misaligned flow need not create any cooling problems
- Misalignments can be tolerated in all directions without significantly affecting flow attachment.
- The adapter plate does not demonstrate enough benefit from either a flow dynamics or cooling standpoint to warrant the complexity of applying it to an in-airframe application. (The acoustic benefit of such an adapter is investigated at full scale and reported in Reference 1.)

TABLE 1. SINGLE ENGINE TAILPIPE MISALIGNMENT TEST CONFIGURATIONS

NOTE ALL DIMENSIONS IN INCHES

CONFIGURATION NUMBER	PRIMARY		ADAPTER	NOZZLE EJECTOR MISALIGNMENT	DATA		
	NOZZLE DIAMETER	FLOW CONDITION			SURFACE P_s & T_m	EXIT P_t & T_t	TEST RUN NUMBER
1	4 31	FULL MILITARY	NONE	NONE	X	X	21
2	4 31	FULL MILITARY	NONE	MODEL 1 DOWN	X	X	23
3	4 31	FULL MILITARY	NONE	MODEL 1 UP	X	X	22
4	4 31	FULL MILITARY	NONE	MODEL 1 TO SIDE	X	X	33
5	4 31	FULL MILITARY	4 62 DIAMETER	NONE	X	X	38
6	4 31	FULL MILITARY	4 62 DIAMETER	MODEL 1 DOWN	X	X	40
7	4 31	FULL MILITARY	4 62 DIAMETER	MODEL 1 UP	X	X	39
8	4 31	FULL MILITARY	4 62 DIAMETER	MODEL 1 TO SIDE	X	X	37
9	6 18	FULL AFTER-BURNING	NONE	NONE	X	X	53
10	6 18	FULL AFTER-BURNING	NONE	MODEL 1 DOWN	X	X	52
11	6 18	FULL AFTER-BURNING	NONE	MODEL 1 UP	X	X	54
12	6 18	FULL AFTER-BURNING	NONE	MODEL 1 TO SIDE	X	X	46
13	6 18	FULL AFTER-BURNING	6 63 DIAMETER	NONE	X	X	43
14	6 18	FULL AFTER BURNING	6 63 DIAMETER	MODEL 1 DOWN	X	X	41
15	6 18	FULL AFTER-BURNING	6 63 DIAMETER	MODEL 1 UP	X	X	44
16	6 18	FULL AFTER-BURNING	6 63 DIAMETER	MODEL 1 TO SIDE	X	X	45

TABLE 2. ONE-SIXTH SCALE EXHAUST NOZZLE FLOW CONDITIONS SIMULATING TF30-P-12A ENGINE AT SEA LEVEL STANDARD

ENGINE CONDITION	EPR (P_{t10} P_{t2})	EGT (T_{t10}) °F	AIRFLOW (W_a) LBS/SEC
IDLE	1.05	270	1.90
FULL MILITARY	2.12	730	6.86
FULL AFTERBURNING	1.93	2920	6.67

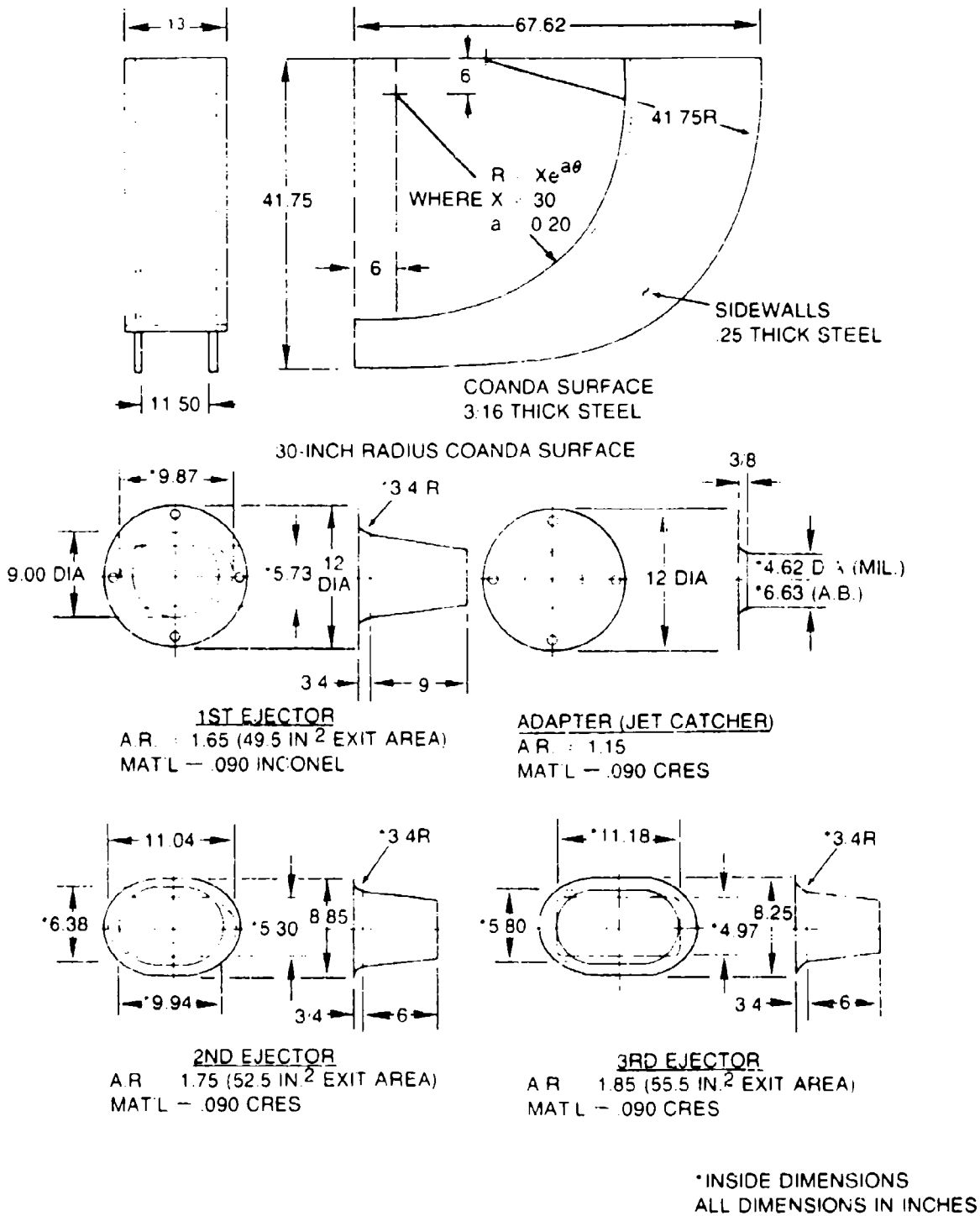

Figure 4. Dimensional drawings of single engine Coanda surface, ejectors and adapter

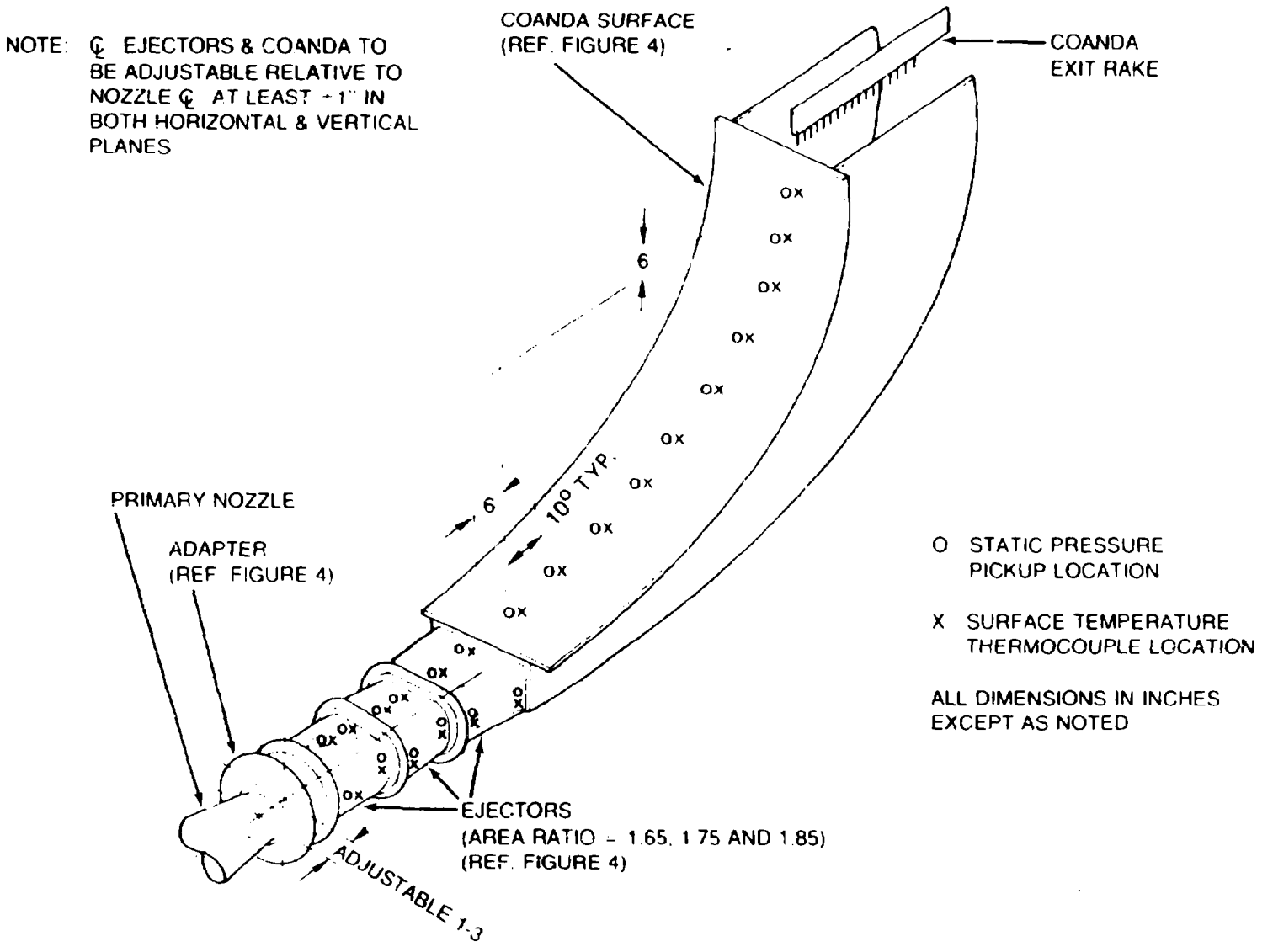

Figure 5. Single engine Coanda and ejector test setup and instrumentation.

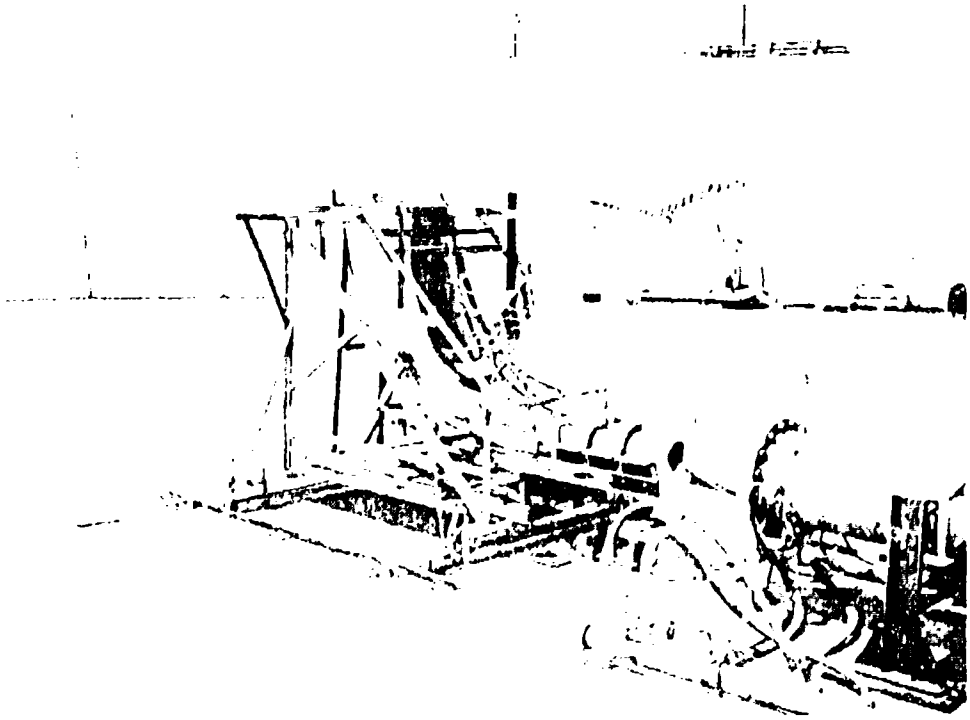

Figure 6. Single engine misalignment test model in Acoustic Arena.

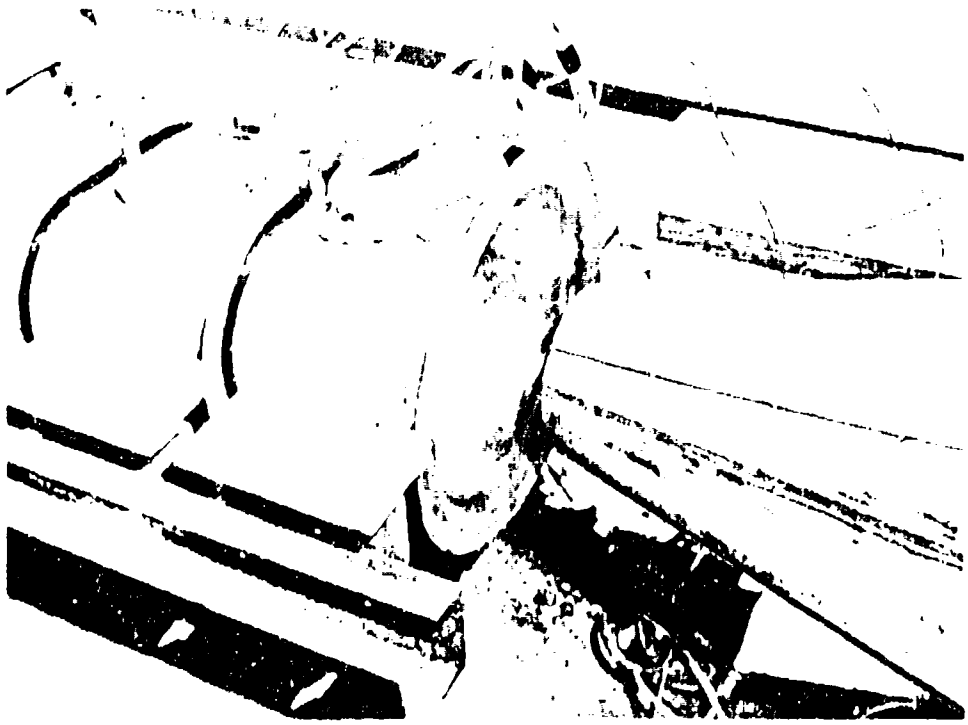

Figure 7. Ejector transition and exhaust model.

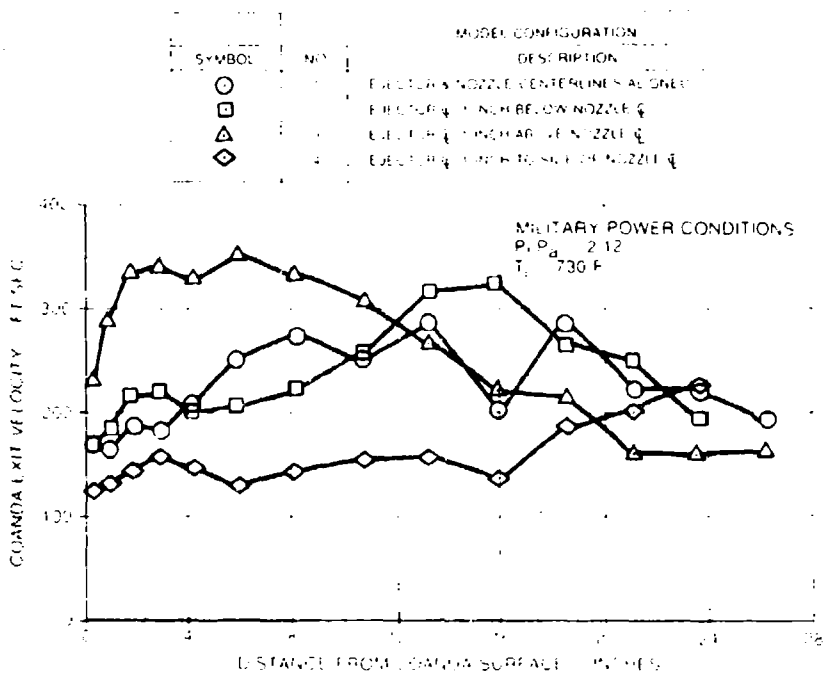

Figure 8. Coanda exit velocity profiles – misalignment test – no adapter – military power.

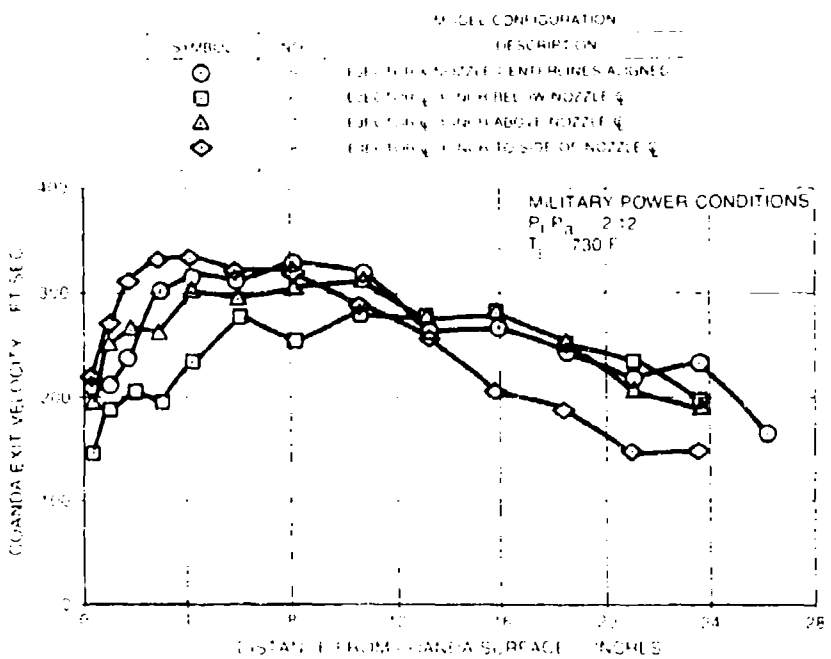

Figure 9. Coanda exit velocity profiles – misalignment test – with adapter – military power.

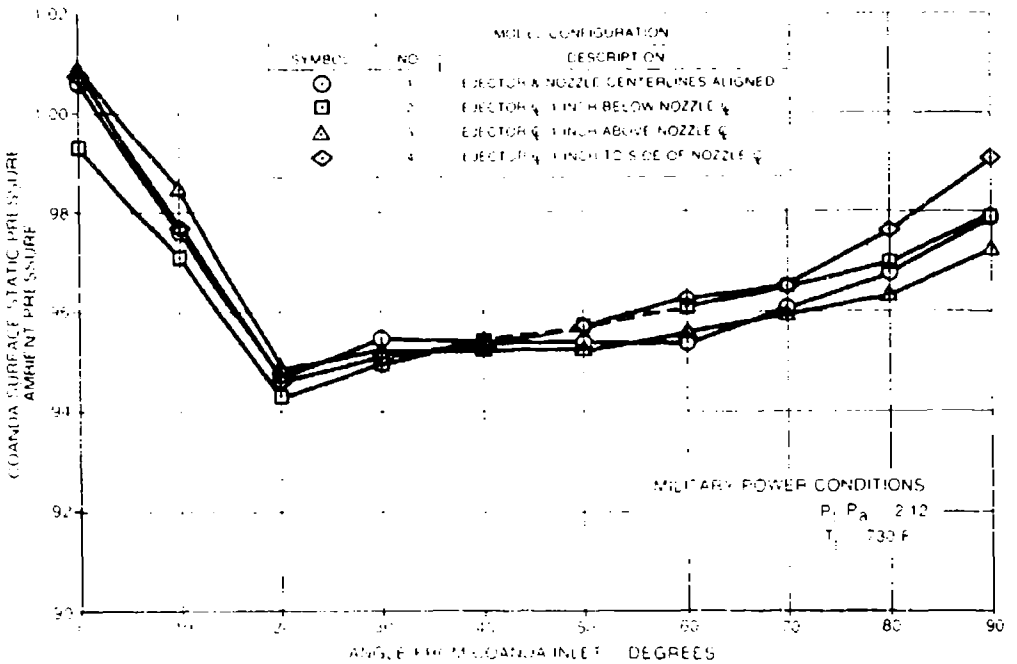

Figure 10. Coanda surface static pressures – misalignment test – no adapter -- military power.

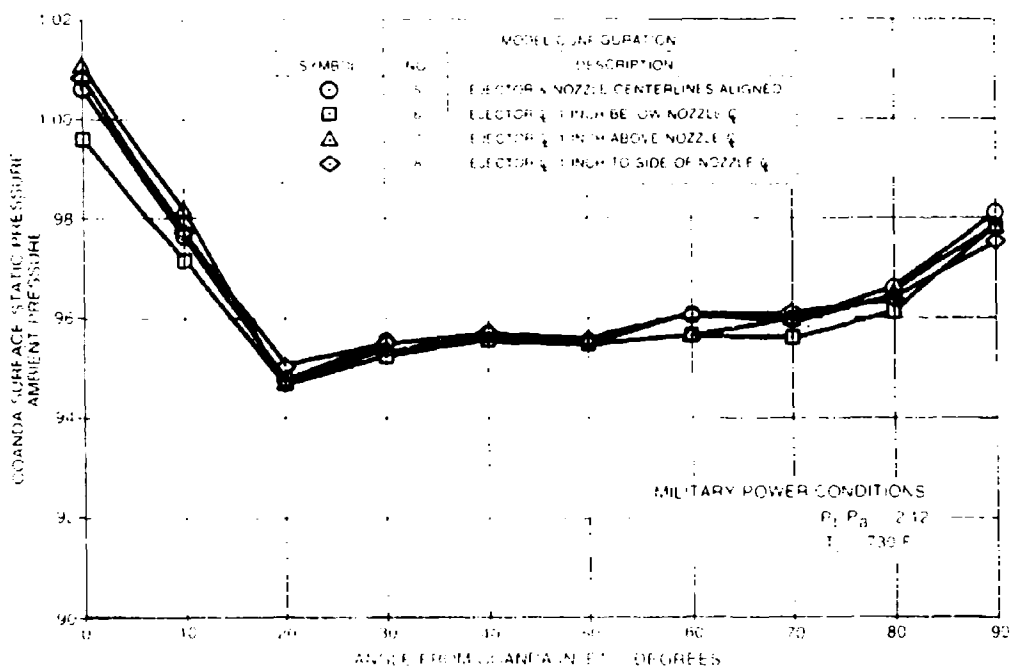

Figure 11. Coanda surface static pressures – misalignment test – with adapter – military power.

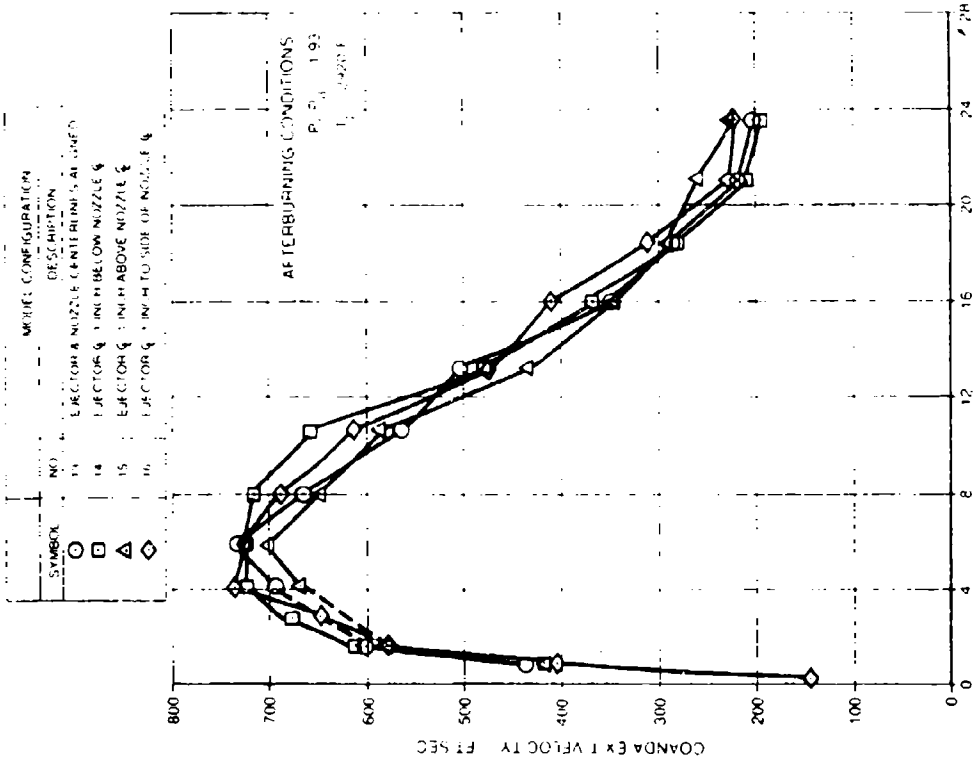

Figure 13. Coanda exit velocity profiles – misalignment test – with adapter – afterburning power.

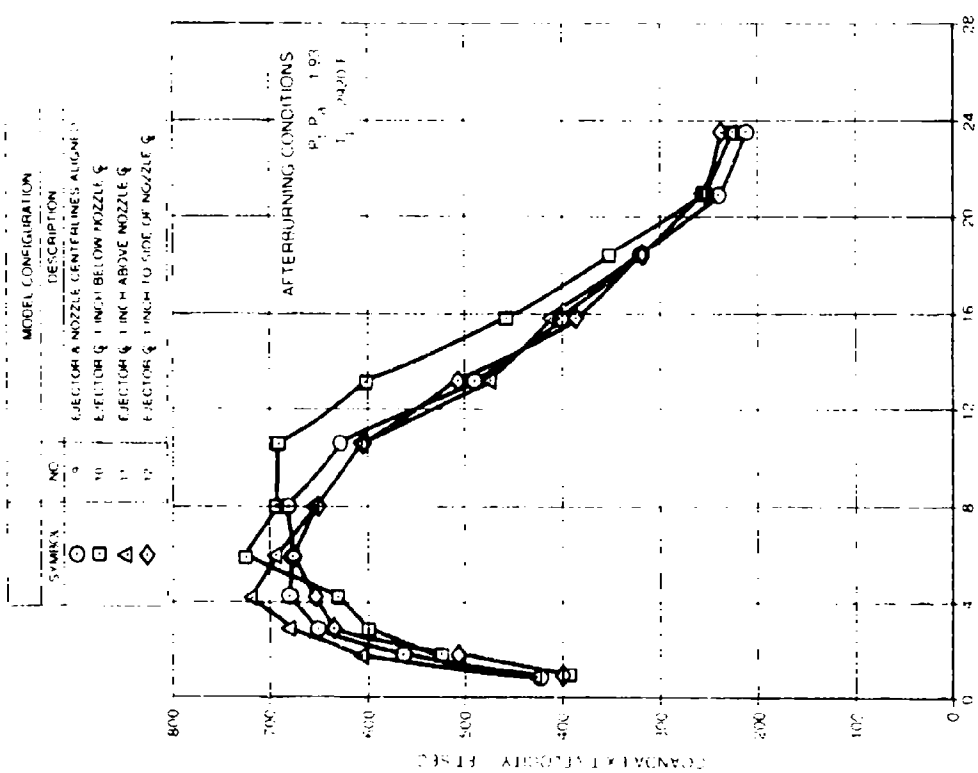

Figure 12. Coanda exit velocity profiles – misalignment test – no adapter – afterburning power.

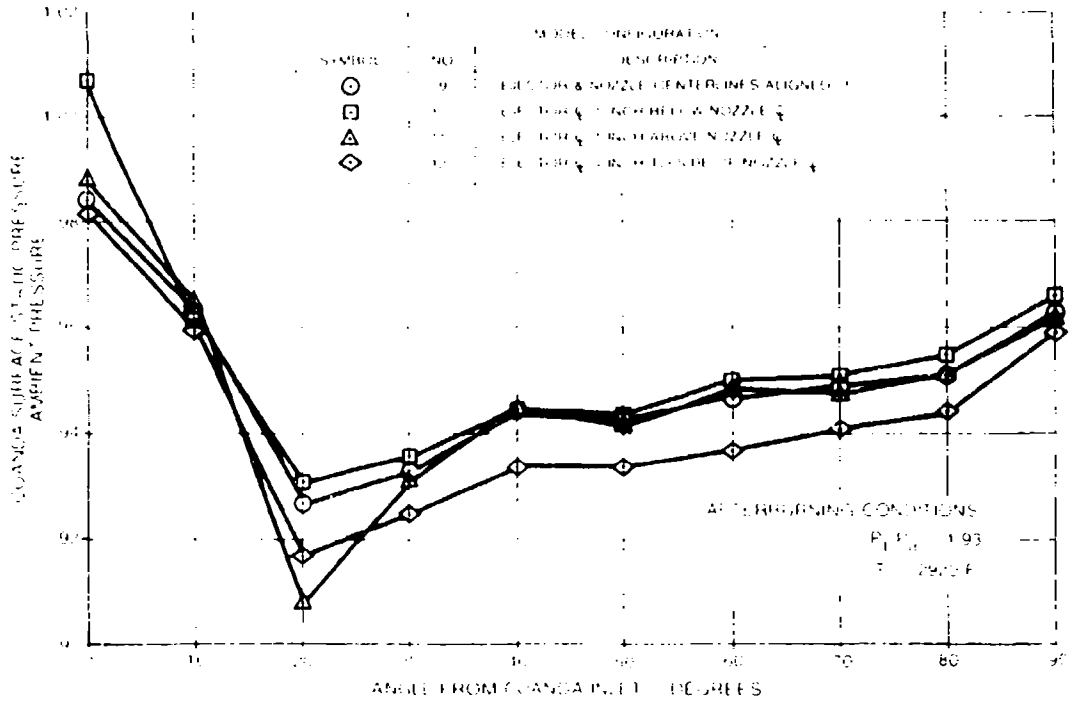

Figure 14. Coanda surface static pressures – misalignment test – no adapter – afterburning power.

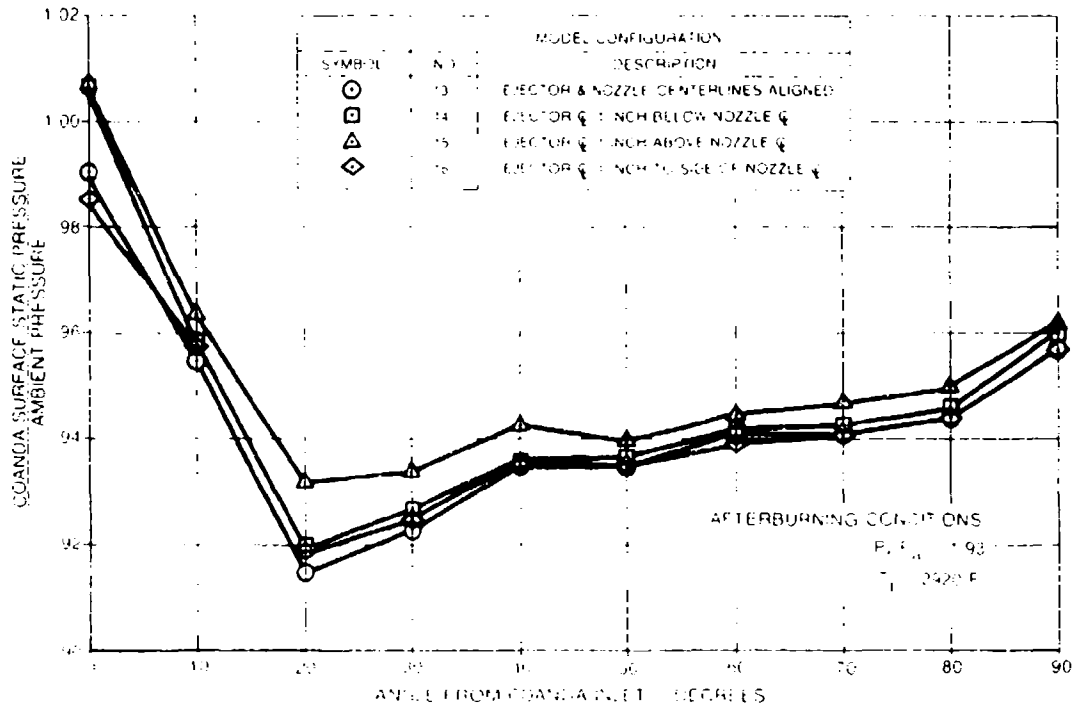

Figure 15. Coanda surface static pressures – misalignment test – with adapter – afterburning power.

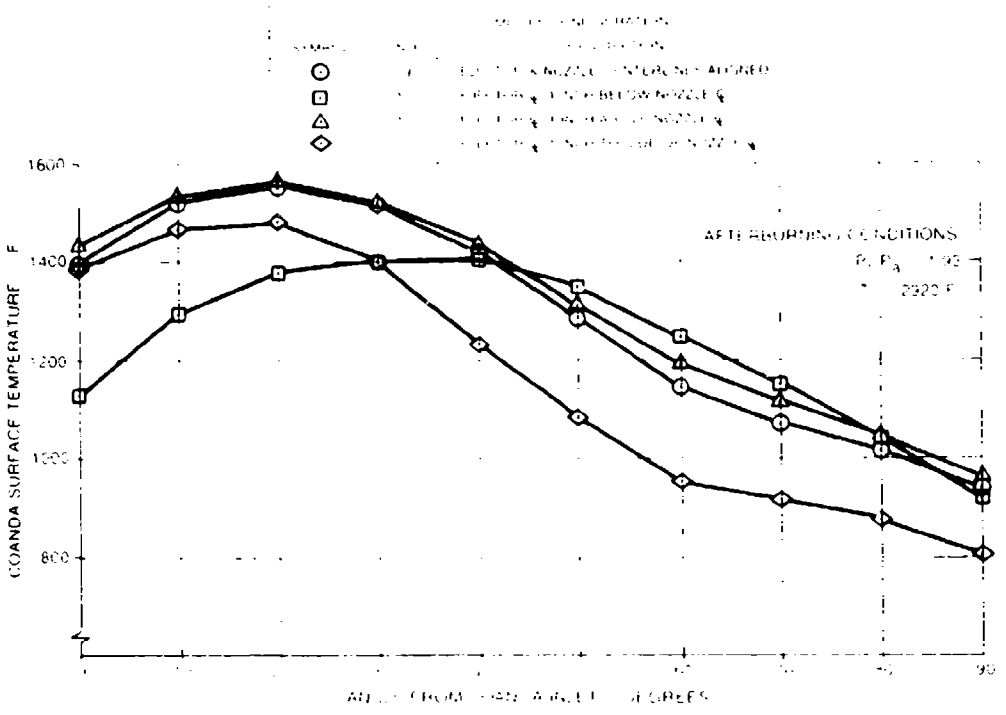

Figure 16. Coanda surface temperatures – misalignment test – no adapter – afterburning power.

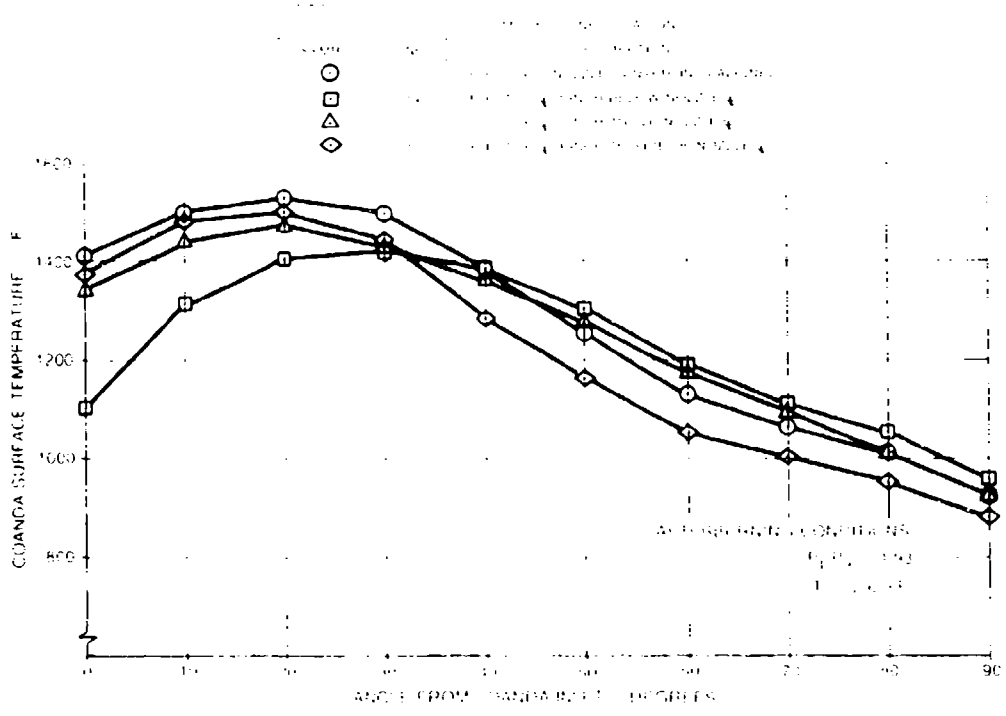

Figure 17. Coanda surface temperatures – misalignment test – with adapter – afterburning power.

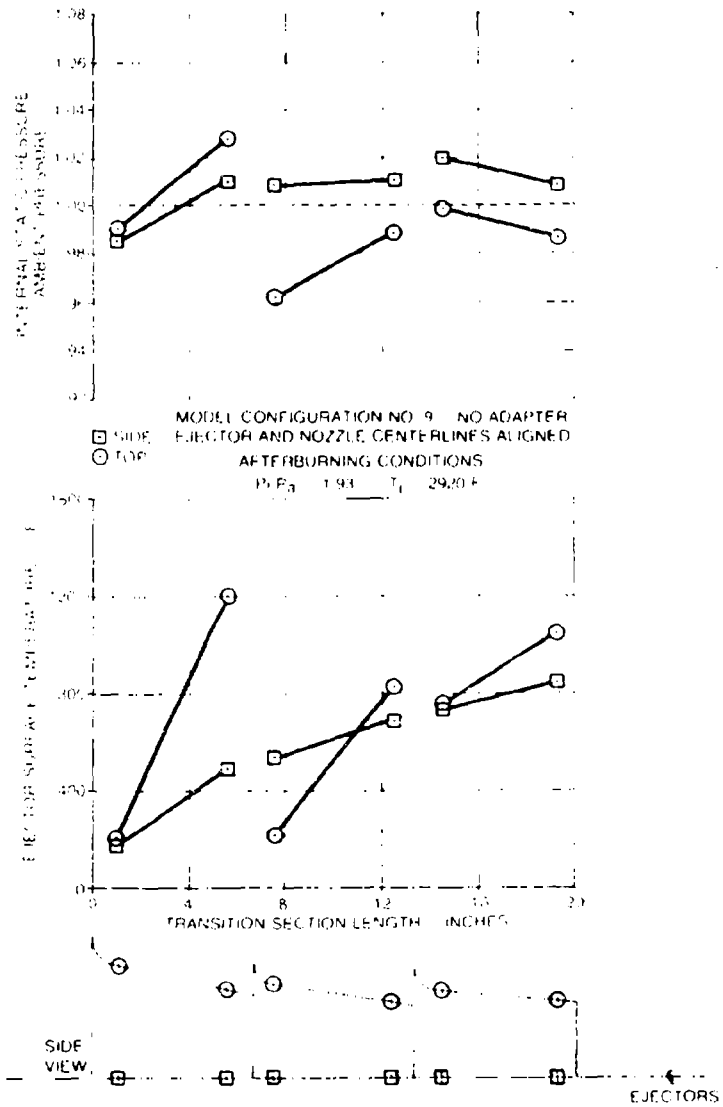

Figure 18. Transition ejector data – misalignment test – ejector and nozzle centerlines aligned – no adapter – afterburning power.

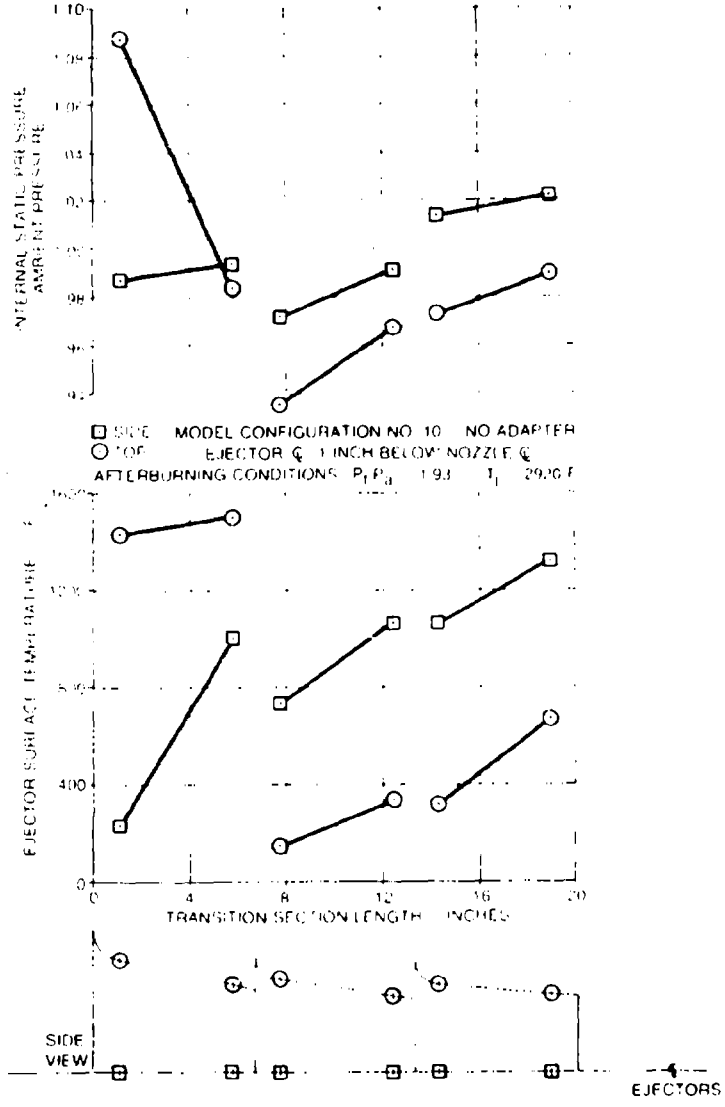

Figure 19. Transition ejector data – misalignment test – nozzle misaligned upward – no adapter – afterburning power.

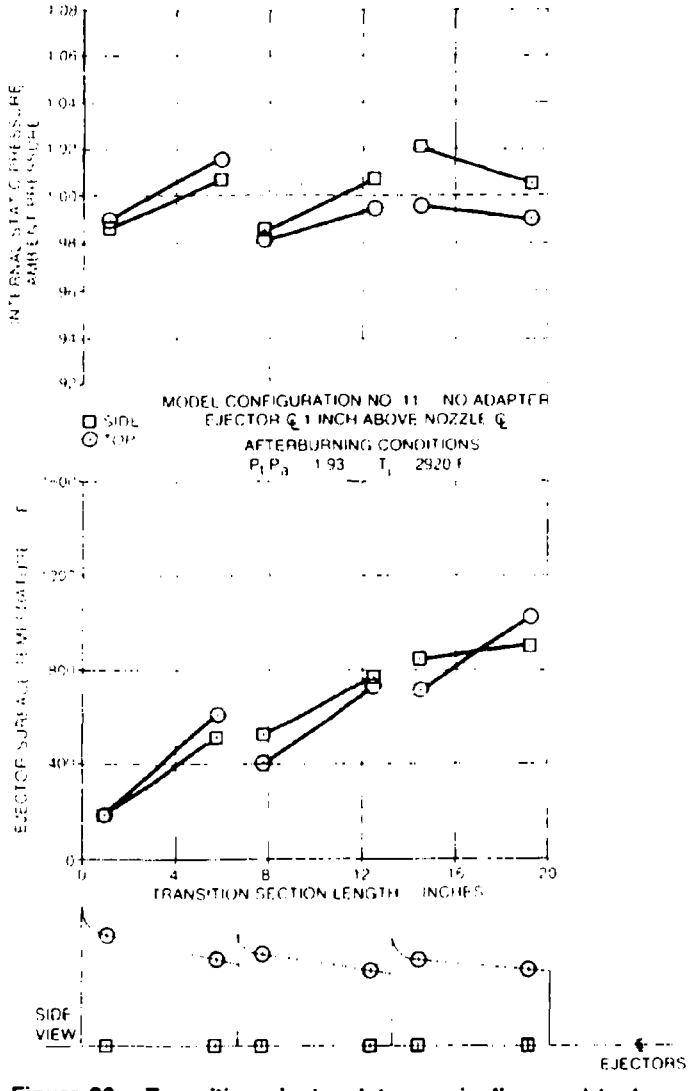

Figure 20. Transition ejector data – misalignment test – nozzle misaligned downward – no adapter – afterburning power.

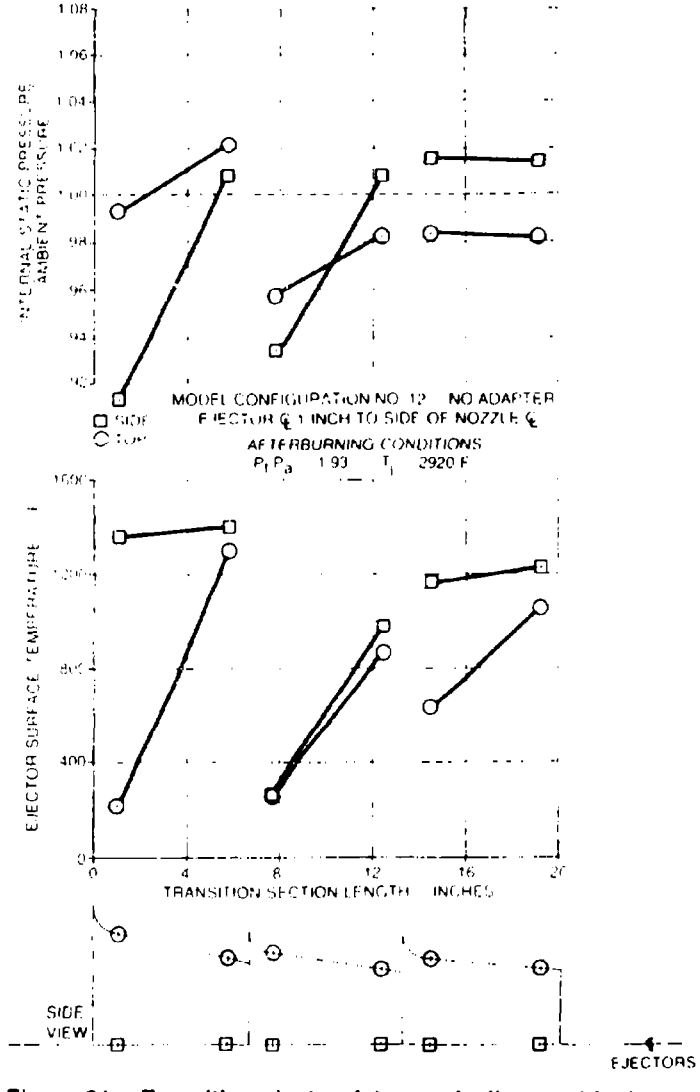

Figure 21. Transition ejector data – misalignment test – nozzle misaligned to side – no adapter – afterburning power.

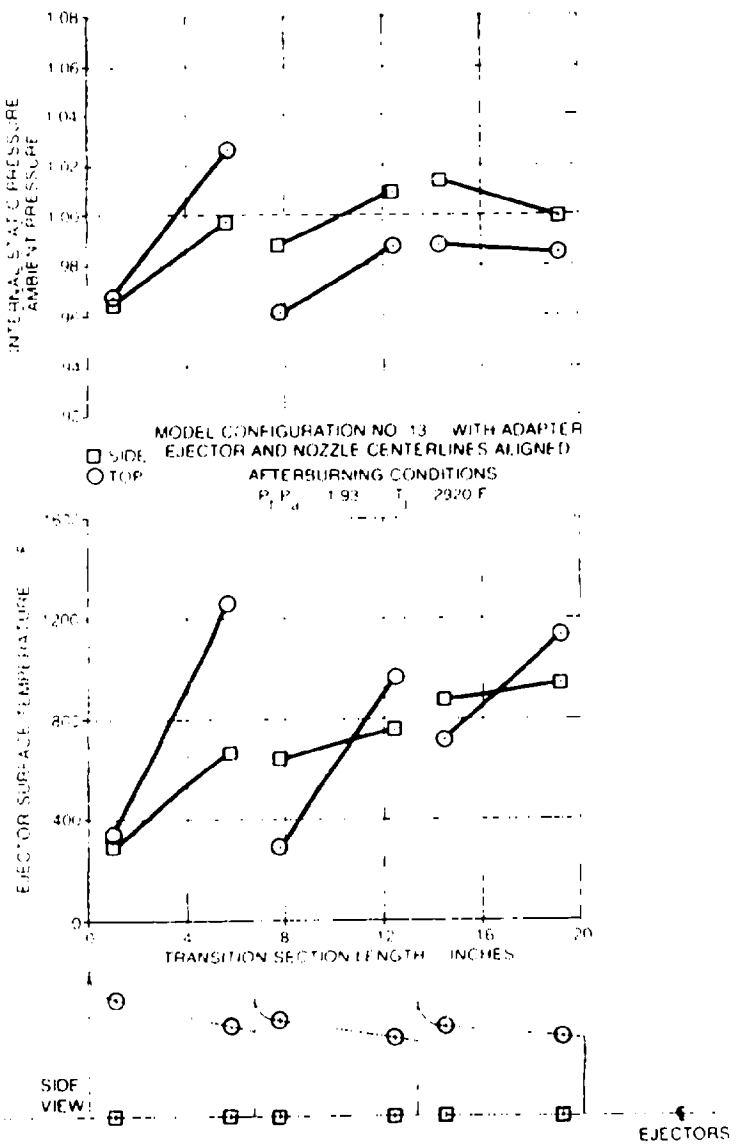

Figure 22. Transition ejector data – misalignment test – ejector and nozzle centerlines aligned – with adapter – afterburning power.

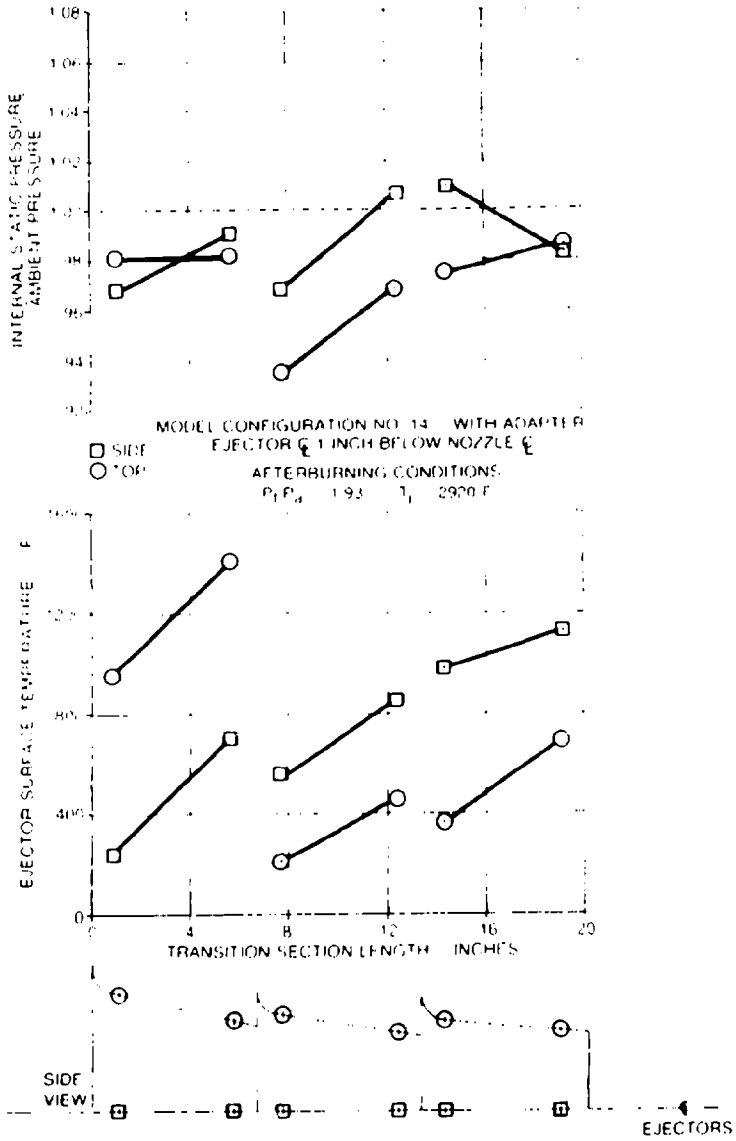

Figure 23. Transition ejector data – misalignment test – nozzle misaligned upward – with adapter – afterburning power.

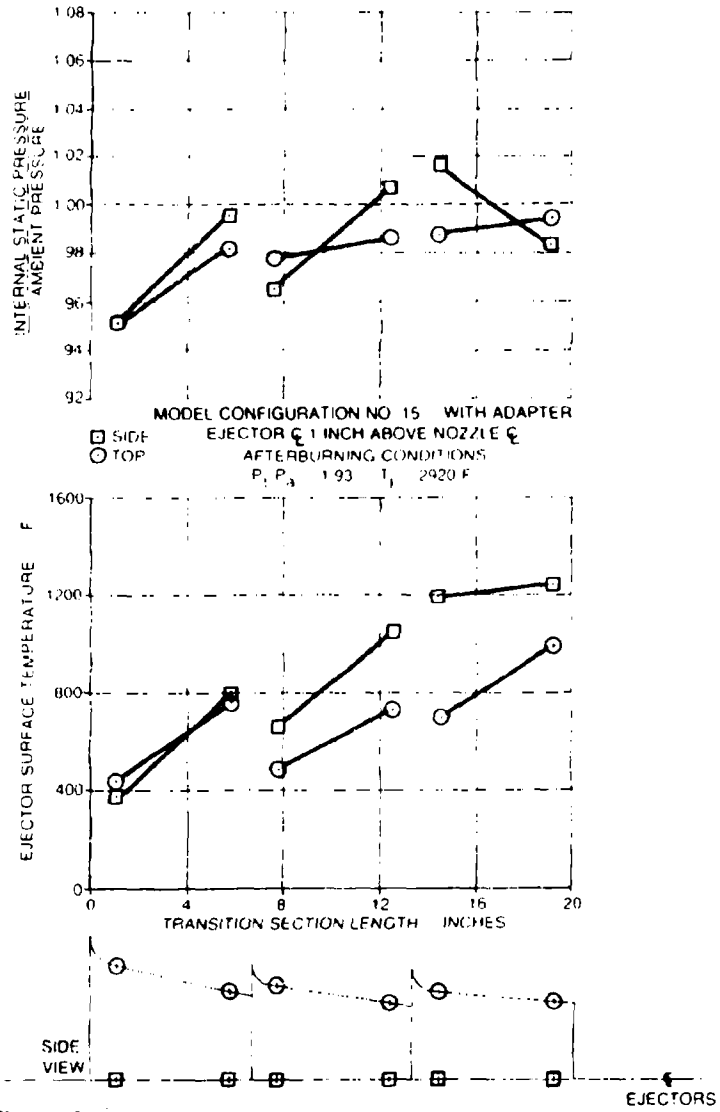

Figure 24. Transition ejector data – misalignment test – nozzle misaligned downward – with adapter – afterburning power.

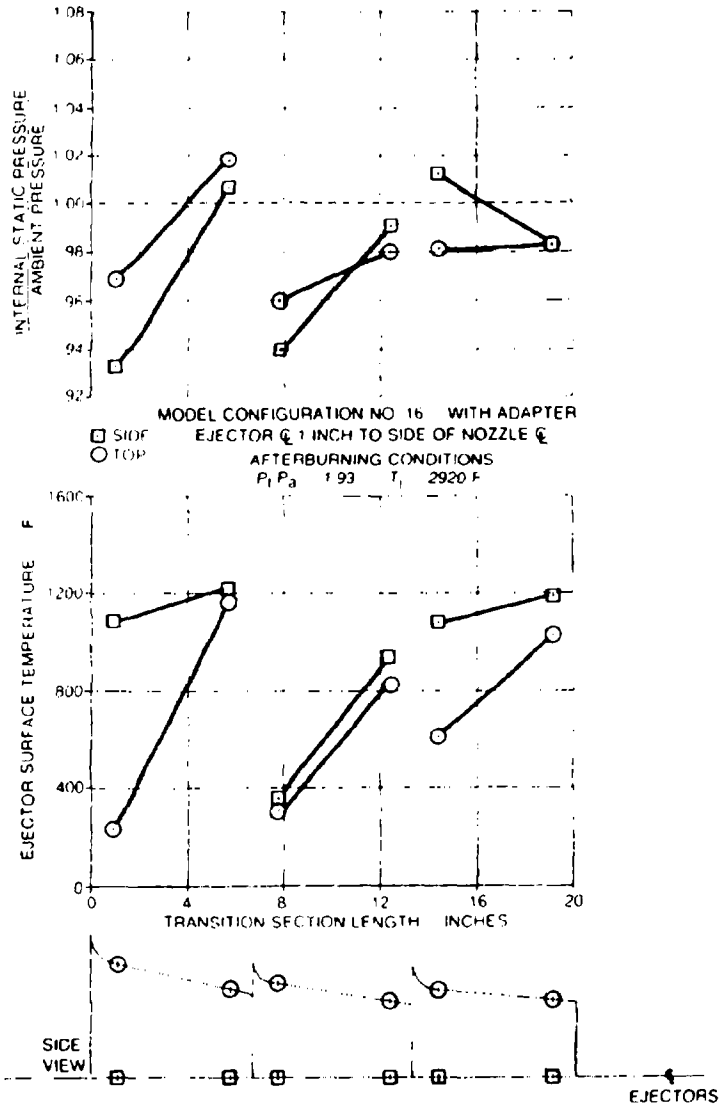

Figure 25. Transition ejector data – misalignment test – nozzle misaligned to side – with adapter – afterburning power.

4.0 COANNULAR FLOW TEST

4.1 Objectives

This model test series was conducted to determine the effects on Coanda flow attachment of the coannular flow produced in fan engines such as the TF41 and TF30-P-408. These are nonafterburning turbofan engines with the fan flow mixed with the primary flow just prior to the exhaust nozzle, which results in a highly stratified coannular flow. The model tests were to evaluate the effects on jet deflection of exhaust flow with a high velocity annulus of cooler gas surrounding the hot exhaust primary core flow. Since the full scale test program (Reference 1) involved only testing with a turbojet afterburning engine, these scale model tests provided data and operational trends that may be extrapolated to full scale operation of long duct, coannular flow, turbofan engines. A secondary objective of these tests was to determine a means for sizing the flow transitioning and deflecting components for suppressor systems to handle nonafterburning engine airflows up to 600 lbs/sec. (The current full scale configuration was designed for up to 300 lbs sec.)

4.2 Model Description and Test Apparatus

The Acoustic Arena facility described in Section 2.0 was used for the coannular flow test. A dual flow system with the center flow heated to the TF30-P-408 primary conditions and sized to one-sixth scale was provided. The bypass ratio (fan airflow primary airflow) is 1.01 for this engine simulation. Figure 26 is a schematic of the coannular flow engine simulation rig.

The transition ejectors, Coanda surface, and support frame used for the coannular flow test were existing hardware from previous testing, Reference 2, and were the model components used to develop the configuration of the full scale test and demonstration article. The first ejector was revised to enlarge its inlet to allow for misalignments as in the test of the preceding section of this report. Figure 27 presents dimensional drawings of the transition ejector and Coanda surface model components used for this test series. The first ejector had an inlet area of 62.5 in^2 and exit area of 43.5 in^2, which results in an exit area ratio (ejector exit area/exit nozzle area) of 2.98, based on the exit nozzle area of 14.60 in^2 of the coannular flow engine simulation rig shown on Figure 26. The area ratio of these ejectors seem large because they are based on the nozzle area of a nonafterburning nozzle whereas those area ratios quoted for previous models were for afterburning nozzle areas (30.0 in^2 at model scale). The first ejector is the only one of this set with a convergent area progression. The second ejector has an area of 46.5 in^2 at the inlet and exit which is an area ratio of 3.18. The third ejector has a constant area progression at 51.0 in^2 resulting in a 3.49 area ratio. The exhaust nozzle used was 4.31 inches in diameter and the exit flow was the combined, coannular primary and fan flow simulating the exhaust of the TF30-P-408 engine.

A schematic of the model test setup is shown on Figure 28. Static pressures are provided on the nozzle lip to measure the pressure changes that may affect engine operating conditions. Static pressure ports are provided on the internal wall of the ejectors to determine the ejector pumping characteristics, and along the Coanda surface centerline to measure the extent of the pressure gradient that produces the flow turning. Thermocouples are provided on the ejectors and Coanda surface to measure the metal surface temperatures. A total pressure and total temperature rake is provided at the Coanda surface exit to obtain exit flow conditions (Mach number, velocity, etc.) and to determine the extent of flow attachment.

Figure 29 is a photograph of the coannular flow simulation rig and Coanda model setup in the Acoustic Arena test facility and running with smoke added to the flow for visualization purposes. The ejectors are positioned such that the exit plane of one coincides with the inlet plane of the next. The exhaust nozzle to ejector inlet spacing was 2.0 inches.

4.3 Test Plan

Table 3 presents the test configurations that were run for evaluating the coannular flow exhaust in a single engine

Coanda deflector system. Also listed are the data that were recorded for each configuration. The location of the pressure and temperature instrumentation on the model is shown on Figure 28. The configuration numbers are listed on all data shown in this report as an aid in identification. The test included misalignment configurations similar to those accomplished in the preceding pure turbojet flow simulation test. It should be noted in the column of Table 3 that describes the misalignment direction that the model was moved rather than the nozzle. This was necessary because of the stationary attachment of the burner and nozzle system to the facility floor. When the configuration is described as "Model 1 inch down" the exhaust nozzle centerline is one inch above the ejector model centerline, and for "Model 1 inch up" nozzle centerline is one inch below the ejector model centerline. All ambient conditions such as temperature, pressure, relative humidity, wind velocity, etc., were recorded along with the data shown in Table 3. Two sets of exhaust nozzle flow parameters were recorded: the primary jet and the cooler annulus of fan airflow. The flow conditions listed in Table 3 are simulated TF30-P-408 engine conditions (scaled to one-sixth scale) and are defined in Table 4.

4.4 Test Results and Conclusions

4.4.1 Coanda Flow Turning Data

Figures 30, 31, and 32 present velocity profiles calculated from total pressure and temperature data measured at the exit of the Coanda surface for idle, 75 percent, and 100 percent intermediate power, respectively. Data for both aligned and misaligned configurations are presented. The profiles indicate the amount of mixing (from their level) and the quality of flow attachment (from the location of the peak velocity) to the Coanda surface. These data indicate excellent mixing and flow attachment for the aligned configuration and for the nozzle misaligned toward the bottom of the ejector inlet. However, the configurations with the nozzle misaligned either to the side or top of the ejector inlet show some degradation of flow attachment at all power settings, as indicated by the movement of the higher velocity streamlines to a greater distance from the Coanda surface. The degradation of flow attachment for those configurations is not significant enough, however, to create any problem with any acoustic enclosure that would be placed around the deflector surface.

Figures 33 and 34 show the Coanda surface static pressure data for aligned and misaligned configurations at 75 percent and 100 percent intermediate power, respectively. These data verify the excellent flow attachment indicated by the velocity profiles because the lowest static pressure levels are as low as those seen previously only with high velocity afterburning flow (Figures 14 and 15). However, the abrupt decrease in pressure gradient beyond the 50° position, on the deflection surface, indicates a weakening of flow attachment, probably due to decreased flow velocity caused by more complete mixing than with the previous afterburning flow. The fact that the static pressure has nearly recovered to ambient level at the 90° position indicates a weakening of attachment to the surface.

4.4.2 System Size Analysis

The evidence from all previous model tests and from the full scale tests (References 1 and 3) indicates that the present system size will operate satisfactorily for the required engines ranging in airflow from 143 lbs/sec to 263 lbs sec (full scale). However, to extend the range to include 600 lbs/sec airflow engines would require more than one size unit. It may be possible to cover the range up to 600 lbs/sec engines with only two unit sizes: one that will handle engines up to 300 lbs/sec and another for engines from approximately 350 to 600 lbs/sec. The determination of the necessary size can be based on the model scale tests. These tests were run at one-sixth scale to the TF30 engine which means the scaled mass flow was

$$(1/6)^2 \ (242) \ = \ 6.72 \text{ lbs/sec}$$

If these models are considered to be variable scale factor models, then for a 600 lbs/sec engine simulation, the scale factor would be

$$S.F. = \sqrt{W_{ms} / W_{fs}} = \sqrt{6.72/600} = .106$$

This means the model scale dimensions would be multiplied by 1.106 for the 600 lbs/sec unit which makes it about 1.5 times the size of the present Coanda and ejector system. This assumes the flow dynamics and thermodynamic characteristics of the system scale similarly at 1/10 scale as they have for the current 1/6 scale which is reasonable.

4.4.3 Conclusions

The conclusions that may be made from the results of the coannular flow test are:

- There are no significantly adverse effects on flow attachment at any power level due the the cooler fan air surrounding the primary flow for low bypass ratios such as the TF30-P-408 and TF41 engines. However, operation with higher bypass ratio turbofan engines, such as the TF34 (6 to 1 bypass ratio), was not evaluated.

- With the presence of the fan flow, there are no system cooling problems.

- Full scale units for larger airflow engines may be sized simply by using the correct model scale factor (within reasonable scaling factor limits) based on the model airflow and full scale airflow requirement.

TABLE 3. COANNULAR FLOW TEST CONFIGURATIONS

CONFIGURATION NUMBER	FLOW CONDITION* (TF30-P-408 ENGINE)	NOZZLE EJECTOR MISALIGNMENT	DATA		
			SURFACE P_s & T_m	EXIT P_t & T_t	TEST RUN NUMBER
17	IDLE	NONE	X	X	127
18	75 PERCENT	NONE	X	X	127
19	INTERMEDIATE	NONE	X	X	127
20	IDLE	MODEL 1° DOWN	X	X	128
21	75 PERCENT	MODEL 1° DOWN	X	X	128
22	INTERMEDIATE	MODEL 1° DOWN	X	X	128
23	IDLE	MODEL 1° UP	X	X	129
24	75 PERCENT	MODEL 1° UP	X	X	129
25	INTERMEDIATE	MODEL 1° UP	X	X	129
26	IDLE	MODEL 1° TO SIDE	X	X	130
27	75 PERCENT	MODEL 1° TO SIDE	X	X	130
28	INTERMEDIATE	MODEL 1° TO SIDE	X	X	130

*PRESSURE RATIO AND TEMPERATURE CONDITIONS ARE PROVIDED IN TABLE 4.

TABLE 4. ONE-SIXTH SCALE EXHAUST NOZZLE FLOW CONDITIONS SIMULATING TF30-P-408 ENGINE AT SEA LEVEL STANDARD

ENGINE CONDITION	PRIMARY			SECONDARY		
	EPR (P_{t7} / P_{t2})	EGT (T_{t7}) °F	AIRFLOW ($\dot{W}_p$) LBS/SEC	FPR ($P_{t2.5}$ / P_{t2})	FGT ($T_{t2.5}$) °F	AIRFLOW ($\dot{W}_s$) LBS/SEC
IDLE	1.055	320	1.00	1.05	60	1.00
75 PERCENT	2.04	875	3.22	1.73	60	3.24
INTERMEDIATE	2.48	1160	3.55	2.00	60	3.58

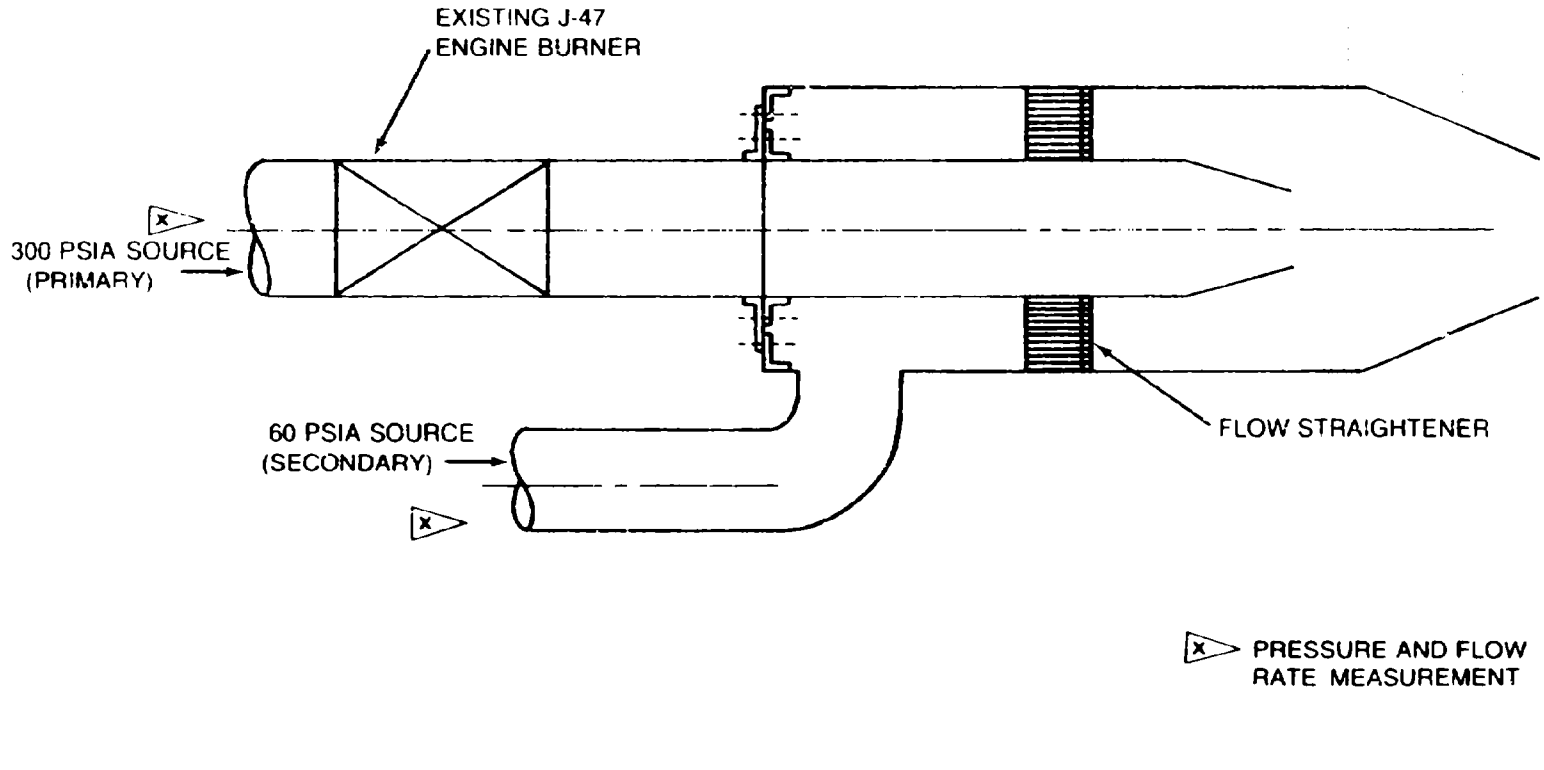

Figure 26. Schematic of coannular flow engine simulation rig.

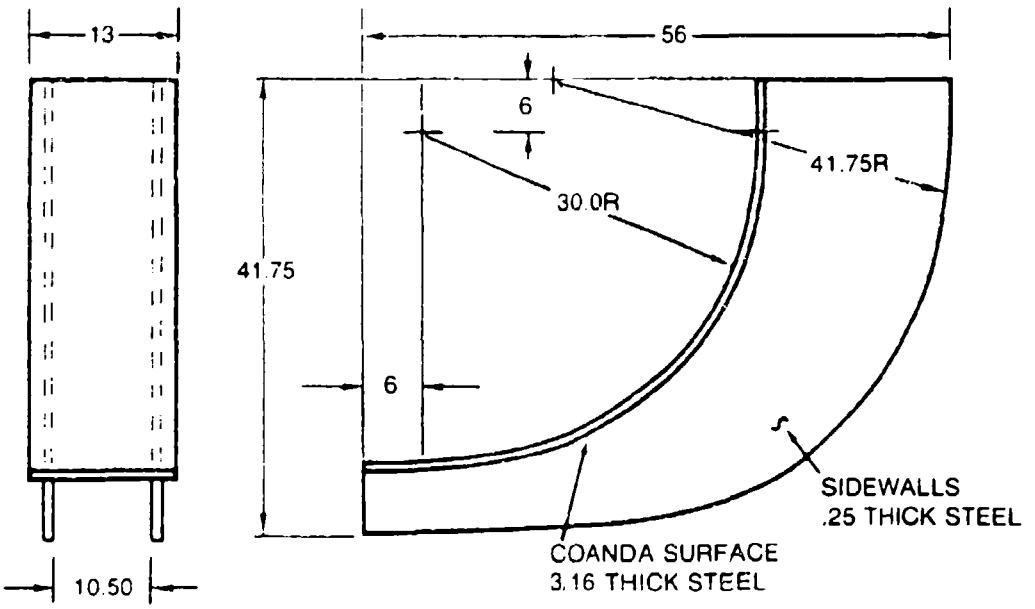

30-INCH RADIUS COANDA SURFACE

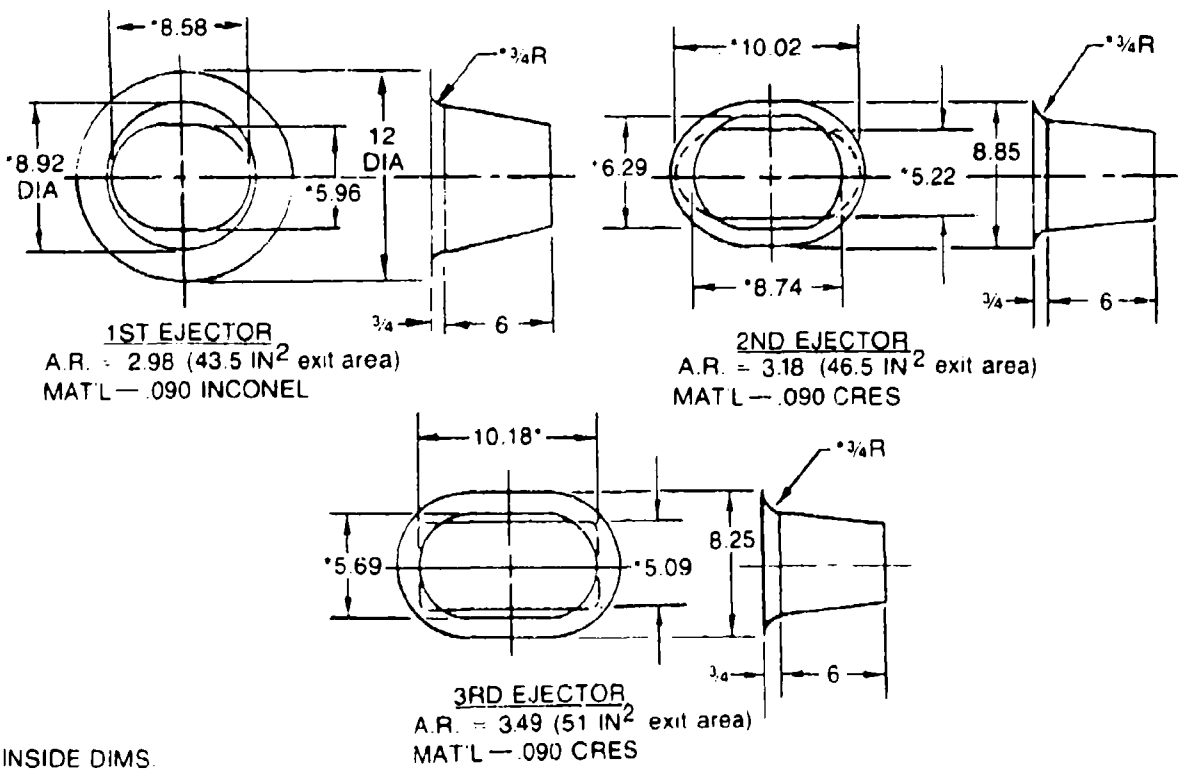

*INSIDE DIMS.

Figure 27. Dimensional drawings of single engine Coanda surfaces and ejectors for coannular flow test.

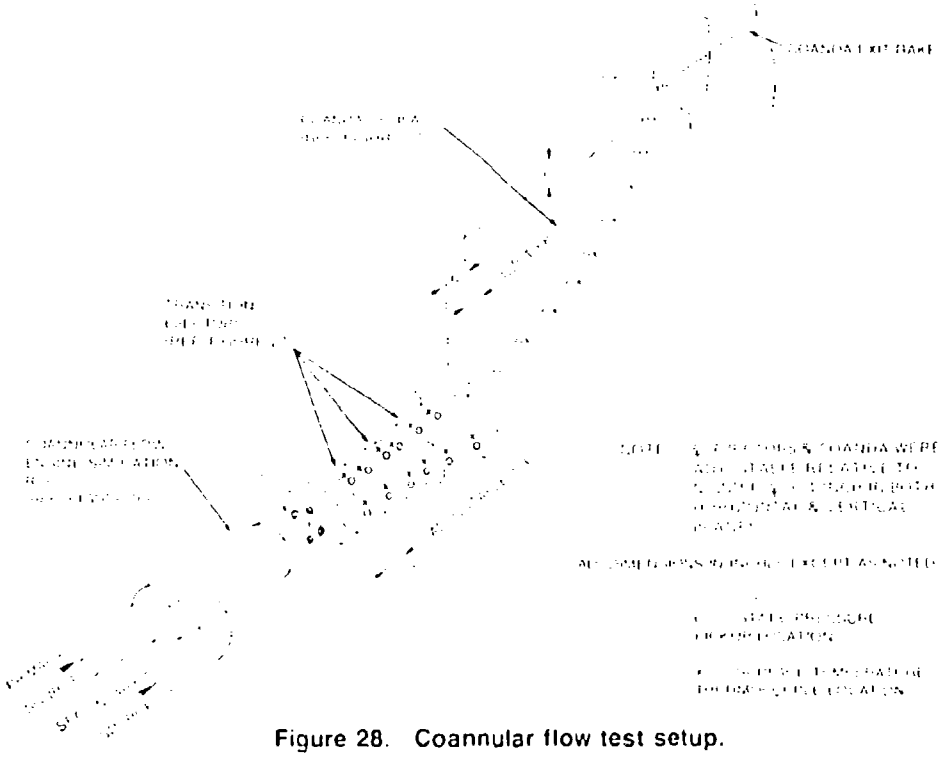

Figure 28. Coannular flow test setup.

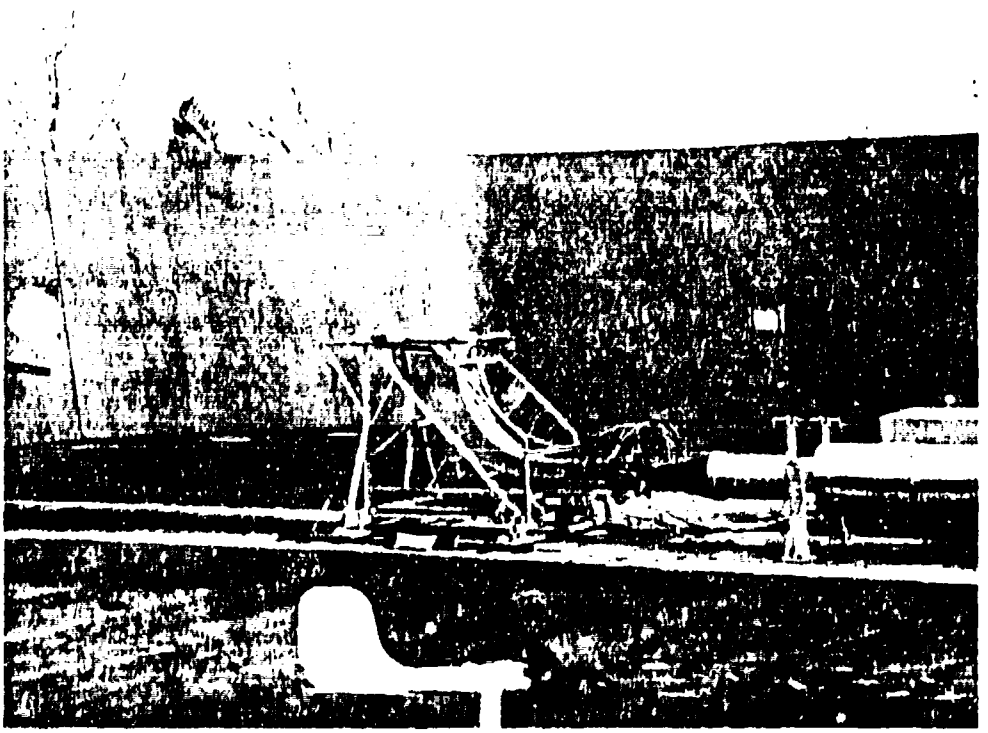

Figure 29. Coannular flow test in Acoustic Arena.

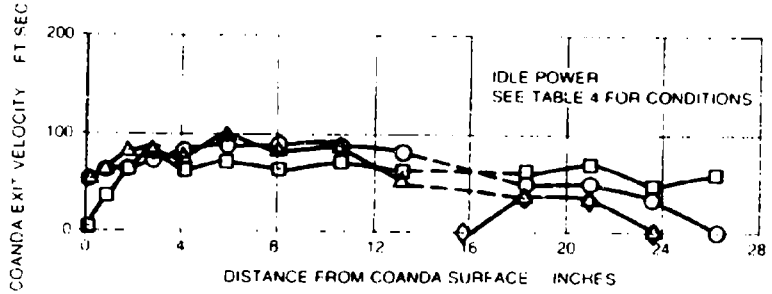

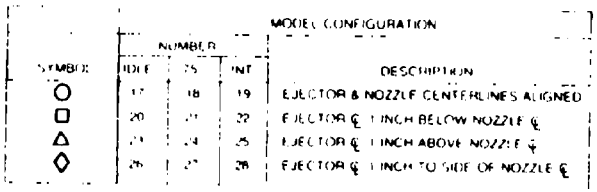

Figure 30. Coanda exit velocity profiles – coannular flow test – idle power.

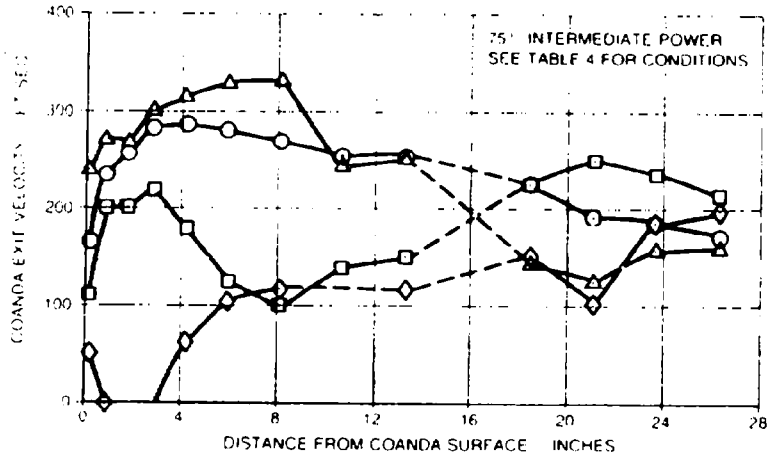

Figure 31. Coanda exit velocity profiles – coannular flow test – 75% intermediate power

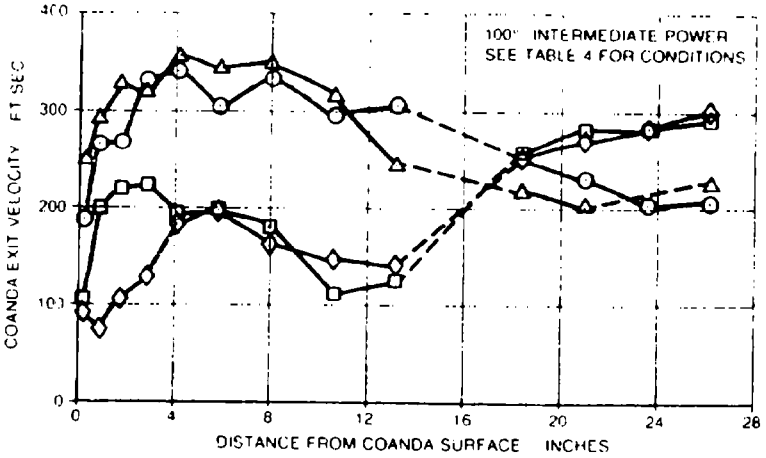

Figure 32. Coanda exit velocity profiles – coannular flow test – intermediate power.

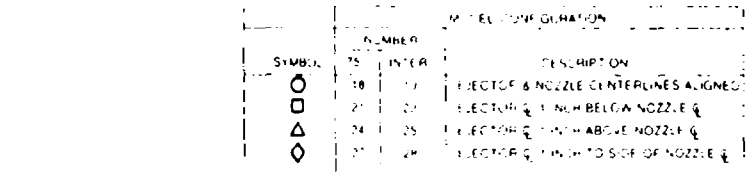

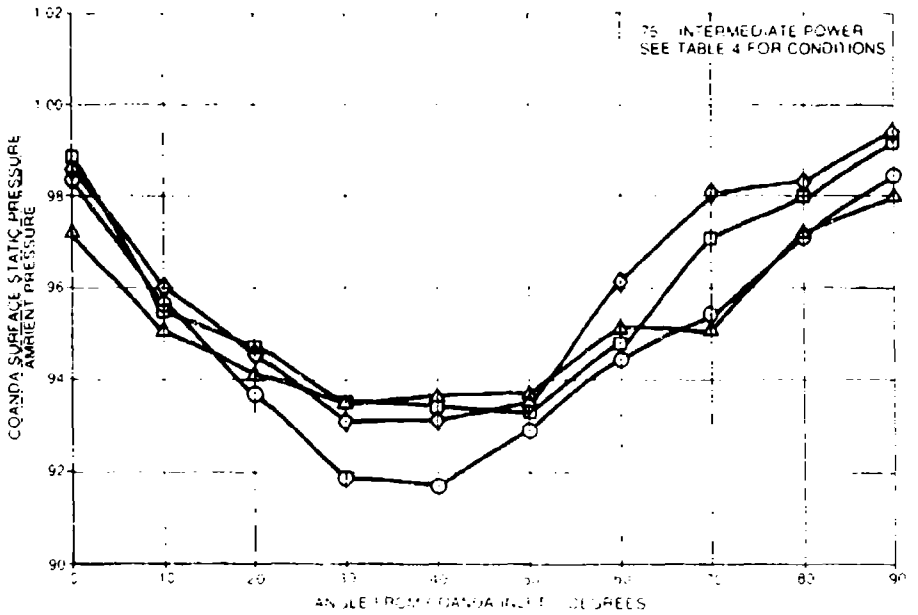

Figure 33. Coanda surface static pressures – coannular flow test – 75% intermediate power

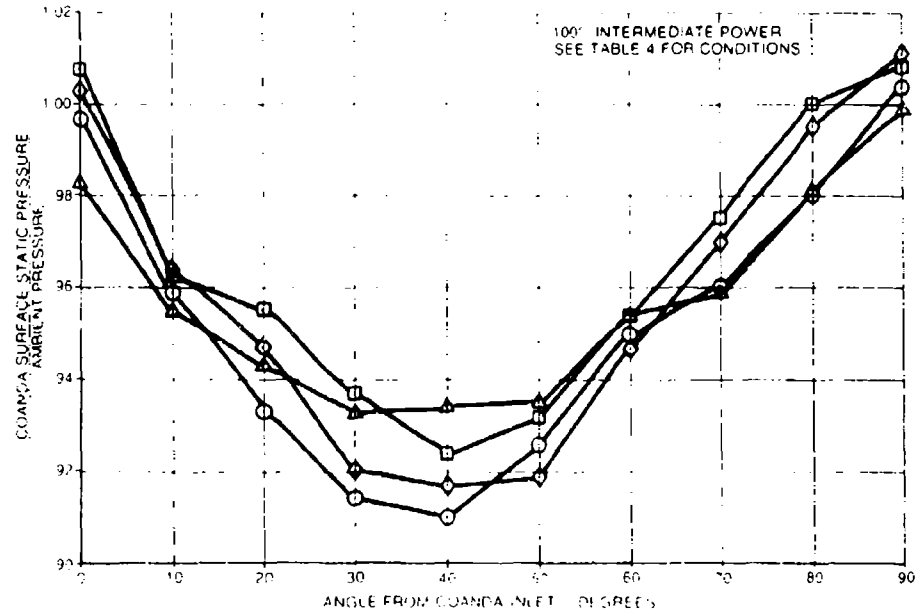

Figure 34. Coanda surface static pressures – coannular flow test – 100% intermediate power

5.0 INITIAL TWIN ENGINE TEST

5.1 Objectives

The third model test of the series was an initial step in developing a Coanda flow turning system for twin engine aircraft with closely spaced engines (such as the F-4, F-111, and F-15 aircraft). The F-14 engine exhaust centerlines are wide enough apart to easily adapt to two separate single engine transition ejector/Coanda deflector systems housed in one acoustic enclosure, therefore, its engine spacing was not included in this series of model tests.

The object of these initial twin engine simulation tests was to observe: (1) The effects of concurrent jet deflection of two distinct power jet sheets in the same deflection chamber, (2) any adverse boundary conditions between two distinct energy levels of dynamic gases which might adversely affect attachment, and (3) to determine if a divider wall is required between the two flows. The results of this test were used to influence the configuration of the model for the twin engine misalignment test discussed later in Section 7.0.

5.2 Model Description and Test Apparatus

This test series was run in the Boeing-Wichita Acoustic Arena Test Facility described earlier in Section 2.0. The data acquisition system was the same as that outlined in that section. Facility changes were required to provide the second nozzle flow with an exit centerline simulating the distance between aircraft (F-4, F-111, and F-15) engines at one-sixth scale. The nozzles were placed nine inches apart which is equivalent to 54 inches full scale. The second nozzle flow system was provided with a J47 engine burner and controls to heat the air to the required temperature for exhaust simulations up to 1500°F.

A new model was fabricated for this test consisting of a three ejector transition with removable internal splitters and a "double wide" Coanda deflection surface with a removable splitter. Dimensional drawings of the model components are shown on Figure 35. With the removable splitters installed, the ejectors have the following flow passage (per engine) areas:

	Inlet		Exit	
Ejector	Area	Area Ratio	Area	Area Ratio
1	63.0 in^2	2.10	45.0 in^2	1.50
2	51.0 in^2	1.70	51.0 in^2	1.70
3	57.0 in^2	1.90	57.0 in^2	1.90

These areas indicate a convergent first ejector and constant area progression second and third ejectors. The first ejector is of necessity, convergent, so the inlet is large enough to capture misaligned flow. However, the second and third ejectors are constant area which is preferable as seen in previous testing. The areas (per side) will change somewhat (enlarge) with the splitters removed; however, this is insignificant when it is considered that the whole ejector (both sides) is open to the combination of flows from both engines which is usually a high power setting on one side and idle on the other.

The Coanda surface has the same rotated logarithmic spiral curvature that was developed in previous testing (Reference 3) for the full scale test article. The "double wide" surface has a center divider (splitter) that is removable.

Figure 36 is a schematic of the transition ejectors and Coanda deflection surface setup behind the twin engine

simulation rig. Also shown is the static pressure and metal temperature instrumentation used for this test. Only one side of the twin system was instrumented for metal surface temperatures, internal static pressures and flow attachment data (Coanda exit pressure and temperature rake). The other side was run at idle conditions and system symmetry assumed for the case of interchanged power settings. Static pressures were provided at the nozzle lip to measure the pressure changes that may affect engine operating conditions. Static pressure ports are provided on the internal wall of the ejectors to determine the ejector pumping characteristics and along the Coanda surface centerline (of one side) to measure the extent of the pressure gradient that produces the flow turning. The metal surface thermocouples are to determine the effects of configuration changes on system cooling. A total pressure and temperature rake is provided at the Coanda surface exit to obtain exit flow conditions (Mach number, velocity, etc) and to determine the extent of flow attachment at the 90° deflected position.

Figure 37 is a photograph showing the twin engine flow simulation rig installed in the Acoustic Arena.

Figures 38, 39, and 40 are photographs of the initial twin engine Coanda model in the Acoustic Arena. A new Coanda surface and transition ejector support frame was fabricated to accept the "double wide" twin model. The ejectors were positioned such that the exit plane of one coincided with the inlet plane of the next. The exhaust nozzle to ejector inlet spacing was 1.75 inches.

5.3 Test Plan

Table 5 presents the test configurations that were initially planned as well as those additional runs that were added as the testing progressed. The test runs that were planned with both nozzles at military power conditions were not accomplished. (It should be noted that current airplane ground test limitations restrict the second engine to idle power while the first engine is at any power up to afterburning). Model configurations were tested alternately with one engine at afterburning and the other at idle; with one engine at full military and the other at idle; and with both engines at idle power settings. The tests were repeated with and without the Coanda surface center splitter and different combinations of ejector splitters. Once the best configuration was found with the nozzle and ejectors aligned, test conditions were run with nozzle to ejector inlet misalignments (offsets) in the vertical and horizontal directions similar to the single engine misalignment test of Section 3.0. As in previous tests, the misalignments were accomplished by moving the model as the nozzle is stationary mounted. Ambient conditions, as well as the two exhaust nozzle flow parameters, were recorded along with the data indicated in Table 5. The configuration numbers are listed on all data shown in Paragraph 5.4 as an aid to identification. The flow conditions listed in Table 5 are simulated TF30-P-12A engine conditions and were defined previously in Table 2 in Paragraph 3.3.

5.4 Test Results and Conclusions

5.4.1 Coanda Flow Turning Data

Figure 41 presents the Coanda exit velocity profiles calculated from total pressure and temperature data recorded by the exit rake at the end of the Coanda surface for various model configurations at afterburning power. These data indicate the only acceptable configurations for flow attachment are those with the Coanda surface center splitter installed either with or without the ejector splitters. The presence of the ejector splitters does not have much effect on flow attachment with the Coanda splitter installed; however, the ejector splitters seem to further reduce the flow attachment when the Coanda divider is not present. The Coanda surface static pressure data at afterburning power shown on Figure 42 indicate the same results as the flow profiles discussed above. The configurations without the Coanda surface divider (splitter) demonstrate surface static pressures, beyond the 20° turned position, that are higher (closer to ambient) than those with the Coanda splitter installed. This results in a lower pressure gradient across the flow and less chance of good flow attachment. All of these configurations, even those whose data indicate good flow attachment, produce high Coanda surface static pressures (low pressure gradients) when compared to the single engine results reported previously in Paragraphs 3.4 and 4.4. A comparison of the Coanda exit velocity profiles from those previous tests and this test indicate a much lower exit velocity for the twin Coanda configuration which explains the high surface static pressures.

Figure 43 presents the Coanda exit velocity profiles for the model with various splitter configurations at full military and idle power conditions. The data at idle power is not conclusive for comparison of configurations as the total pressure data was too low for good resolution. It is presented only to show that the flow attaches at idle conditions. The military power data show the same result as the afterburning data; i.e., the Coanda splitter has to be installed for good flow attachment. There is some evidence (Configuration 38 S-2) that removal of the ejector splitters increases the flow attachment at military power. The Coanda surface static pressure data for various splitter configurations presented on Figure 44 verify the flow attachment conclusions drawn from the exit flow profile data at military power.

Figures 45 and 46 present the Coanda exit velocity profiles and corresponding Coanda surface static pressures, respectively, for vertical and horizontal nozzle to ejector misalignments at afterburning power. The misalignment of nozzle to ejector centerlines was one inch model scale which is equivalent to six inches full scale. The model configuration was without any ejector splitters and with the Coanda surface splitter installed. These data indicate virtually no degradation to flow attachment due to any of the misalignments.

Figures 47 and 48 present the Coanda exit velocity profiles and corresponding Coanda surface static pressures, respectively, for vertical and horizontal misalignments at full military power simulation. Again, the ejector centerlines were offset from the nozzle centerline one inch at model scale and the model configuration used was without ejector splitters and with Coanda surface splitter installed. These data indicate only a slight degradation of flow attachment with a sideways misalignment of the primary flow toward the outer sidewall (away from the splitter) as shown by the slightly irregular shape of the exit velocity profile in the region 0 - 12 inches from the Coanda surface.

5.4.2 System Cooling Data

Figure 49 shows the Coanda surface temperatures for model configurations with ejector and Coanda splitter variations at afterburning power conditions. The temperature levels measured indicate inadequate cooling provided by the transition ejectors. This was attributed to the inability of the ejectors (as designed) to entrain secondary air in the area between the two flows at the second and third ejector inlets. The temperature levels on the Coanda surface are unacceptable and a new ejector design was developed for the next twin engine test discussed later in Section 7.0. The configurations with the Coanda splitter installed produced the lowest peak Coanda surface temperatures, again indicating the necessity of that splitter. The Coanda surface temperatures for the configurations without the Coanda divider decrease more rapidly beyond the 30° position because of poor flow attachment to the surface in that area.

Figure 50 presents Coanda surface temperature data for the model configurations with misalignments of one inch (model scale) in the vertical and horizontal directions at afterburning simulation. These data indicate very little change in Coanda surface temperatures due to any misalignment direction. The significance of these data is that it may be expected that misalignments of at least six inches may be tolerated in a full scale suppressor without causing any additional cooling problem at the Coanda surface.

Coanda splitter and sidewall temperature data for misalignment configurations with afterburning power primary flow simulations are presented on Figure 51. The model configuration used was with no ejector splitters but with the Coanda surface splitter installed. Of primary importance is the indication that all misalignments cause both the splitter and sidewall to be hotter than when nozzle and ejector centerlines are aligned. A further indication that lack of secondary air entrainment between the flows is the cooling problem is seen with the nozzle misaligned to the side (closer to the sidewall). The sidewall temperature increases by about 340° but the splitter does not demonstrate any corresponding decrease in temperature.

Figure 52 gives the transition ejector surface temperatures with splitter variations at afterburning power. The temperatures at the upper surface, especially at the aft end of each ejector, is the hottest because of the oval shape of the ejector exit which allows the flow to impinge on these surfaces as it is spread into the rectangular shape of the transition exit. The much higher temperature of the splitters in the second and third ejectors again indicate

inadequate cooling air between the two engine flows. The presence of the splitters in the ejectors does not appreciably affect the ejector side and upper surface temperatures.

Figure 53 presents the transition ejector surface temperature data with primary nozzle misalignments. The model configuration used was without ejector splitters and with the Coanda surface splitter. The significant results shown by these data are that the surface of the first ejector toward which the misalignment is made increases in temperature to levels well above the 1000°F design goal. The effect of misalignment on the temperatures of the second and third ejector is much less pronounced and generally results in temperatures below the 1000°F goal.

Figure 54 is a summary of the transition ejector internal static pressure data for splitter and misalignment configuration variations at afterburning power. Indications are that, with nozzle and ejector centerlines aligned and with or without the ejector splitters, the third ejector does not entrain secondary flow. This conclusion is drawn from the fact that all the inlet static pressures for that ejector are above ambient pressure. Increasing the area of the last ejector would probably relieve the problem. The upper (and lower) surface static pressures at the aft edge of the first ejector are above ambient pressure because of the flow impingement on those convergent surfaces which causes the desired spreading effect to the primary flow. Misalignment of the flow toward the upper (or lower) surface causes the first stage ejector inlet pressure on that surface to increase to well above ambient, again because of the inward slope of those surfaces. This stagnation of the edge of the primary flow at the upper and lower surfaces is the reason for the high first ejector inlet temperatures seen with vertical misalignment on Figure 53. Misalignment to the side causes the inlet static pressure of the first stage at the side closest to the flow to decrease further below ambient because the ejector side surfaces slope away (diverge) from the flow. This does not allow any stagnation to occur and the higher velocity flow close to the ejector inner surface causes a lower static pressure.

5.4.3 Conclusions

The following conclusions may be made from the results of the initial twin engine model test:

- The Coanda suppressor system may be adapted to in-airframe runups of twin engine aircraft with closely spaced engines.

- The transition ejector set used in this test did not provide adequate self-cooling. It is not entirely clear whether splitters in the ejectors serve any useful purpose. It appeared from the results of these tests that they only served to block air entrainment between the two nozzles. This inability to educt air between the two closely spaced jets was the reason for the insufficient cooling of the Coanda surface and splitters and also contributes to the lack of firm flow attachment to the Coanda surface.

- Flow turning at military power was not satisfactory. For most configurations, the main body of the flow seemed to be turning only about 60°. Although firm attachment was not achieved, satisfactory flow turning was obtained at afterburning conditions both with and without the ejector splitters (Coanda surface splitter installed).

- The twin engine Coanda ground noise suppressor requires a splitter on the Coanda surface to separate the two flow streams. When a high power and a low power jet stream are discharged over a Coanda surface with the proximity of the typical twin engine aircraft, the higher power stream almost completely entrains the lower power jet. While this is not inherently undesirable, it does seem to have a detrimental effect on attachment to the Coanda surface.

- Misalignments in any direction may be tolerated without any adverse effects on flow attachment. Some increase in temperature will accompany misalignments at the first ejector and Coanda surface. A configuration of transition ejectors to improve secondary entrainment between the engine exhausts and at the third ejector inlet should help alleviate the cooling deficiencies.

TABLE 5. INITIAL TWIN ENGINE TEST CONFIGURATIONS

NOTE ALL DIMENSIONS IN INCHES

CONF NUMBER	PRIMARY NOZZLE DIA LEFT HAND	PRIMARY NOZZLE DIA RIGHT HAND	PRIMARY FLOW CONDITION LEFT HAND	PRIMARY FLOW CONDITION RIGHT-HAND	EJECTOR CONFIGURATION	COANDA CONFIGURATION	NOZZLE/EJECTOR MISALIGNMENT	DATA SURFACE P_s & T_{im}	DATA EXIT P_t & T_t	DATA TEST RUN NUMBER
29	4.31	4.31	IDLE	IDLE	NO SPLITTERS	NO SPLITTER	NONE	X	X	14
30	4.31	4.31	MILITARY	IDLE	NO SPLITTERS	NO SPLITTER	NONE	X	X	15
31	4.31	4.31	MILITARY	MILITARY	NO SPLITTERS	NO SPLITTER	NONE	—	—	NOT RUN
32	6.18	4.31	FULL AFTER BURNING	IDLE	NO SPLITTERS	NO SPLITTER	NONE	X	X	17
33	4.31	4.31	IDLE	IDLE	WITH ALL SPLITTERS	NO SPLITTER	NONE	X	X	5
34	4.31	4.31	MILITARY	IDLE	WITH ALL SPLITTERS	NO SPLITTER	NONE	X	X	6
35	4.31	4.31	MILITARY	MILITARY	WITH ALL SPLITTERS	NO SPLITTER		—	—	NOT RUN
36	6.18	4.31	FULL AFTER BURNING	IDLE	WITH ALL SPLITTERS	NO SPLITTER	NONE	X	X	18
37	4.31	4.31	IDLE	IDLE	WITH ALL SPLITTERS	WITH SPLITTER	NONE	X	X	1
37 S 1	4.31	4.31	IDLE	IDLE	WITH EJECTOR 1 & 2 SPLITTERS ONLY	WITH SPLITTER	NONE	X	X	7
					WITH EJECTOR 1 SPLITTER ONLY	WITH SPLITTER	NONE	X	X	9
37 S 3	4.31	4.31	IDLE	IDLE	WITH EJECTOR 1 & 3 SPLITTERS ONLY	WITH SPLITTER	NONE	X	X	11
38	4.31	4.31	MILITARY	IDLE	WITH ALL SPLITTERS	WITH SPLITTER	NONE	X	X	2
38 S 1	4.31	4.31	MILITARY	IDLE	WITH EJECTOR 1 & 2 SPLITTERS ONLY	WITH SPLITTER	NONE	X	X	8
38 S 2	4.31	4.31	MILITARY	IDLE	WITH EJECTOR NO 1 SPLITTER ONLY	WITH SPLITTER	NONE	X	X	10
38 S 3	4.31	4.31	MILITARY	IDLE	WITH EJECTOR 1 & 3 SPLITTERS ONLY	WITH SPLITTER	NONE	X	X	13
39	4.31	4.31	MILITARY	MILITARY	WITH ALL SPLITTERS	WITH SPLITTER	NONE	—	—	NOT RUN
40	6.18	4.31	FULL AFTER BURNING	IDLE	WITH ALL SPLITTERS	WITH SPLITTER	NONE	X	X	19

TABLE 5. INITIAL TWIN ENGINE TEST CONFIGURATIONS (CONT'D)

NOTE ALL DIMENSIONS IN INCHES

CONF. NUMBER	PRIMARY NOZZLE DIA LEFT HAND	PRIMARY NOZZLE DIA RIGHT HAND	PRIMARY FLOW CONDITION LEFT HAND	PRIMARY FLOW CONDITION RIGHT HAND	EJECTOR CONFIGURATION	COANDA CONFIGURATION	NOZZLE-EJECTOR MISALIGNMENT	DATA SURFACE P_s & T_m	DATA EXIT P_t & T_t	DATA TEST RUN NUMBER
40 S 1	6.18	4.31	FULL AFTER BURNING	IDLE	NO SPLITTERS	WITH SPLITTER	NONE	X	X	20
41	4.31	4.31	MILITARY	IDLE	NO SPLITTERS	WITH SPLITTER	MODEL 1" DOWN	X	X	21
42	4.31	4.31	MILITARY	MILITARY	NO SPLITTERS	WITH SPLITTER	MODEL 1" DOWN			NOT RUN
43	6.18	4.31	FULL AFTER BURNING	IDLE	NO SPLITTERS	WITH SPLITTER	MODEL 1" DOWN	X	X	26
44	4.31	4.31	MILITARY	IDLE	NO SPLITTERS	WITH SPLITTER	MODEL 1" UP	X	X	22
45	4.31	4.31	MILITARY	MILITARY	NO SPLITTERS	WITH SPLITTER	MODEL 1" UP			NOT RUN
46	6.18	4.31	FULL AFTER BURNING	IDLE	NO SPLITTERS	WITH SPLITTER	MODEL 1" UP	X	X	25
47	4.31	4.31	MILITARY	IDLE	NO SPLITTERS	WITH SPLITTER	MODEL 1" TO SIDE	X	X	23
48	4.31	4.31	MILITARY	MILITARY	NO SPLITTERS	WITH SPLITTER	MODEL 1" TO SIDE			NOT RUN
49	6.18	4.31	FULL AFTER BURNING	IDLE	NO SPLITTERS	WITH SPLITTER	MODEL 1" TO SIDE	X	X	24

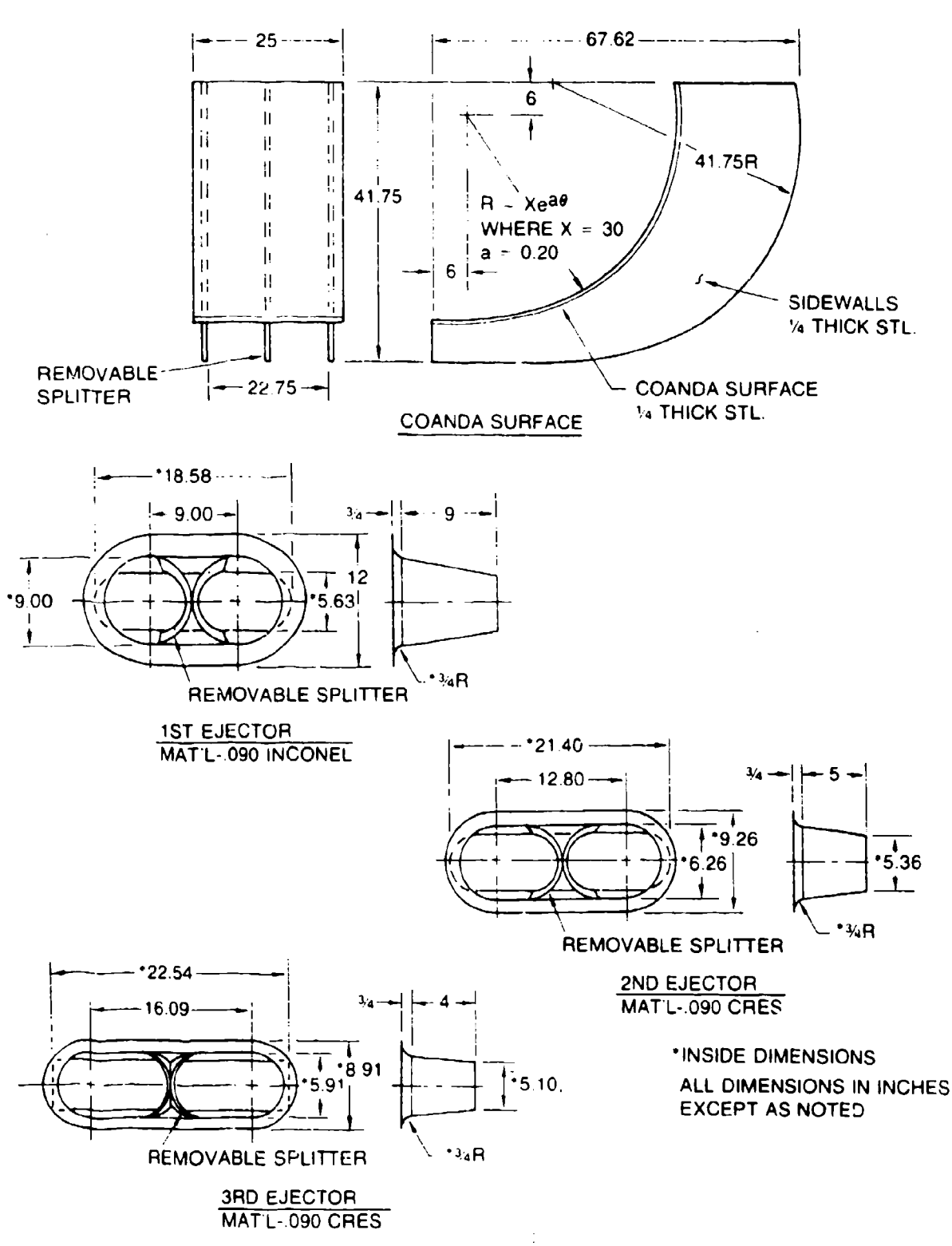

Figure 35. Dimensional drawings of two engine Coanda surface and ejectors.

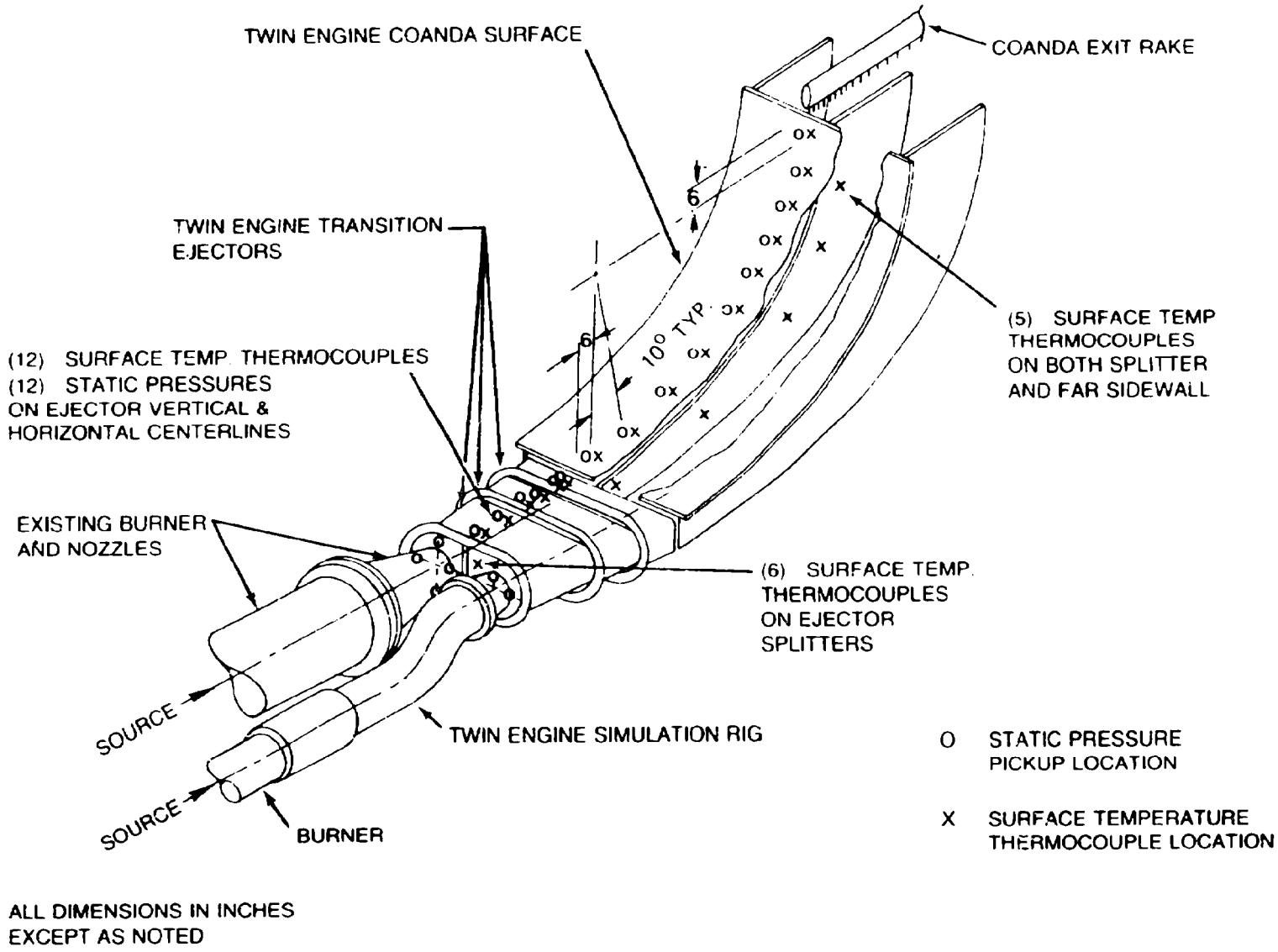

Figure 36. Initial twin engine Coanda and ejector test setup.

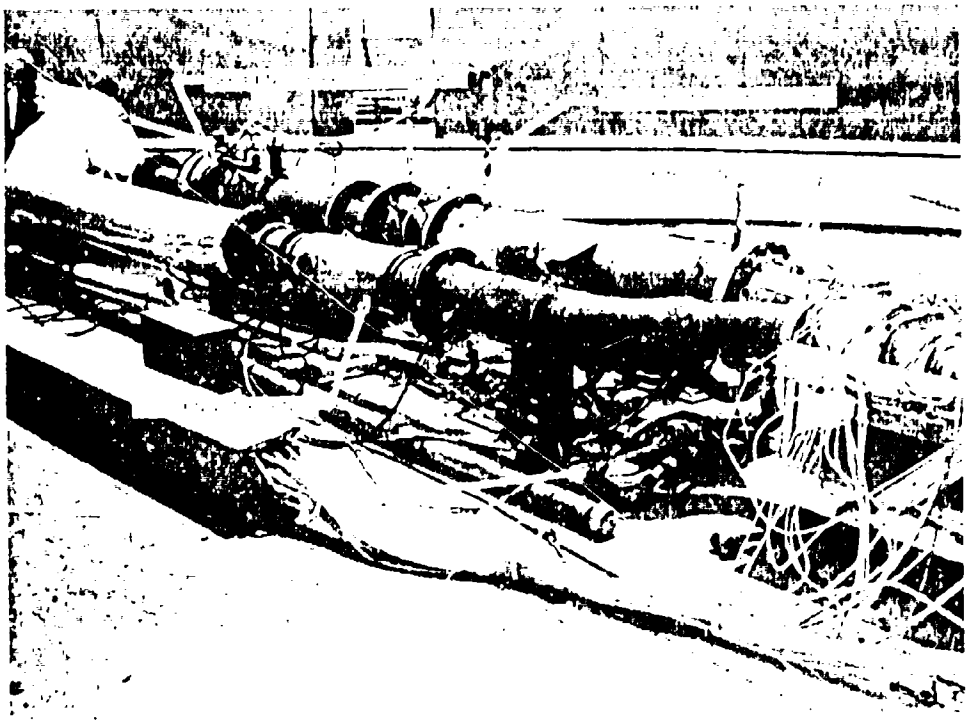

Figure 37. Twin engine flow simulation rig in acoustic arena.

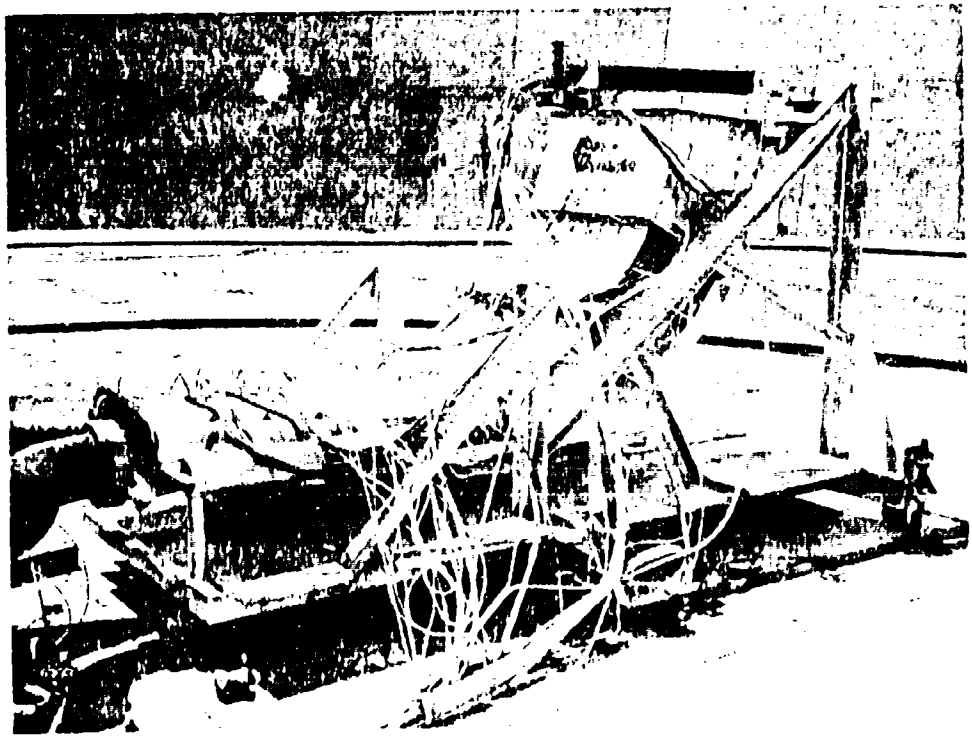

Figure 38. Initial twin engine Coanda model in acoustic arena.

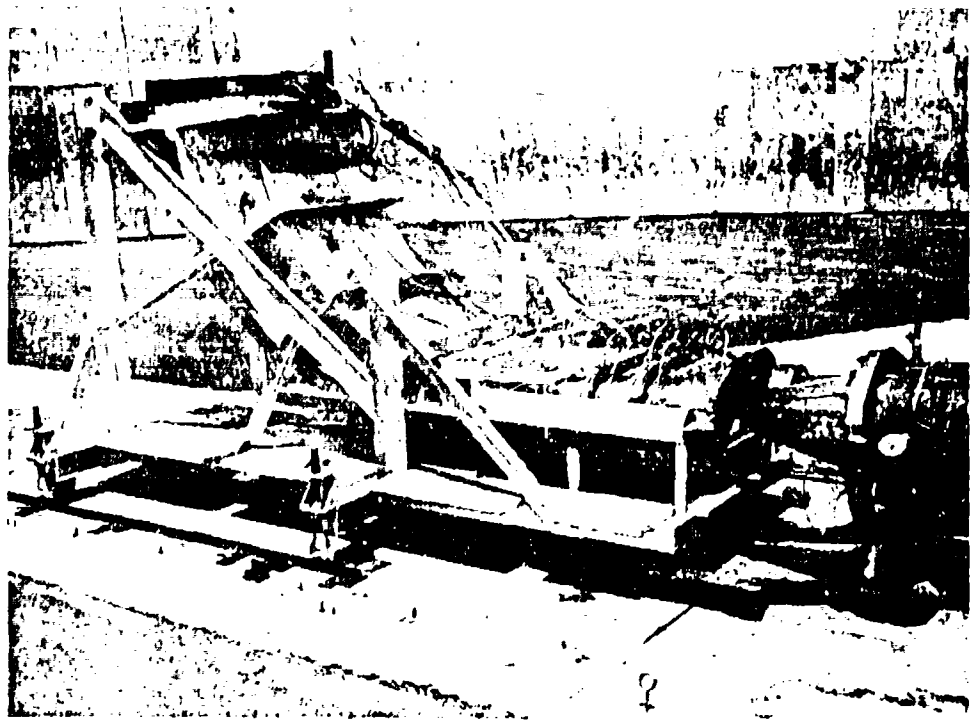

Figure 39. Initial twin engine Coanda model in acoustic arena.

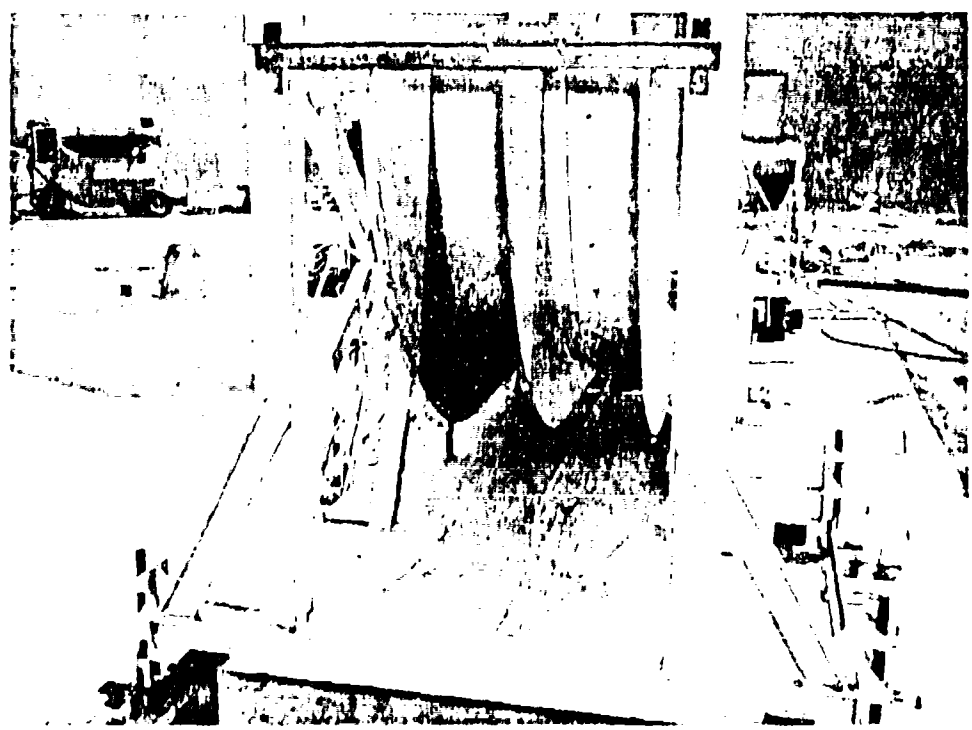

Figure 40. Rear view of initial twin engine Coanda model.

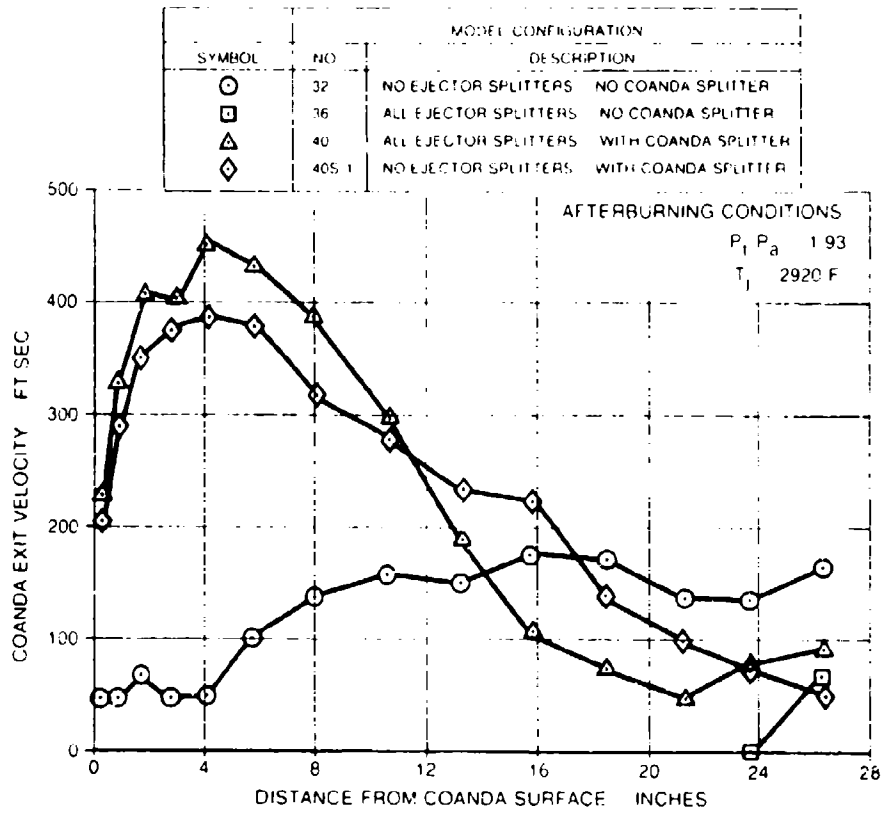

Figure 41. Coanda exit velocity profiles – initial twin engine model test – spiltter variations – afterburning power

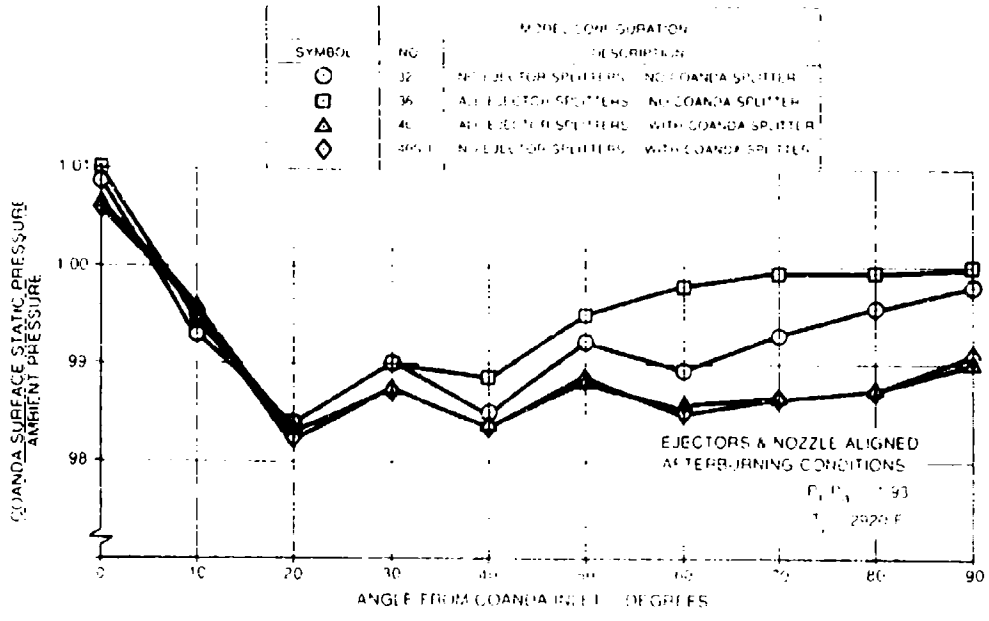

Figure 42. Coanda surface pressures – initial twin engine test – splitter variations – afterburning power.

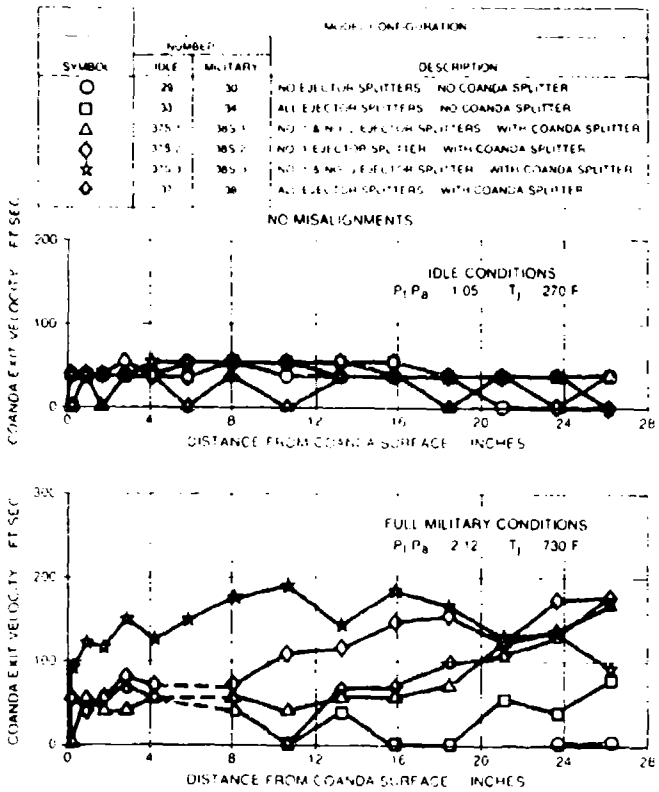

Figure 43. Coanda exit velocity profiles – initial twin engine test – splitter variations – idle and full military power.

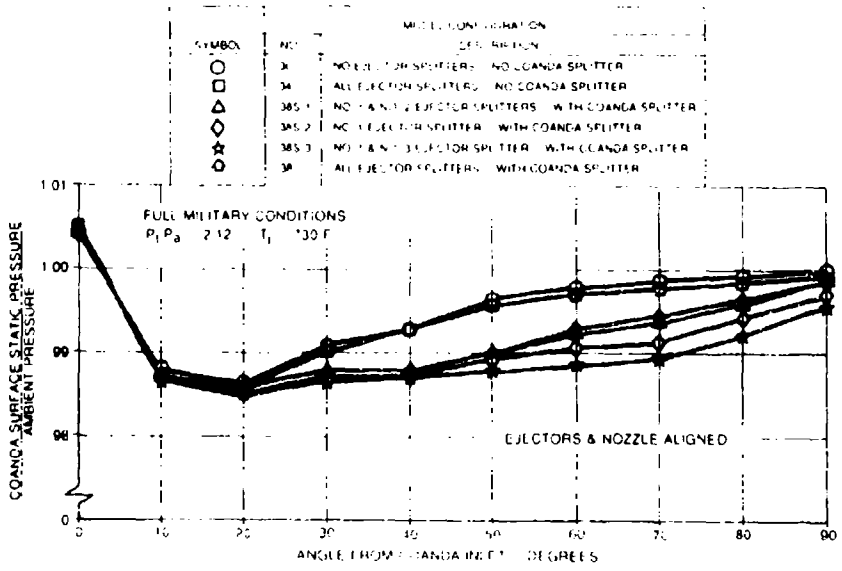

Figure 44. Coanda surface pressures – initial twin engine test – splitter variations – full military power.

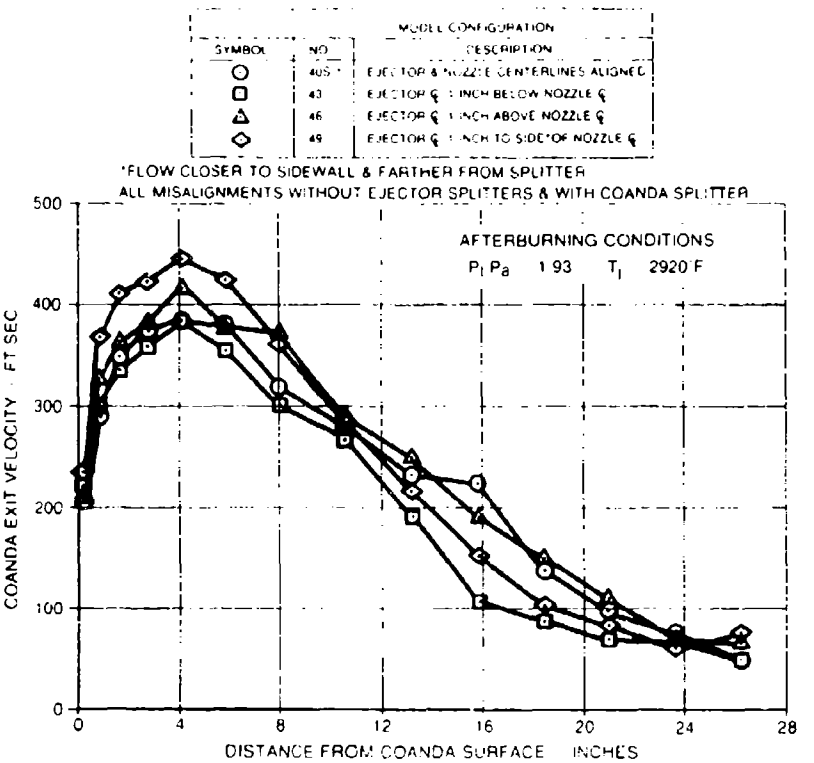

Figure 45. Coanda exit velocity profiles – initial twin engine test – with misalignment – afterburning power.

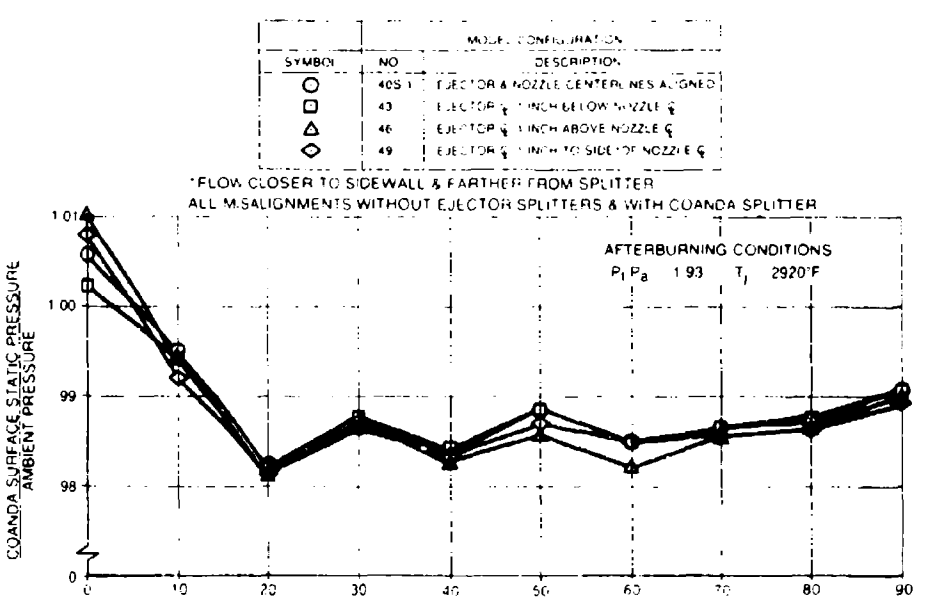

Figure 46. Coanda surface static pressures – initial twin engine test – with misalignment – afterburning power.

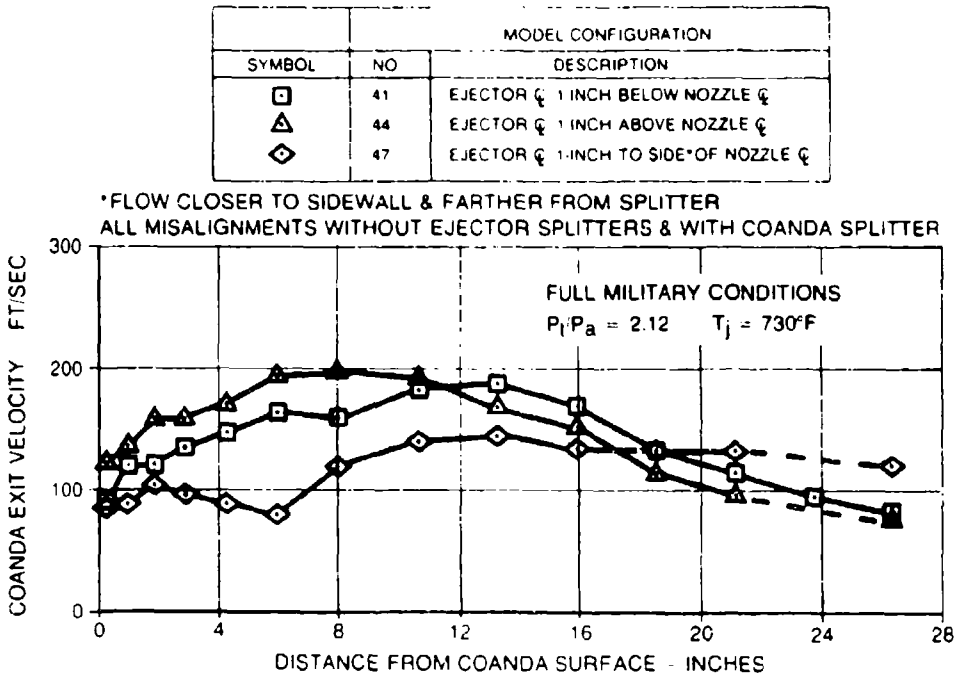

Figure 47. Coanda exit velocity profiles – initial twin engine test – with misalignment – full military power.

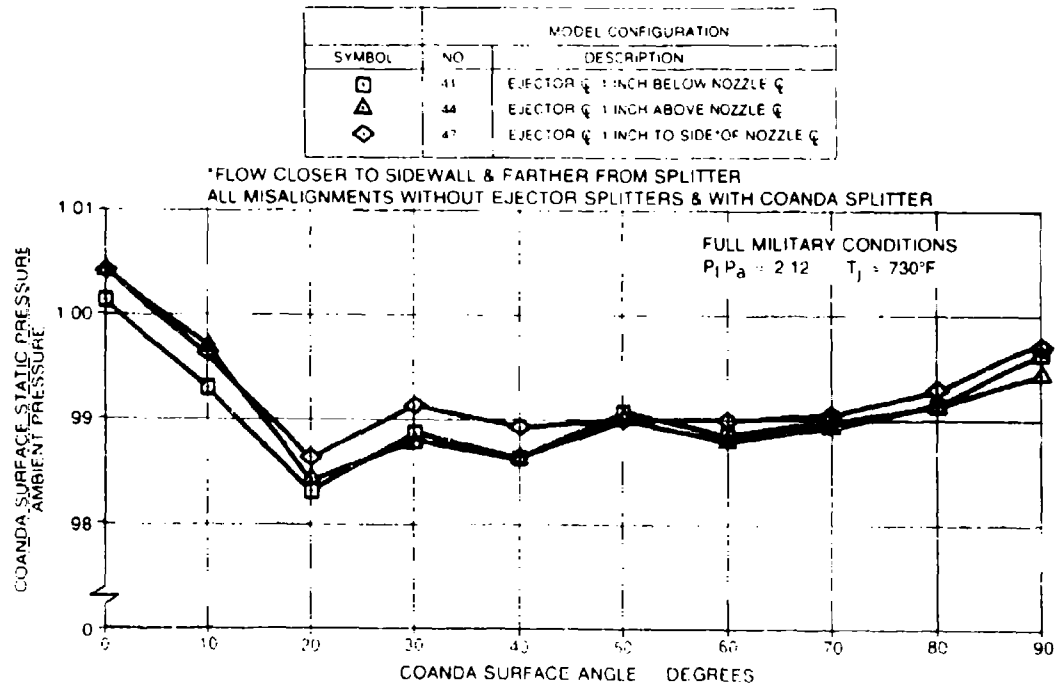

Figure 48. Coanda surface static pressures – initial twin engine test – with misalignment – full military power.

SYMBOL	MODEL CONFIGURATION NO	DESCRIPTION
○	32	NO EJECTOR SPLITTERS - NO COANDA SPLITTER
□	36	ALL EJECTOR SPLITTERS - NO COANDA SPLITTER
△	40	ALL EJECTOR SPLITTERS - WITH COANDA SPLITTER
◇	40S-1	NO EJECTOR SPLITTERS - WITH COANDA SPLITTER

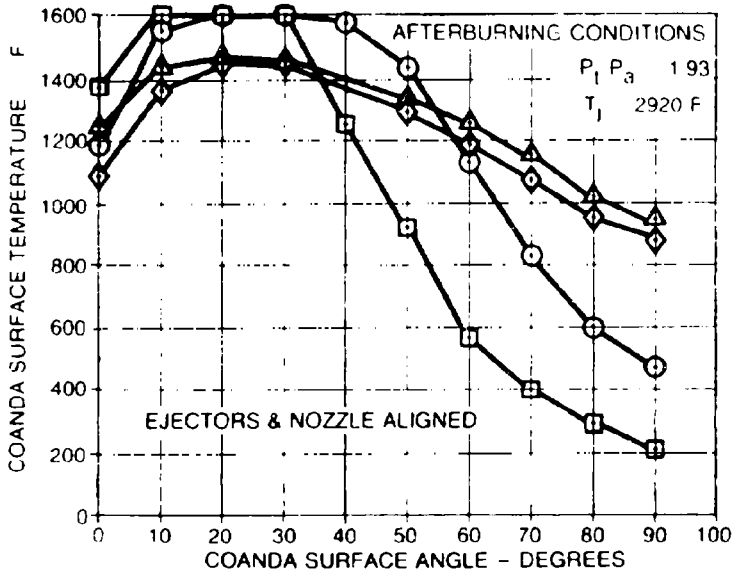

Figure 49. Coanda surface temperatures – initial twin engine model test – splitter variations – afterburning power.

SYMBOL	MODEL CONFIGURATION NO	DESCRIPTION
○	40S-1	EJECTOR & NOZZLE CENTERLINES ALIGNED
□	43	EJECTOR ℄ 1 INCH BELOW NOZZLE ℄
△	46	EJECTOR ℄ 1 INCH ABOVE NOZZLE ℄
◇	49	EJECTOR ℄ 1 INCH TO SIDE* OF NOZZLE ℄

*FLOW CLOSER TO SIDEWALL & FARTHER FROM SPLITTER ALL MISALIGNMENTS WITHOUT EJECTOR SPLITTERS & WITH COANDA SPLITTER

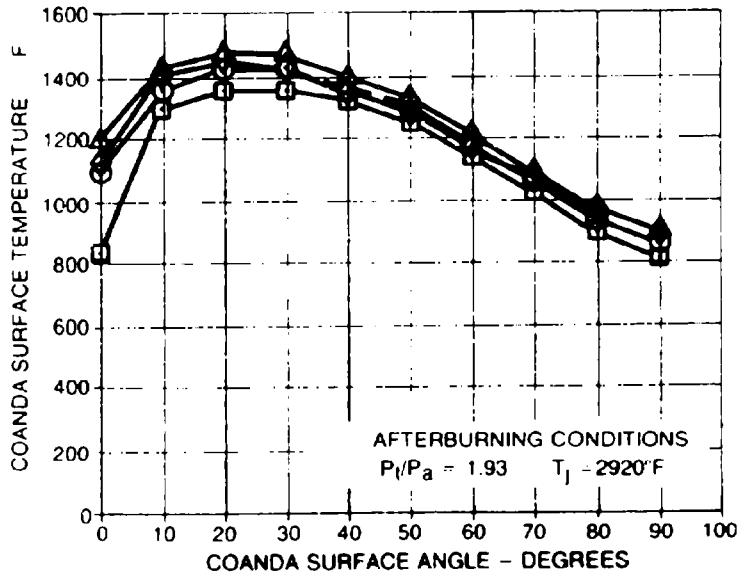

Figure 50. Coanda surface temperatures – initial twin engine model test – with misalignment – afterburning power.

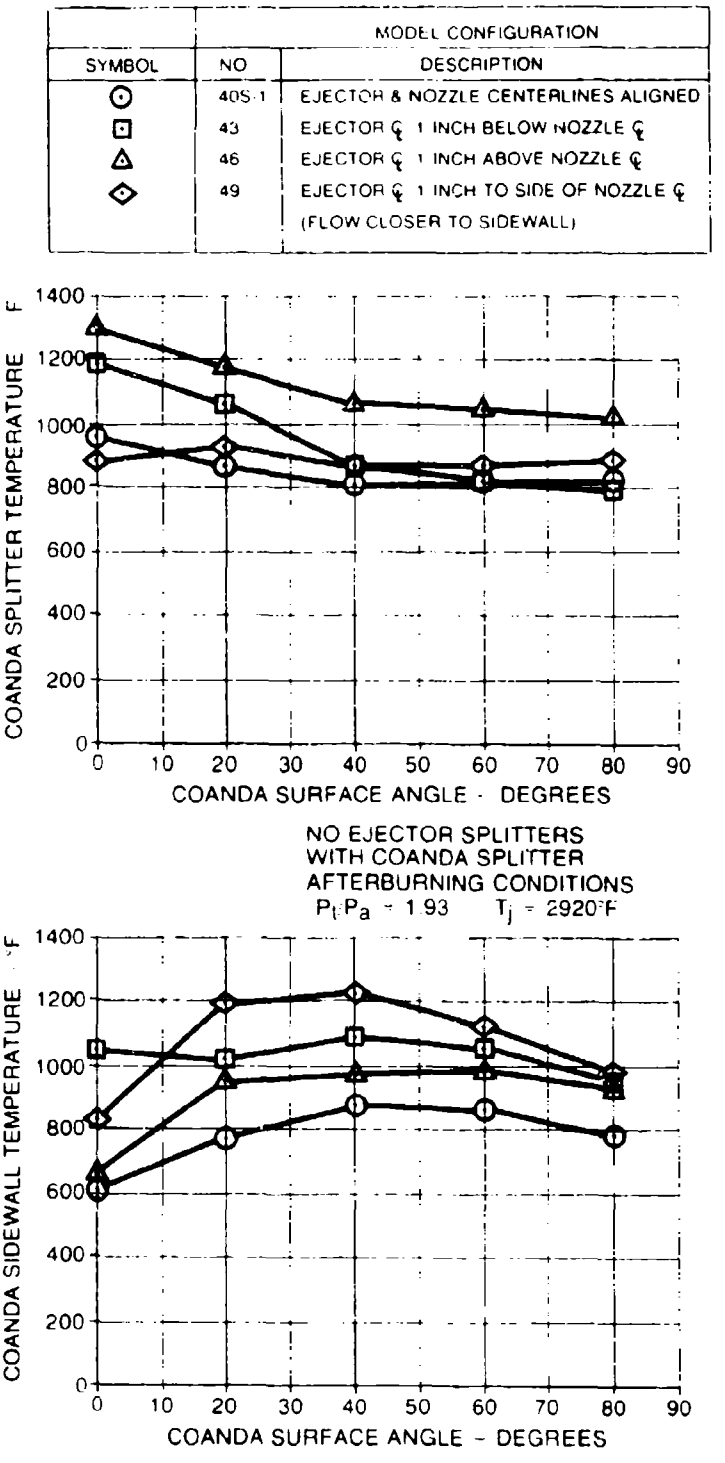

Figure 51. Coanda splitter and sidewall temperatures – initial twin engine model test – with misalignments – afterburning power.

SYMBOL	NO	DESCRIPTION
○ TOP ○ SIDE	32	NO EJECTOR SPLITTERS NO COANDA SPLITTERS
□ TOP □ SIDE	40S-1	NO EJECTOR SPLITTERS WITH COANDA SPLITTER
△ TOP △ SIDE ◇ SPLITTER	40	ALL EJECTOR SPLITTERS WITH COANDA SPLITTER

MODEL CONFIGURATION

EJECTORS AND NOZZLE ALIGNED

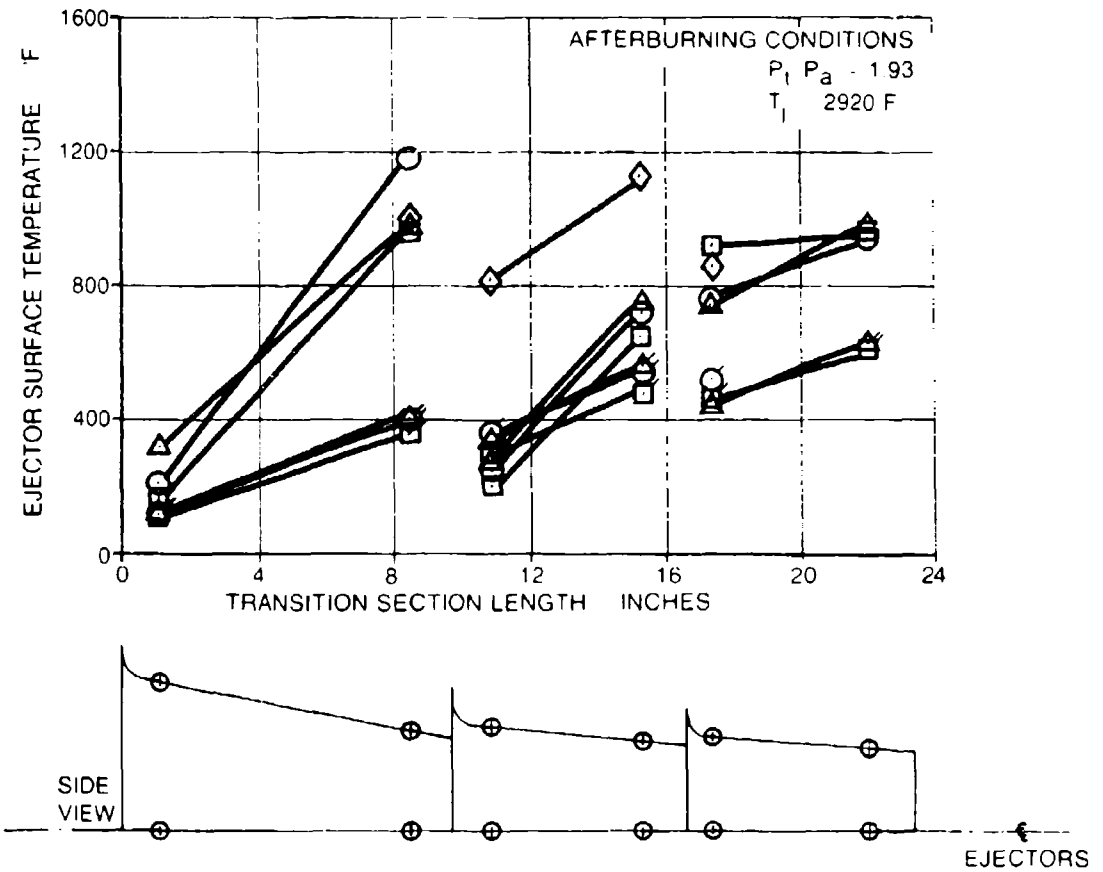

Figure 52. Ejector surface temperatures – initial twin engine model test splitter variations – afterburning power.

SYMBOL	MODEL CONFIGURATION NO	DESCRIPTION
⊙ TOP ⊙ SIDE	40S-1	EJECTOR & NOZZLE CENTERLINES ALIGNED
□ TOP □ SIDE	43	EJECTOR ℄ 1-INCH BELOW NOZZLE ℄
△ TOP △ SIDE	46	EJECTOR ℄ 1-INCH ABOVE NOZZLE ℄
◇ TOP ◇ SIDE	49	EJECTOR ℄ 1-INCH TO SIDE OF NOZZLE ℄ (FLOW CLOSER TO SIDEWALL)

ALL MISALIGNMENTS WITHOUT EJECTOR SPLITTERS
& WITH COANDA SPLITTER

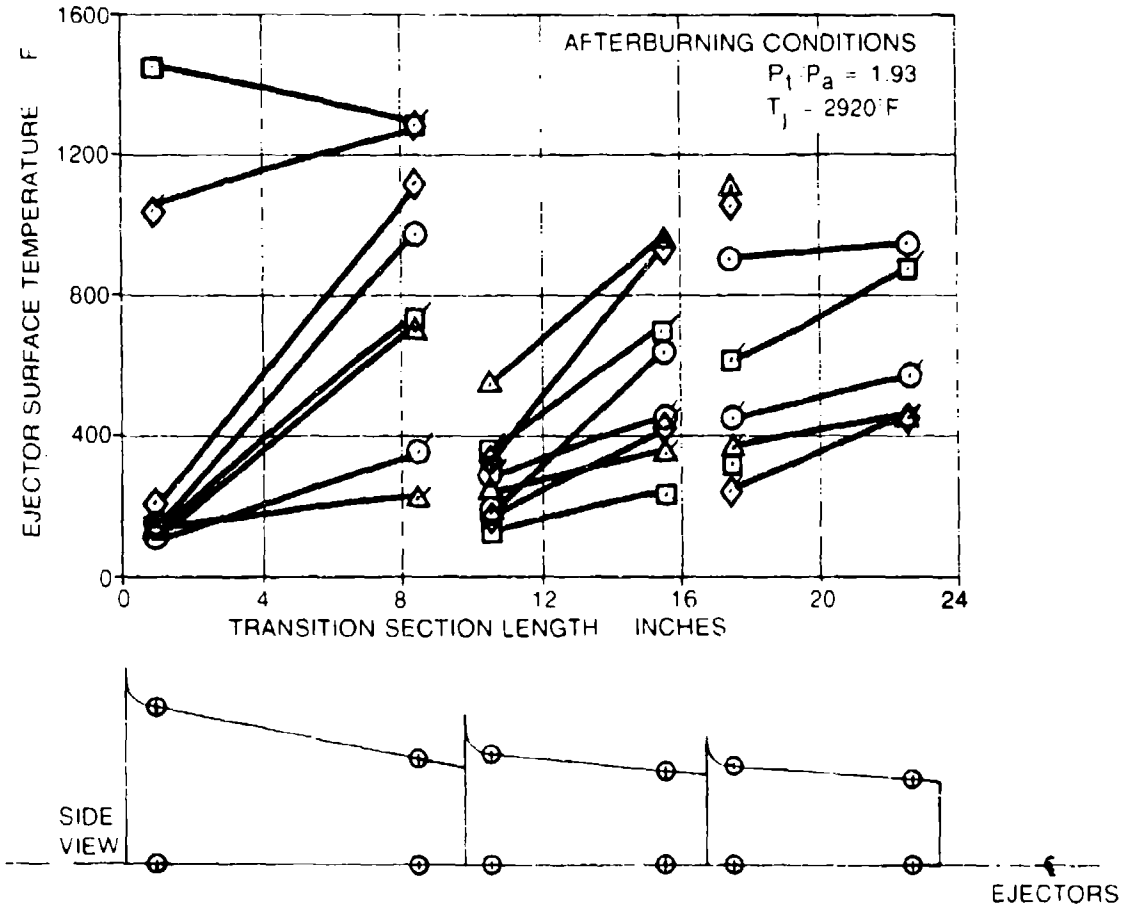

Figure 53. Ejector surface temperatures – initial twin engine model test – with misalignment – afterburning power.

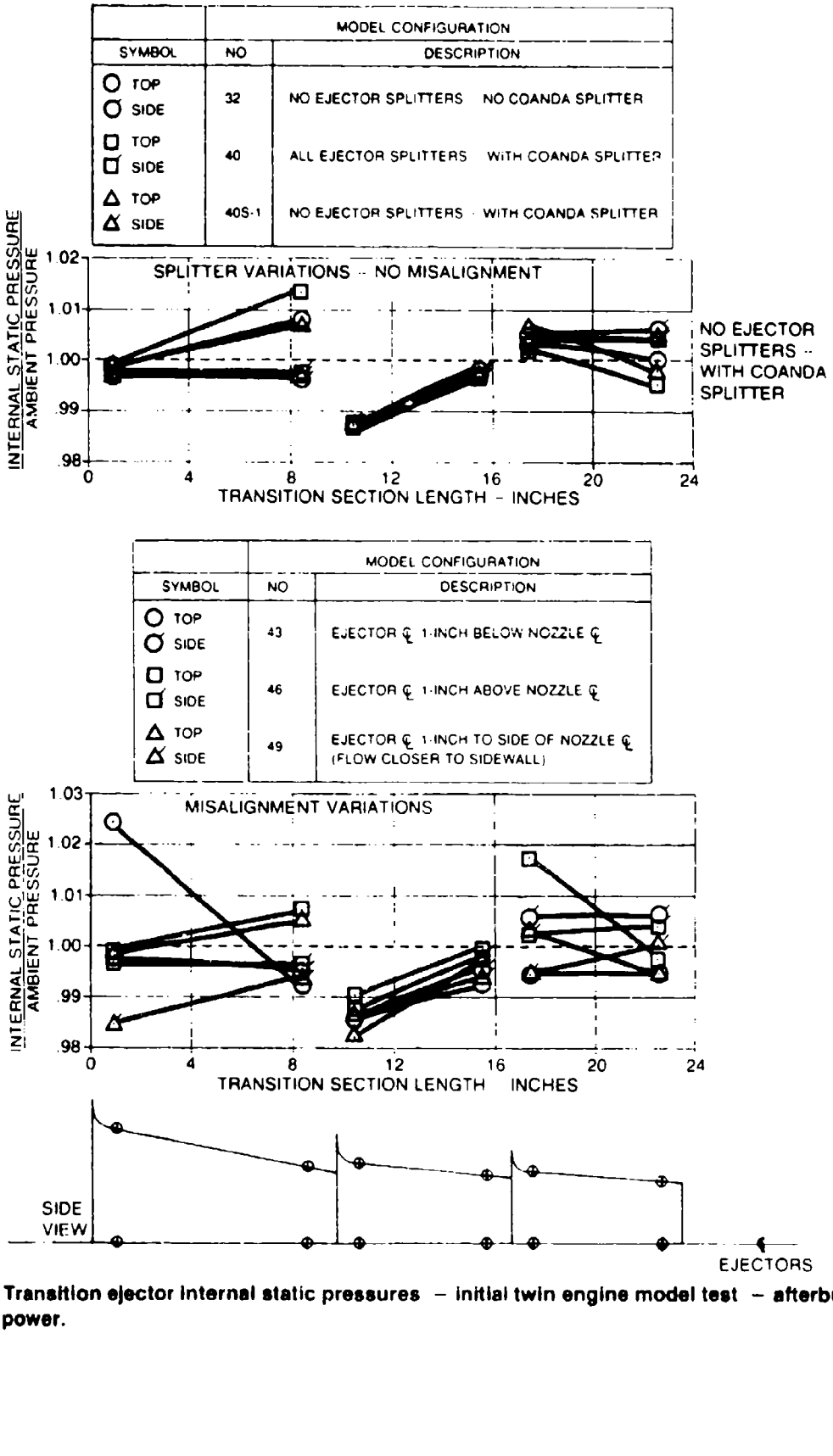

Figure 54. Transition ejector internal static pressures – initial twin engine model test – afterburning power.

6.0 SINGLE ENGINE TAILPIPE/SUPPRESSOR TRANSLATION TEST

6.1 Objectives

The purpose of the fourth test series was to determine the effect on flow attachment and system cooling of varying the distance between the engine exhaust nozzle and the suppressor inlet. Engine installation such as on the F-4 aircraft where the engine exhaust is a large distance forward of the aft stabilizer necessitated this study. In such cases, the suppressor inlet cannot be extended near the engine exhaust plane because of possible damage to the aircraft during positioning or during runup movement. This is because of very little clearance between the aircraft aft of the engine exhaust and the suppressor extension. Similarly, in the case of an engine test cell installation, the distance from the engine tailpipe to the ejector inlet varies because the location of the engine thrust trailer in the cell is fixed and the various engines differ in length and in their fore and aft positioning on the thrust trailer.

6.2 Model Description and Test Apparatus

The Acoustic Arena facility and its data acquisition system described in Section 2.0 was used for the single engine translation test described in this section.

The same one-sixth scale model hardware used in the first misalignment test (Paragraph 3.2) was used for this translation test even though the first test results (Paragraph 3.4) indicated the transition ejector set from that model to be inefficient for cooling. This was done to eliminate the cost of fabricating a new model since relative cooling performance could be determined. Dimensional drawings of the ejectors and Coanda surface are shown on Figure 55. The first ejector has an inlet area of 63.6 in^2 and an exit area of 49.5 in^2 which results in an exit area ratio (ejector exit area/primary nozzle area) of 1.65, based on the afterburning nozzle area. The second ejector has an inlet area of 54.7 in^2, an exit area of 52.5 in^2 which is an exit area ratio of 1.75. The third ejector has an inlet area of 57.6 in^2, an exit area of 55.5 in^2, and exit area ratio of 1.85. The primary nozzles used (not shown) are 4.31 inches and 6.18 inches in diameter for military rated thrust and afterburning, respectively. The afterburning nozzle is water jacketed to provide cooling. These nozzles simulate the exit area of a TF30-P-12A engine at military rated thrust and afterburning.

A schematic of the model setup with instrumentation is shown on Figure 56. Static pressures are provided at the nozzle lip to measure the pressure changes that may affect engine operating conditions. Static pressure ports are provided on the internal wall of the ejectors to determine the ejector pumping characteristics and along the Coanda surface centerline to measure the extent of the pressure gradient that produces the flow turning. Thermocouples are provided on the ejectors and Coanda surface to measure the metal surface temperatures so that the effects of configuration changes on system cooling may be determined. A total pressure and total temperature rake is provided at the Coanda surface exit to obtain exit flow conditions (Mach number, velocity, etc.) and to determine the extent of flow attachment.

Figure 57 is a photograph of the model setup in the Acoustic Arena Test Facility and Figure 58 is a close-up of the large inlet ejector and exhaust nozzle. The existing Coanda support frame from previous model tests (Reference 3) was used. The ejectors are positioned such that the exit plane of one coincides with the inlet plane of the next. The exhaust nozzle to ejector inlet spacing was varied by moving the model on a track with a roller system provided on the support frame. Vertical misalignments are accomplished by jack screws provided on the model support frame and sideways misalignment by adjustment of the track that positions the support frame.

6.3 Test Plan

Table 6 presents the model configurations that were tested for evaluating the effects of translation distance coupled with misalignments on flow attachment to the deflection (Coanda) surface and on system cooling. Also listed are the data recorded for each configuration. The configuration numbers are listed on all data shown later in this report as an aid in identification. It should be noted in the column of Table 6 that describes the misalignment direction that the model is moved rather than the exhaust nozzle. This was necessary because of the stationary attachment of the

burner and nozzle system to the facility floor. All ambient conditions such as temperature, pressure, relative humidity, wind velocity, etc , were recorded along with the data shown in Table 6.

The flow conditions listed in Table 6 are simulated TF30-P-12A engine conditions and were defined earlier in Table 2 (Paragraph 3.3).

The configurations consisted of nozzle to ejector translation distances of 2, 6, 12, and 18 inches at military power and 2, 6, and 12 inches at afterburning. The maximum distance the nozzle was translated away from the ejector inlet was limited only by the first ejector inlet size. The afterburning nozzle is larger thus accounting for the lesser translation distance at afterburning. Tufts were placed on the ejector lip to indicate whether the flow was being captured by the ejector inlet or if some was "spilling" around the ejector lip. All configurations shown in the table indicated the entire exhaust plume was captured by the ejector inlet.

6.4 Test Results and Conclusions

6.4 1 Coanda Flow Turning Data

Figure 59 presents a summary of Coanda exit velocity profiles with the nozzle and transition ejectors aligned and at military rated thrust (MRT) for translation distances of 2, 6, 12, and 18 inches (model scale) which is equivalent to 1, 3, 6, and 9 feet full scale. These data indicate that at MRT the flow attachment actually improves with increasing nozzle to ejector inlet distance. This is probably the result of more complete mixing thus a more uniform flow at the Coanda surface entrance. The corresponding Coanda surface static pressure distributions are presented on Figure 60. The pressure gradient shown by these data indicate a very good Coanda surface flow attachment. Data at the 90° deflected position confirm the velocity profile data; i.e., the two-inch translation data shows the least pressure gradient (pressure gradient is the difference between unity and the normalized Coanda surface static pressure) and therefore not as strong flow attachment

Figures 61, 63, 65, and 67 present the Coanda exit flow velocity profiles for the misaligned (vertically and horizontally) configuration at military rated thrust and translation distances of 2, 6, 12, and 18 inches (model scale), respectively. Figures 62, 64, 66, and 68 present the corresponding Coanda surface static pressure distributions for the misaligned configurations at translation distances of 2, 6, 12, and 18 inches, respectively. The data for a two-inch translation distance (Figures 61 and 62) indicate an improvement in flow attachment with the nozzle flow misaligned toward the lower surface of the transition ejectors and a slight detriment to attachment with the flow misaligned horizontally to the side. Misalignment toward the upper ejector surface indicated flow attachment similar to the aligned configuration. These results are indicated by the distance from the Coanda surface at which the peak velocity occurs and the relative level of the normalized surface static pressure at the 90° position.

Data for the six-inch translation distance (Figures 63 and 64) at MRT conditions indicate an improvement in flow attachment for the aligned configuration as was seen previously on Figure 59. The relative variation in flow attachments between the different misalignments remained similar to the two-inch translation, thus the only real improvement was with the aligned configuration.

The 12-inch translation distance flow attachment data at MRT (Figures 65 and 66) indicate an improvement in the attachment for the configurations misaligned to the side and toward the lower ejector surface. This improvement was to the extent that all configurations, aligned and misaligned, produced nearly equal Coanda exit velocity profiles and 90° position Coanda surface static pressures.

Coanda exit velocity profiles and Coanda surface pressure data for the 18-inch translation distance at MRT (Figures 67 and 68) indicate virtually no difference in attachment between any misaligned and aligned configurations.

Figure 69 presents Coanda exit velocity profiles at afterburning conditions for translation distances of 2, 6, and 12 inches (model scale) with the nozzle and transition ejectors aligned. These data show no difference in Coanda flow

attachment or mixing due to the variation in translation distance. The translation distance was limited to 12 inches at afterburning power due to the larger nozzle size (at larger distances the ejector inlet would not be large enough to capture the expanding nozzle flow).

Figures 70 and 71 present Coanda exit velocity profile data at afterburning nozzle conditions and translation distances of two and six inches (model scale), respectively, for the misaligned configuration. These data indicate no appreciable change in flow attachment or mixing due to misalignment in any direction at either translation distance.

Figures 72, 73, and 74 present Coanda surface static pressures normalized by ambient pressure for aligned configurations with translation, two-inch translation with misalignment and six-inch translation with misalignment, respectively. These data verify the analysis of the exit velocity data of Figures 69, 70, and 71; i.e., neither translation distance nor misalignment is detrimental to the Coanda flow attachment at afterburning conditions. All configurations run at afterburning flow conditions illustrate excellent flow attachment.

6.4.2 System Cooling Data

The transition ejector set used for this test was the same hardware that was fabricated for the single engine misalignment test (Section 3.0). It was discovered in that test that the ejector design was not correct for sufficient cooling of the Coanda surface due to convergent area progressions of the ejectors and ejector lengths that were too short (see discussion in Paragraph 3.4.2). It was decided to go ahead as previously planned and use these ejectors even though inadequate cooling would be shown. This was done instead of incurring the additional expense of redesign and fabrication of a new set of ejectors because the relative temperature changes caused by any model configuration would be representative of those in a properly designed system. Therefore, the absolute levels of the following data are not as important as the differences produced by model configuration changes.

Coanda surface temperature data at afterburning conditions are presented on Figure 75 for the configurations with nozzle and ejector centerlines aligned and translation distances of 2, 6, and 12 inches. The peak temperature decreased about 50° with translation distances greater than two inches but did not decrease further between 6 and 12-inch translations.

Coanda surface temperatures for the two-inch translation distance and aligned and misaligned configurations are shown on Figure 76. The results with the ejectors moved one inch up so that the nozzle flow is toward the lower surface of the ejectors are virtually the same as with the nozzle and ejectors aligned. However, with the ejectors moved one inch downward, so that the flow is toward the ejector upper surfaces, the Coanda surface temperature is about 300° cooler at the inlet and remains cooler in decreasing amount until the 45° turned position. The surface temperatures are about the same as for the aligned configuration from that position to the Coanda exit. The initial lower temperature for the ejectors moved one inch down configuration may be a continuation of the "ricochet effect" through the ejectors described later in this section. The fact that the model misaligned one inch to the side configuration shows Coanda surface temperatures lower than the aligned configuration at all positions beyond the Coanda inlet may also be related to this effect.

Figure 77 presents the Coanda surface temperatures at the six-inch translation distance for aligned and misaligned configuration at afterburning power conditions. The greater translation distance tends to equalize the peak temperature for all configurations at a value about 50° less than the highest temperature configurations at the closer distance. The same trends that were evident at the two-inch translation distance are seen in six-inch translation data but not nearly as pronounced.

Misalignments at the 12-inch distance did not allow the first ejector inlet to capture the entire flow as was evidenced by the tufts on the inlet lip turning outward on the side closest to the flow. The trends from the two and six-inch translation data indicate that greater distances would show no difference in Coanda surface temperatures due to any misalignment and a slight overall decrease in temperature due to mixing over the increased translation distance (assuming the transition ejectors were enlarged enough to capture the flow).

Transition ejector internal static pressures for afterburning conditions and translation distances of 2, 6, and 12 inches with no misalignment are shown on Figure 78. The corresponding ejector surface temperature data along the side and top surfaces are shown on Figure 79. The most important aspect of these data is that the greater translation distances allows the jet to expand and more nearly fill the ejectors, which reduces the ejector entrainment (especially the first ejector). This is evidenced by the higher inlet static pressures recorded with increased translation distance (Figure 78) and the corresponding higher ejector temperatures with increased translation distance (Figure 79). This indicates that the ejector area should be sized for the entire entering flow, including entrainment, rather than just the primary flow rate. The higher surface temperatures on the side of the second and third ejector inlets, when compared to the top temperatures, were caused by the smaller gap on the sides of the ejector inlets and, thus, a thinner film of cooling air. The ejectors were designed with the greater amount of the area increase between ejectors at the upper and lower surfaces because the transitioning to rectangular flow requires more cooling of those surfaces.

Figures 80 and 81 present the ejector internal static pressure data and ejector surface temperature data, respectively, for the two-inch translation distance with aligned and misaligned flow at afterburning conditions. Temperatures were highest on the first ejector and lowest on the second and third ejectors for configuration with the flow misaligned toward the upper ejector surface. The lower temperatures on the top of the second and third ejector were probably due to the flow impinging more directly on the upper surface of the first ejector and then ricocheting off and impinging on the lower surface of the second and third ejectors. The peak temperature on the first ejector was increased by about 250° due to misalignment. The configuration with the flow misaligned toward the lower surface of the ejectors has the lowest temperature at the top surface of the first ejector because the flow impinges more directly on the lower surface. The first ejector top surface temperatures for the sideways misaligned configuration were about the same as for the model aligned; however, the side temperature levels were about the same as those recorded at the top with the misalignment toward the upper surface.

Figures 82 and 83 present the ejector internal static pressure data and ejector surface temperature data, respectively, for the six-inch translation distance with aligned and misaligned flow configurations at afterburning conditions. The results are qualitatively the same as for the two-inch translation distance. The peak temperatures are within data repeatability of the values for two-inch translation. The "ricochet" effect is still evident but seems to be less pronounced. This is shown by the temperature measurements of the second and third ejector for the various configurations approaching more equal values. Again, this is caused by a more complete filling of the ejectors with expanding primary flow than is possible at the lower translation distance.

6.4.3 Conclusions

The following conclusions may be made from the results of the single engine tailpipe suppressor translation model test:

- The Coanda suppressor system will operate at the nozzle/ejector inlet translation distance required for the F-4 aircraft as long as the transition ejectors are sized large enough to handle the flow.

- There are no detrimental effects on flow attachment or cooling due to increasing the distance between the nozzle exit and the suppressor (i.e., transition ejector) inlet. On the contrary, the flow attachment appears to be improved with greater translation distances, probably because the jet spreading and mixing which occurs prior to entering the suppressor provides a more uniform flow at the ejector/transition exit.

- The effect of offset misalignments of nozzle and ejector centerlines on Coanda flow attachment was reduced by increasing translation distance (i.e., flow attachment for misaligned configuration was nearly the same as for the aligned configuration at the greater translation distances). Again, this is because the spreading jet "fills" the ejector and provides a more uniform exit flow.

- The ejector areas (and first ejector inlet) have to be increased if the translation distance is too great because the exhaust spreads and entrains more secondary air (prior to the ejector inlet) than the ejector is capable of pumping which would result in back flow

TABLE 6. SINGLE ENGINE TAILPIPE TO SUPPRESSOR TRANSLATION TEST CONFIGURATIONS

NOTE: ALL DIMENSIONS IN INCHES

CONFIGURATION NUMBER	PRIMARY		NOZZLE/EJECTOR TRANSLATION	NOZZLE/EJECTOR MISALIGNMENT	DATA		
	NOZZLE DIAMETER	FLOW CONDITION			SURFACE P_s & T_m	EXIT P_t & T_t	TEST RUN NUMBER
50	4.31	FULL MILITARY	2	NONE	X	X	21
51	4.31	FULL MILITARY	2	MODEL 1" UP	X	X	22
52	4.31	FULL MILITARY	2	MODEL 1" DOWN	X	X	23
53	4.31	FULL MILITARY	2	MODEL 1" TO SIDE	X	X	33
54	4.31	FULL MILITARY	6	NONE	X	X	26
55	4.31	FULL MILITARY	6	MODEL 1" UP	X	X	25
56	4.31	FULL MILITARY	6	MODEL 1" DOWN	X	X	24
57	4.31	FULL MILITARY	6	MODEL 1" TO SIDE	X	X	34
58	4.31	FULL MILITARY	12	NONE	X	X	27
59	4.31	FULL MILITARY	12	MODEL 1" UP	X	X	28
60	4.31	FULL MILITARY	12	MODEL 1" DOWN	X	X	29
61	4.31	FULL MILITARY	12	MODEL 1" TO SIDE	X	X	35
62	4.31	FULL MILITARY	18	NONE	X	X	30
72	4.31	FULL MILITARY	18	MODEL 1" TO SIDE	X	X	36
73	4.31	FULL MILITARY	18	MODEL 1" UP	X	X	31
74	4.31	FULL MILITARY	18	MODEL 1" DOWN	X	X	32
63	6.18	AFTERBURNING	2	NONE	X	X	53
64	6.18	AFTERBURNING	2	MODEL 1" UP	X	X	54
65	6.18	AFTERBURNING	2	MODEL 1" DOWN	X	X	52
66	6.18	AFTERBURNING	2	MODEL 1" TO SIDE	X	X	46
67	6.18	AFTERBURNING	6	NONE	X	X	49
68	6.18	AFTERBURNING	6	MODEL 1" UP	X	X	50
69	6.18	AFTERBURNING	6	MODEL 1" DOWN	X	X	51
70	6.18	AFTERBURNING	6	MODEL 1" TO SIDE	X	X	47
71	6.18	AFTERBURNING	12	NONE	X	X	48

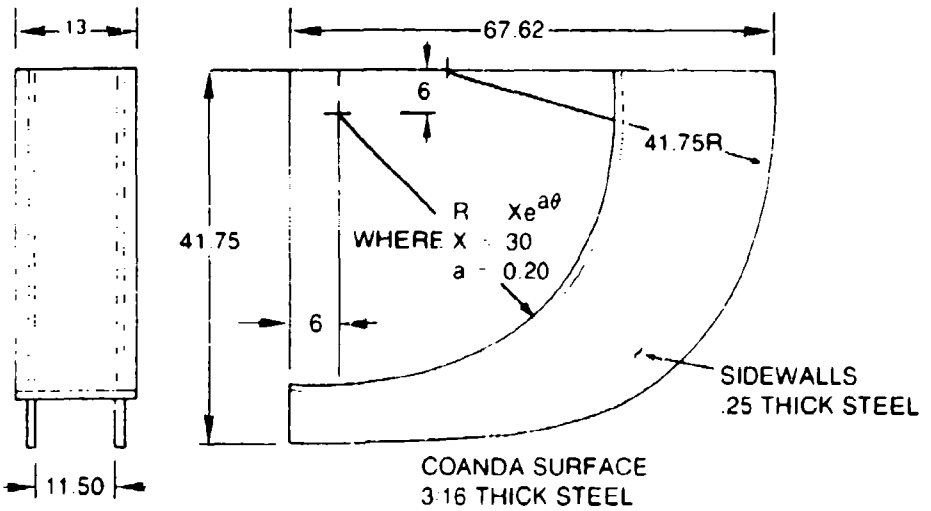

30-INCH RADIUS COANDA SURFACE

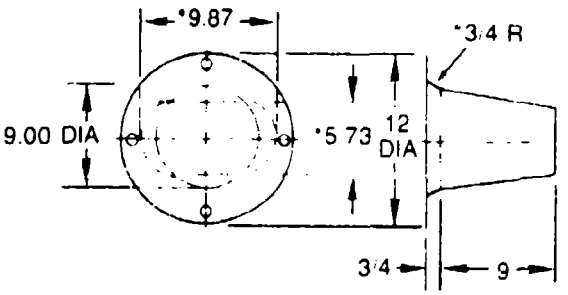

1ST EJECTOR
A.R. = 1.65 (49.5 IN.^{2} EXIT AREA)
MAT'L — .090 INCONEL

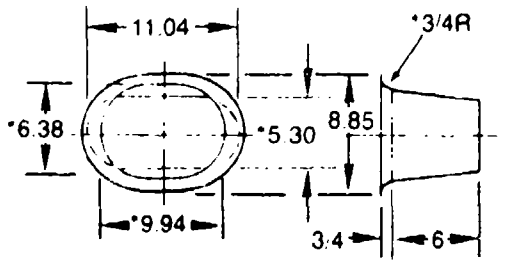

2ND EJECTOR
A.R. = 1.75 (52.5 IN.^{2} EXIT AREA)
MAT'L — .090 CRES

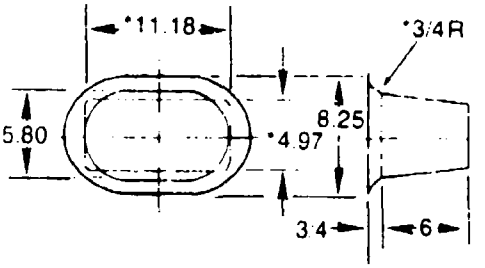

3RD EJECTOR
A.R. = 1.85 (55.5 IN.^{2} EXIT AREA)
MAT'L — .090 CRES

*INSIDE DIMENSIONS
ALL DIMENSIONS IN INCHES

Figure 55. Dimensional drawings of single engine Coanda surface and ejectors.

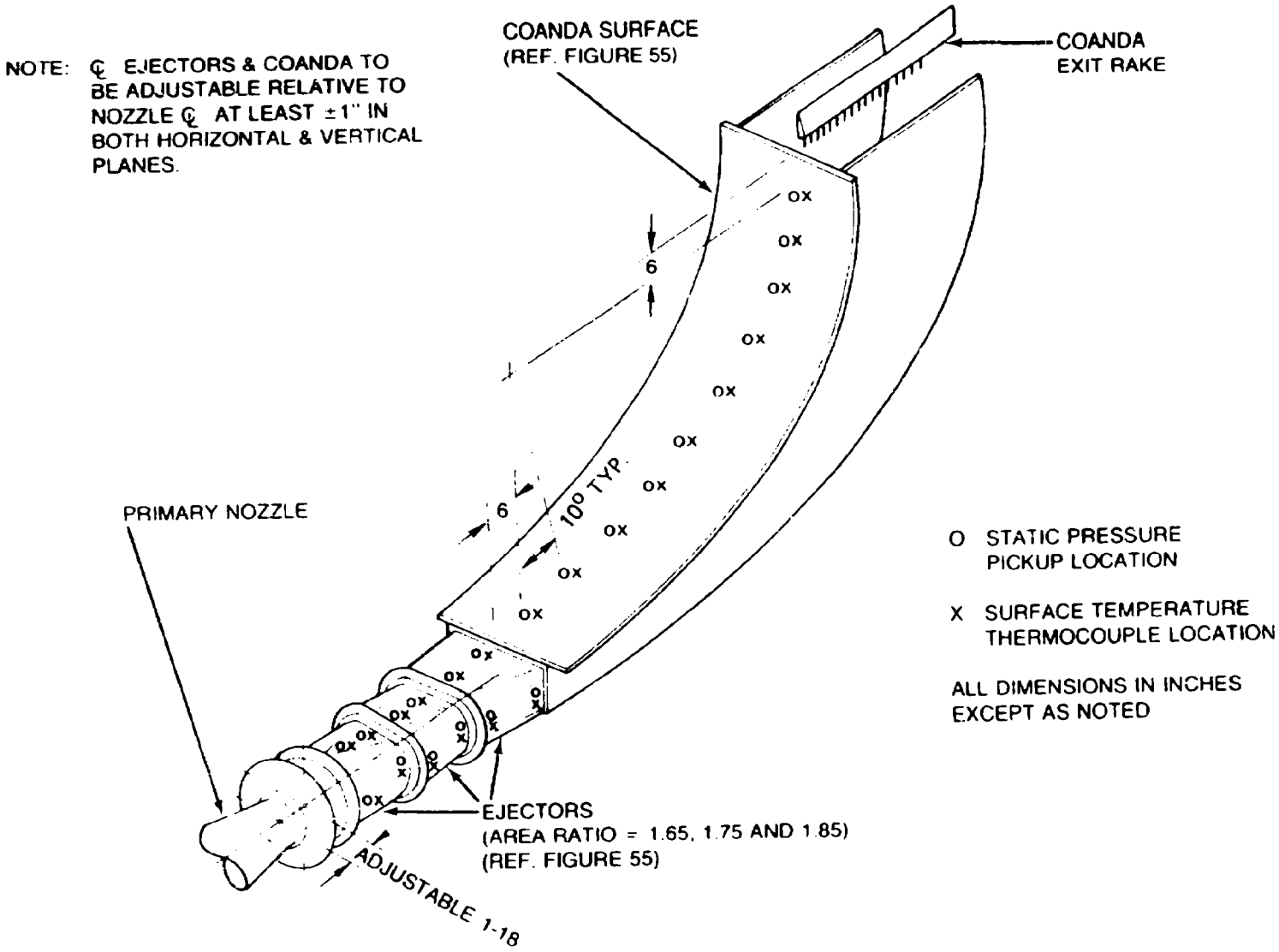

Figure 56. Single engine Coanda and ejector translation test setup and instrumentation.

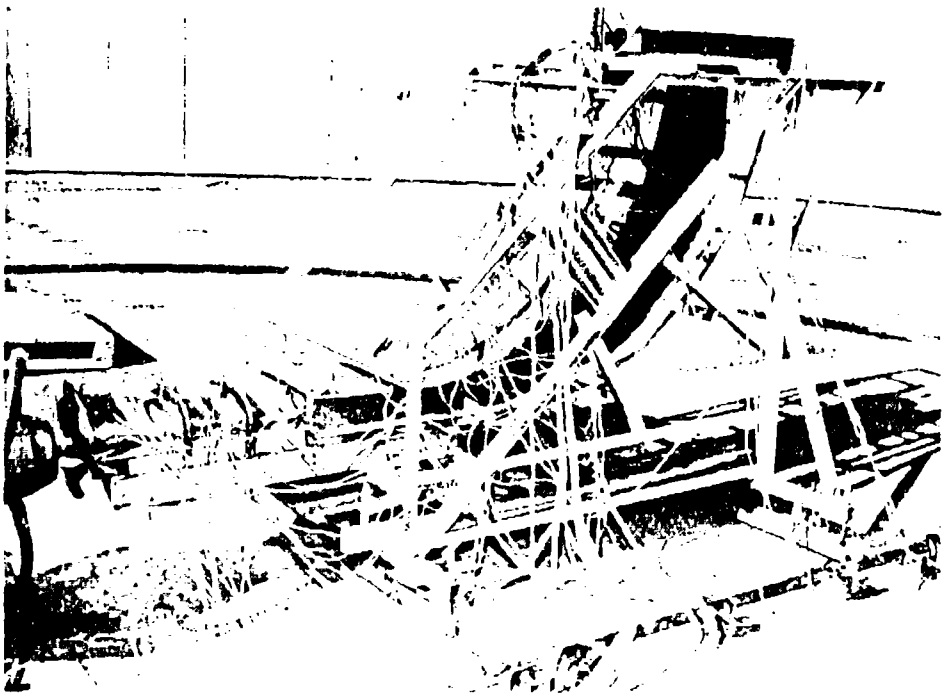

Figure 57. Single engine tailpipe suppressor translation test model setup in Acoustic Arena.

Figure 58. Ejector transition and exhaust nozzle.

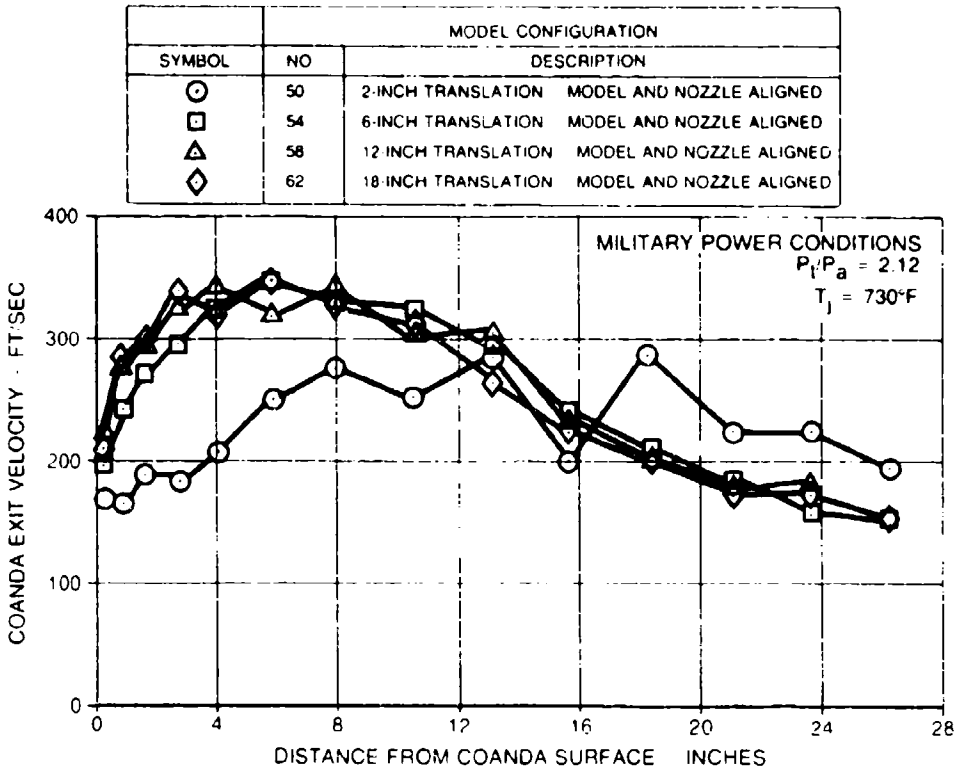

Figure 59. Coanda exit velocity profiles – translation test with model centered (military power).

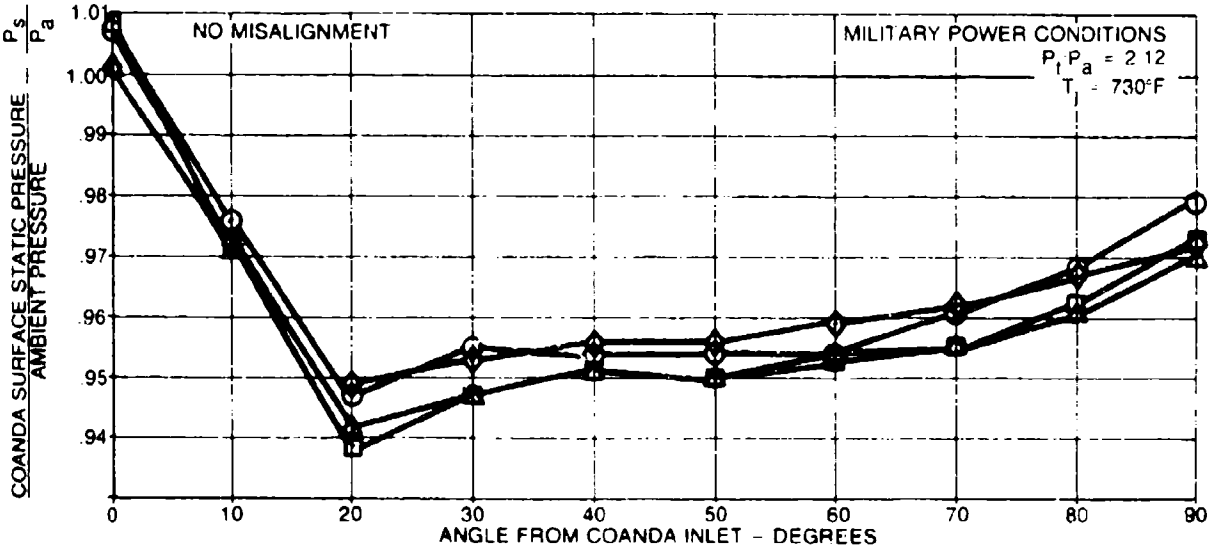

Figure 60. Coanda surface pressure distribution – translation test with model centered (military power).

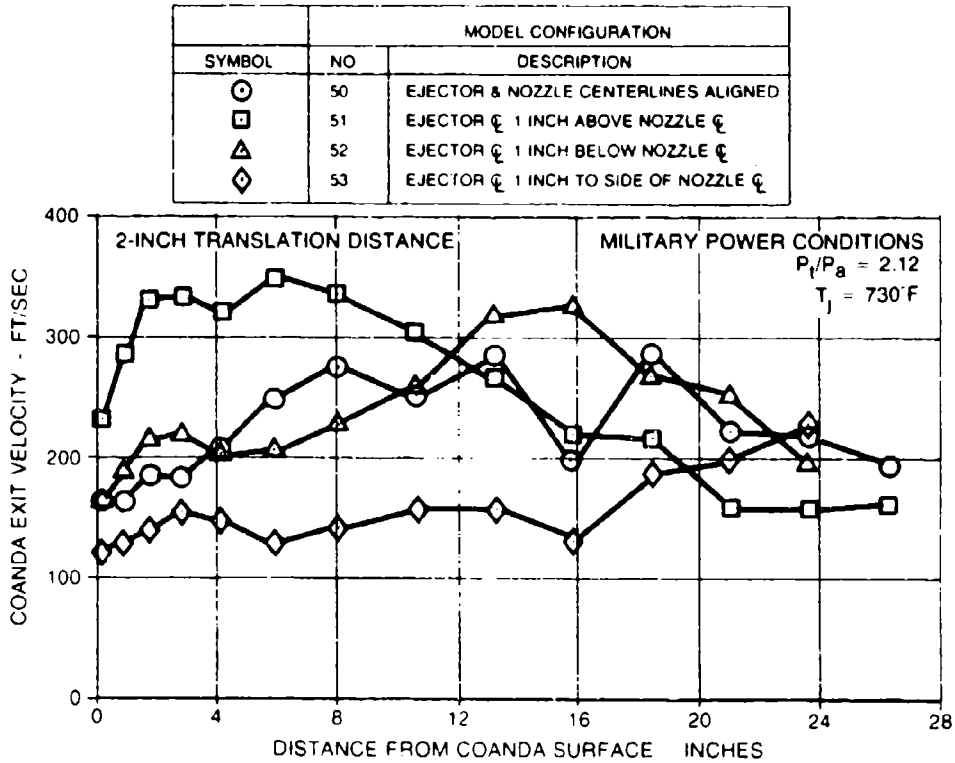

Figure 61. Coanda exit velocity profiles – 2-inch translation with misalignment (military power).

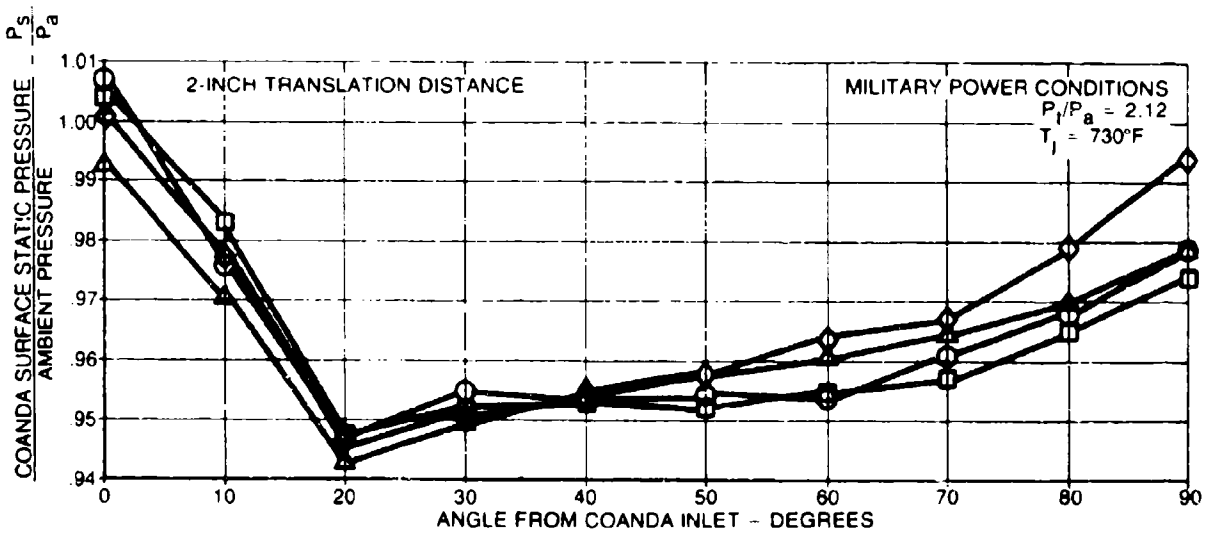

Figure 62. Coanda surface pressure distribution – 2-inch translation with misalignment (military power).

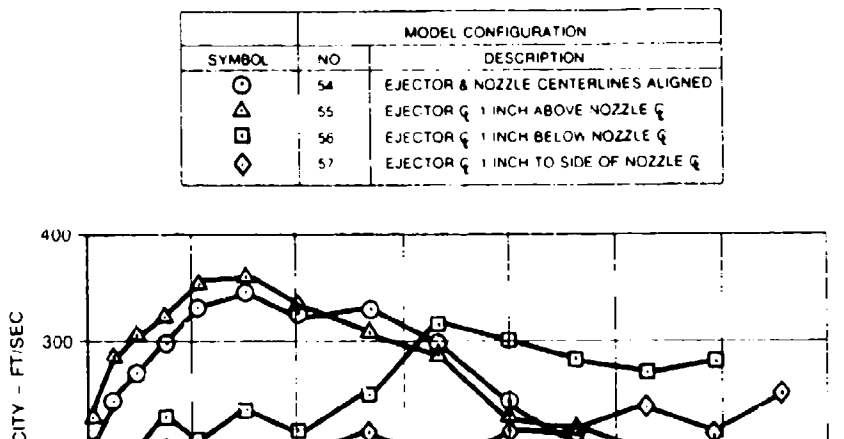

Figure 63. Coanda exit velocity profiles – 6-inch translation with misalignment (military power).

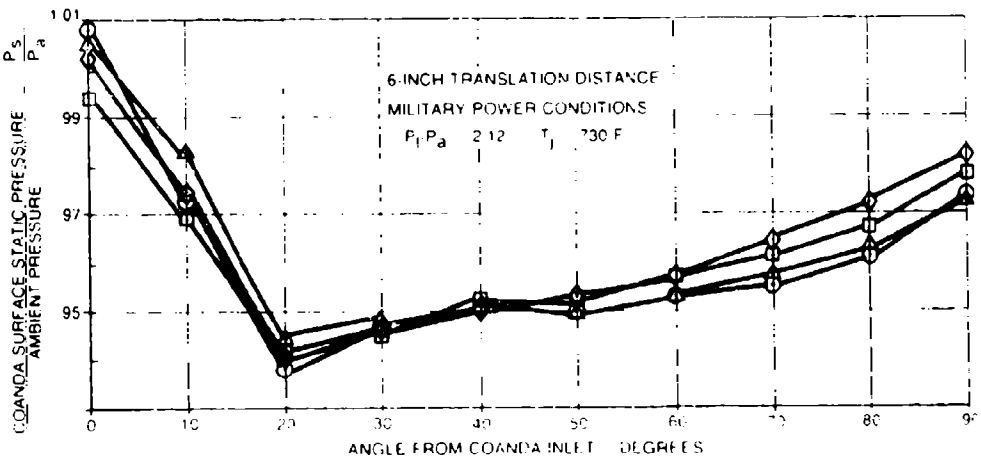

Figure 64. Coanda surface pressure distribution – 6-inch translation with misalignment (military power).

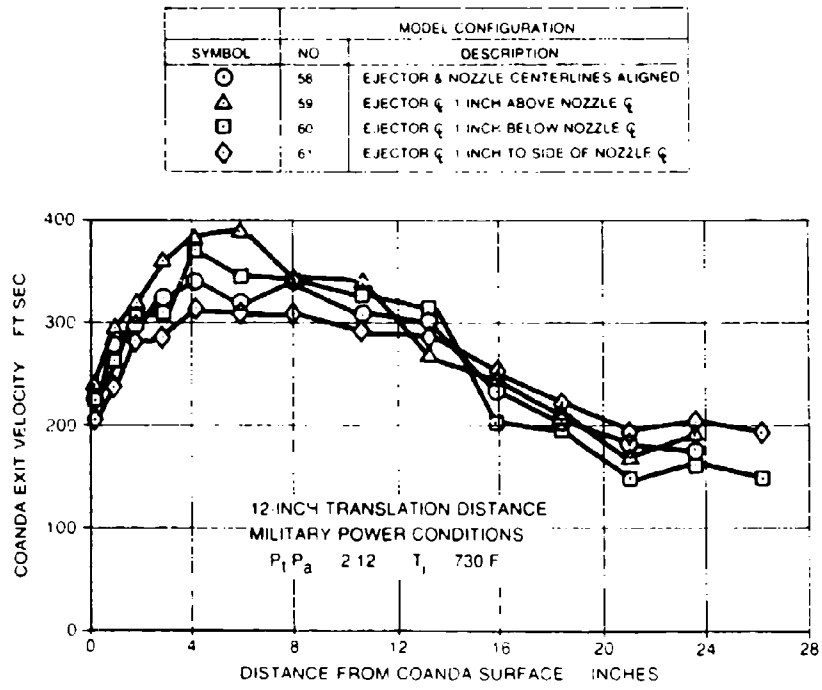

Figure 65. Coanda exit velocity profiles – 12-inch translation with misalignment (military power).

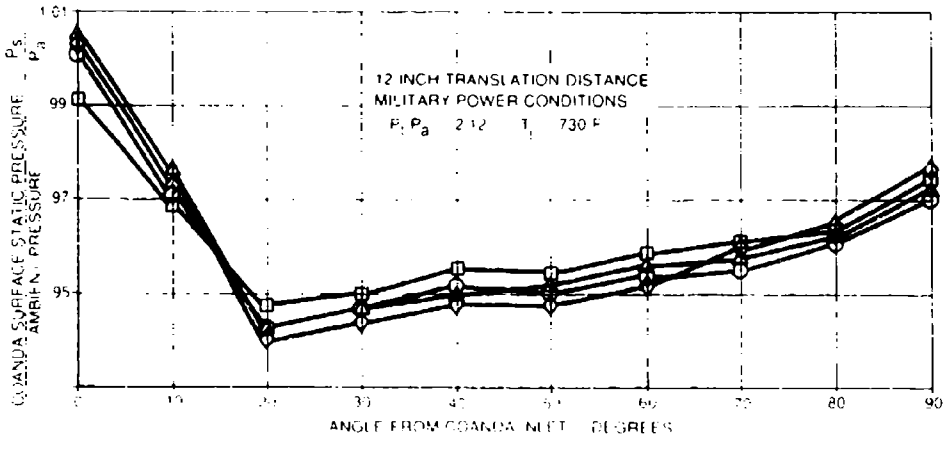

Figure 66. Coanda surface pressure distribution – 12-inch translation with misalignment (military power).

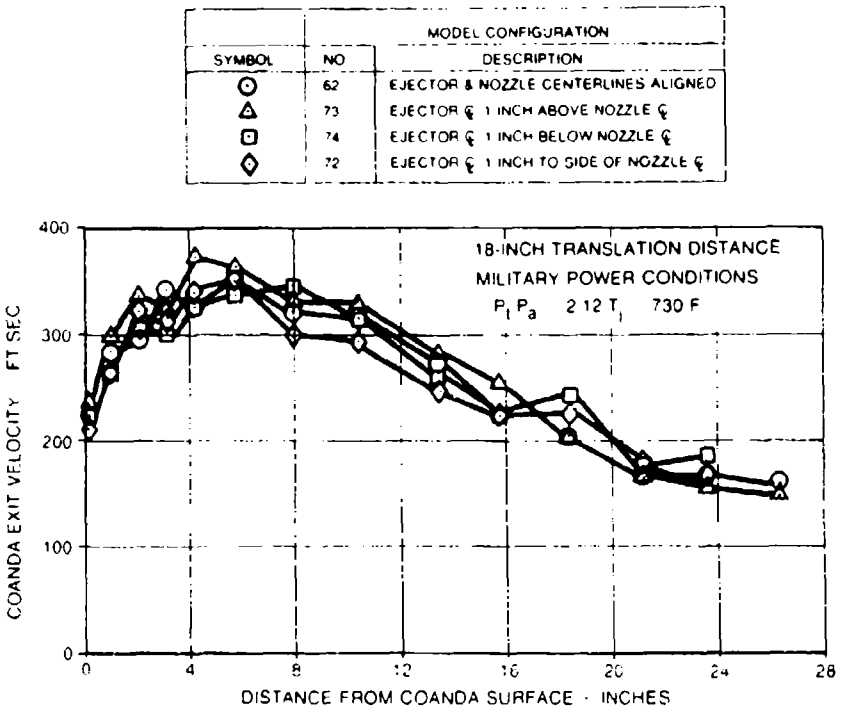

Figure 67. Coanda exit velocity profiles – 18-inch translation with misalignment (military power).

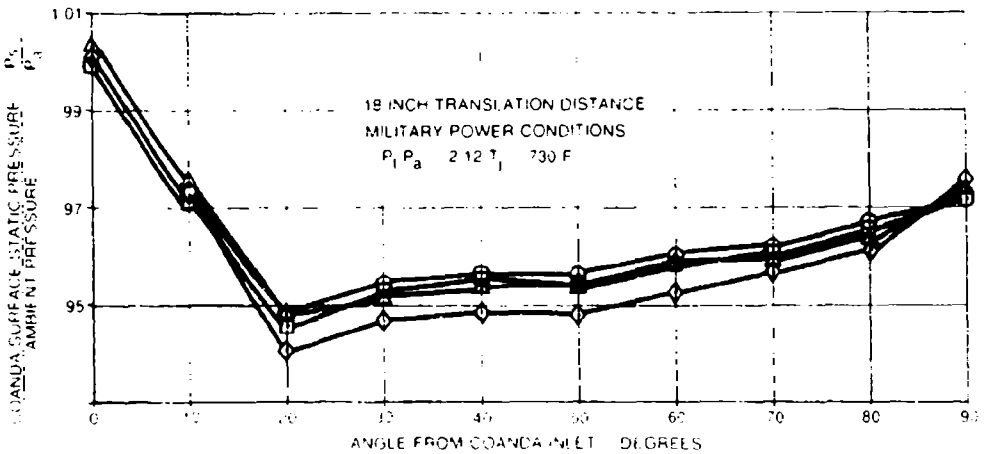

Figure 68. Coanda surface pressure distribution – 18-inch translation with misalignment (military power).

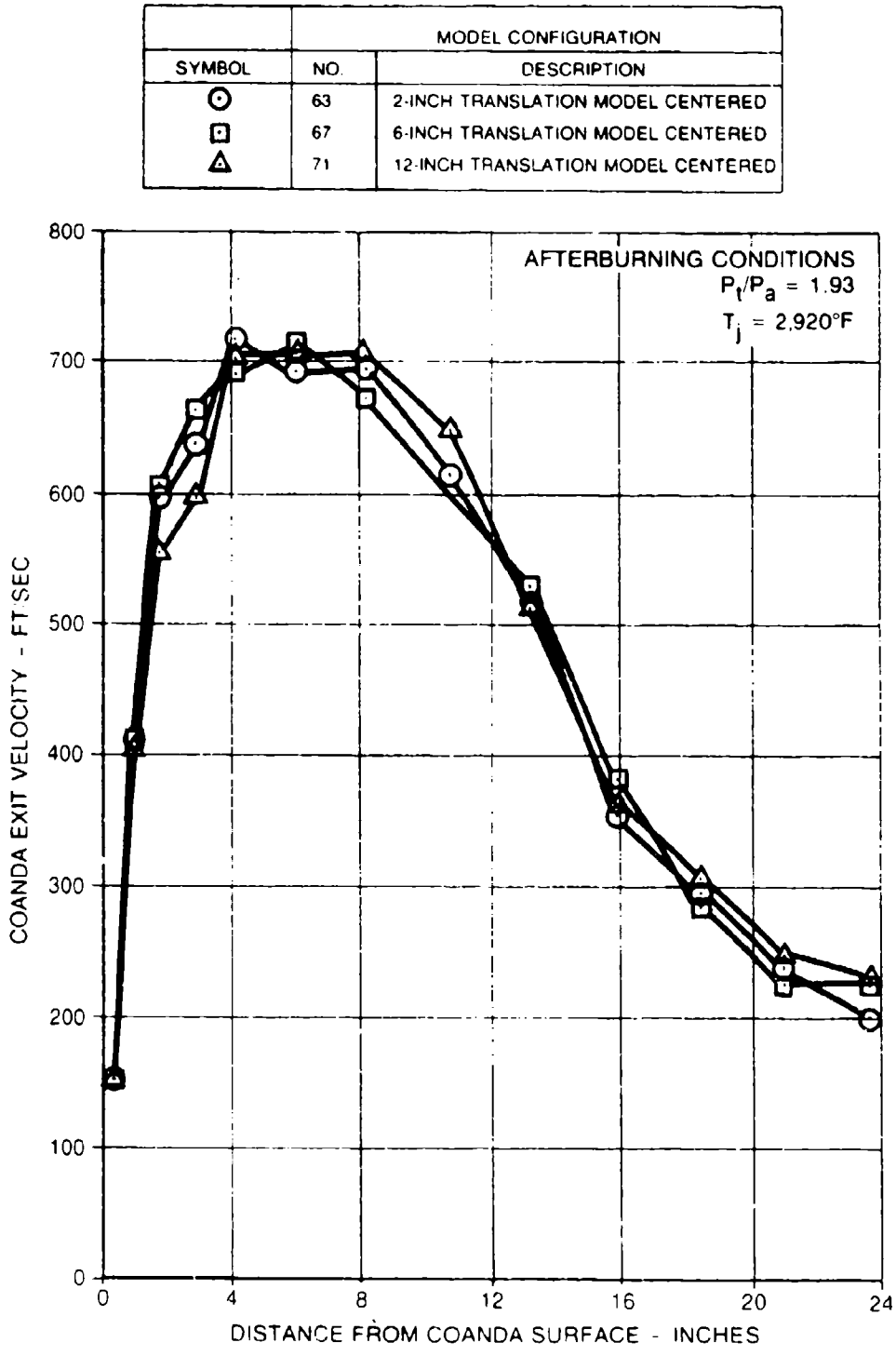

Figure 69. Coanda exit velocity profiles – translation test with model centered (afterburning power).

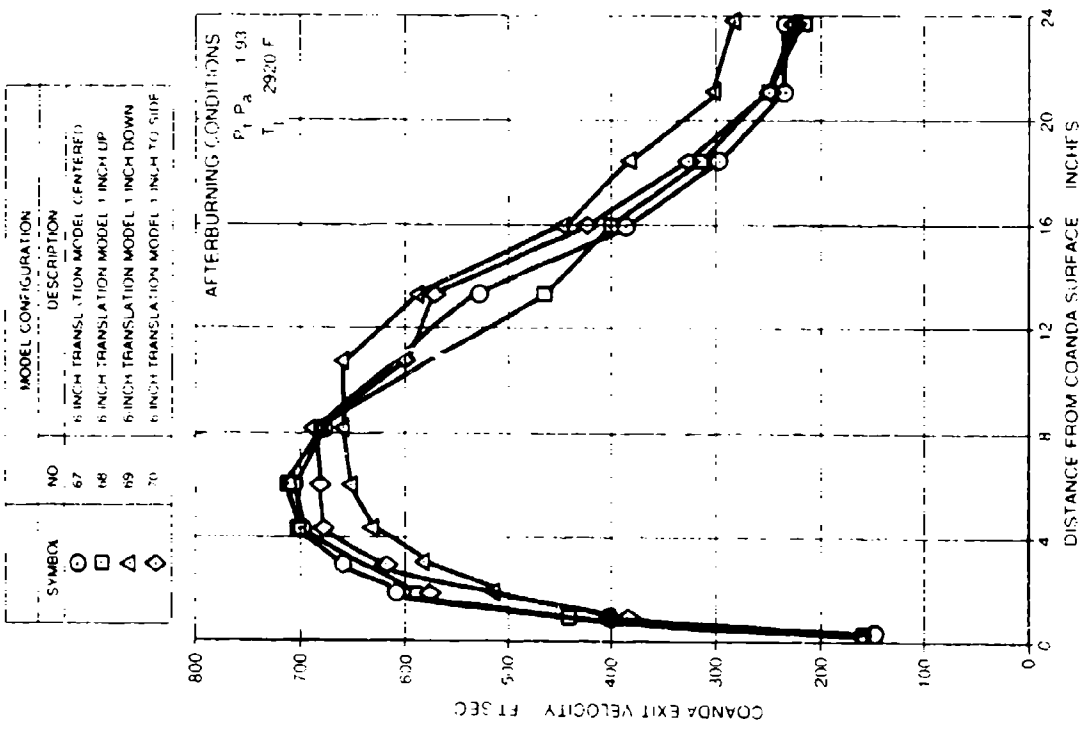

Figure 70. Coanda exit velocity profiles – 2-inch translation test with misalignment (afterburning power).

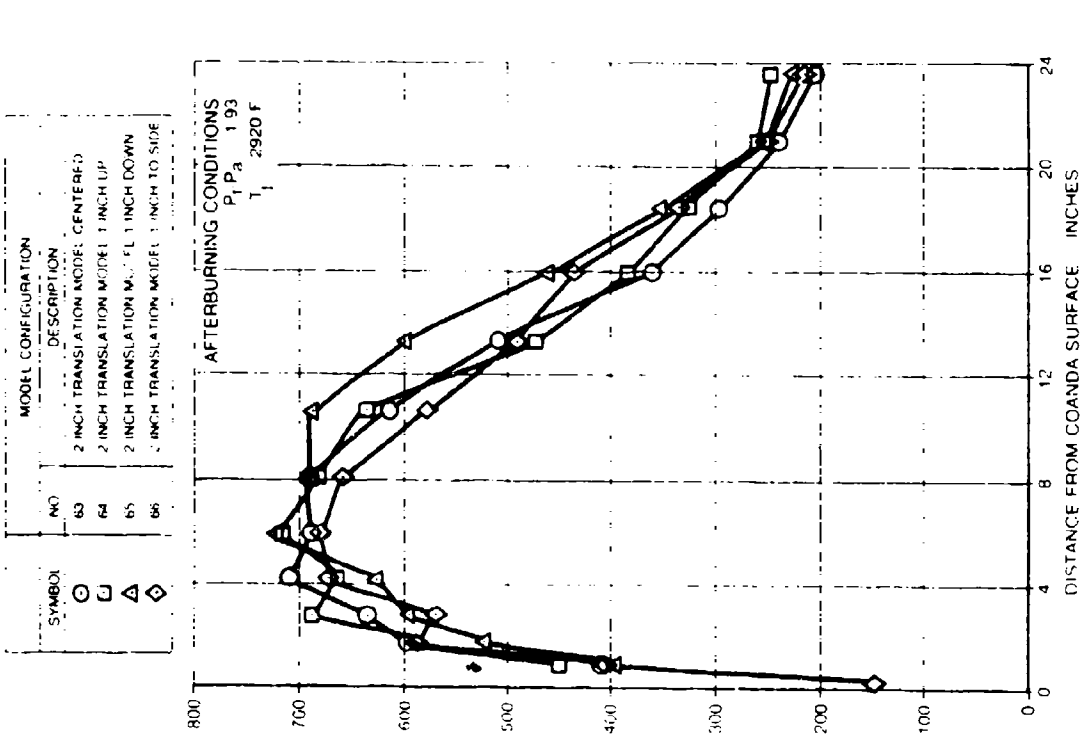

Figure 71. Coanda exit velocity profiles – 6-inch translation test with misalignment (afterburning power).

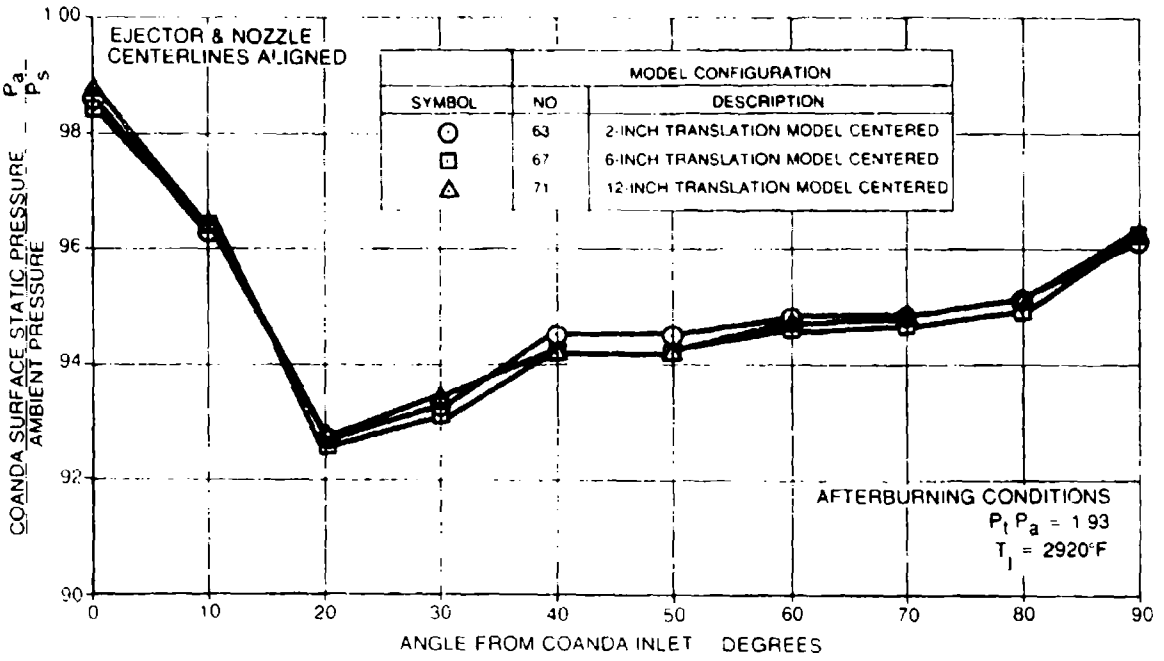

Figure 72. Coanda surface pressure distribution – translation test – model centered (afterburning power).

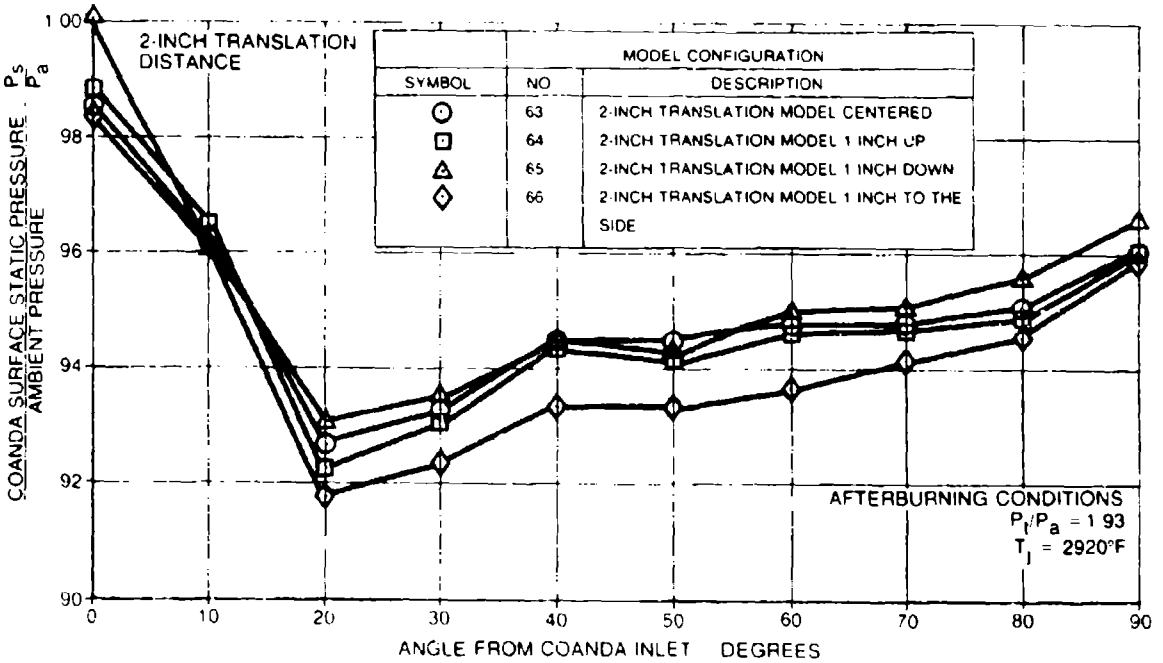

Figure 73. Coanda surface pressure distribution – 2-inch translation with misalignment (afterburning power).

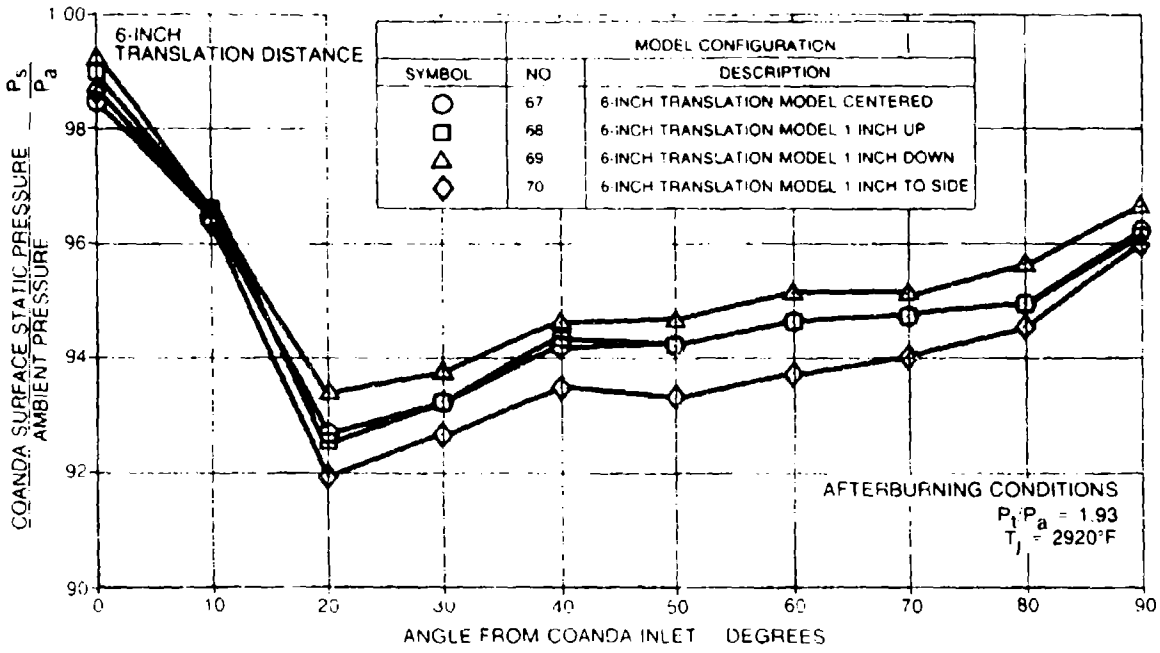

Figure 74. Coanda surface pressure distribution – 6-inch translation with misalignment (afterburning power).

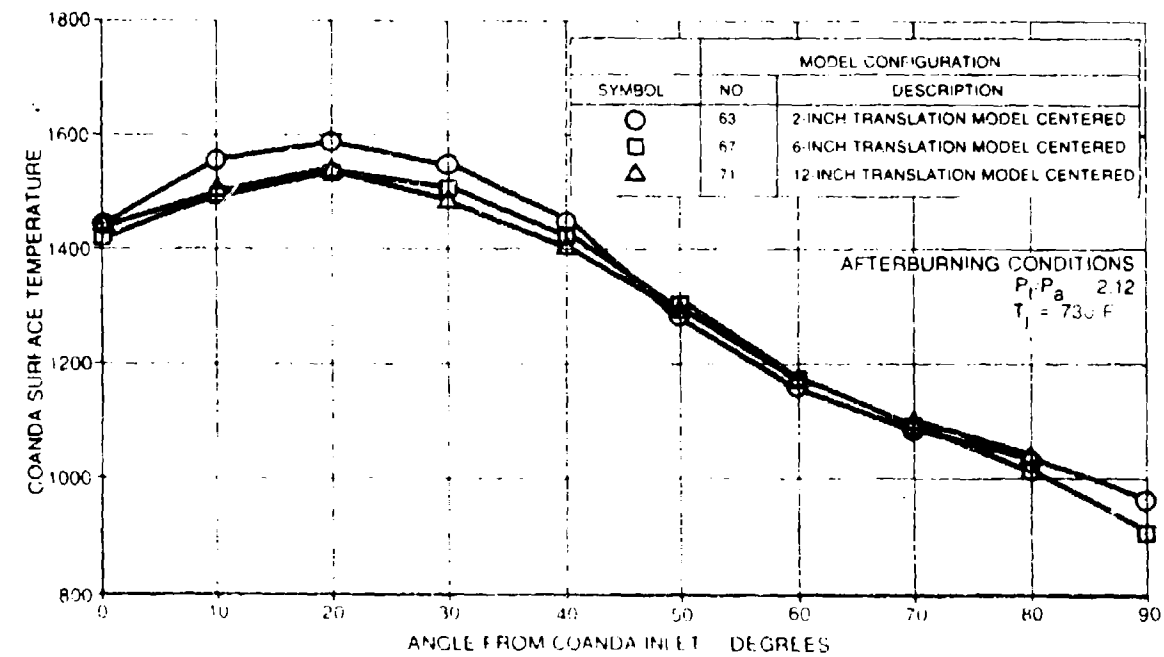

Figure 75. Coanda surface temperature distributions – translation test – model centered (afterburning power).

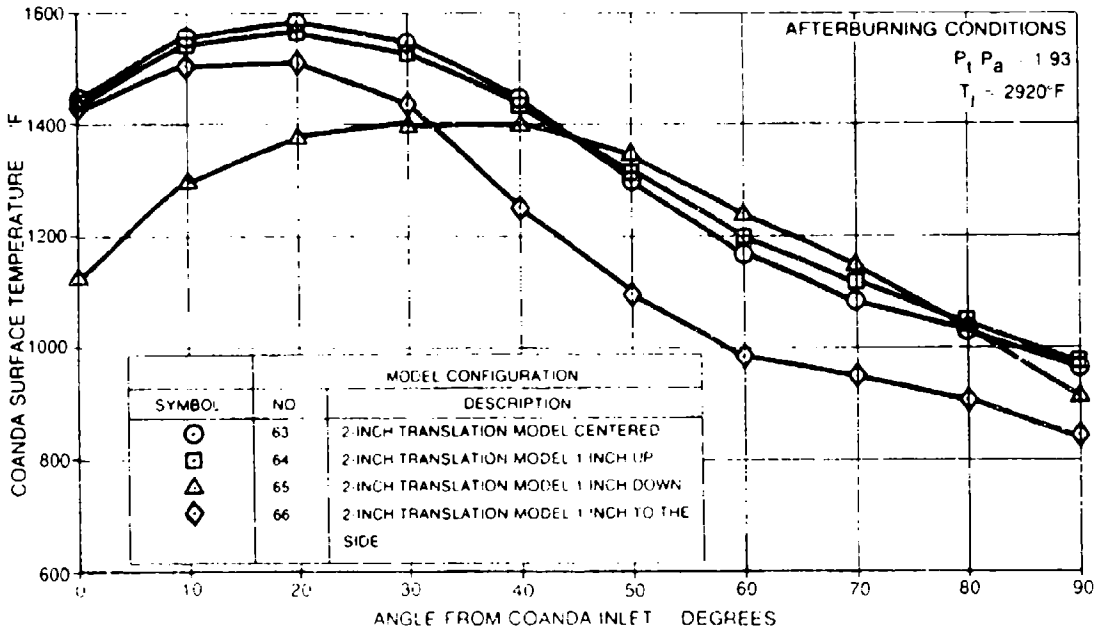

Figure 76. Coanda surface temperature distributions – 2-inch translation with misalignment (afterburning power).

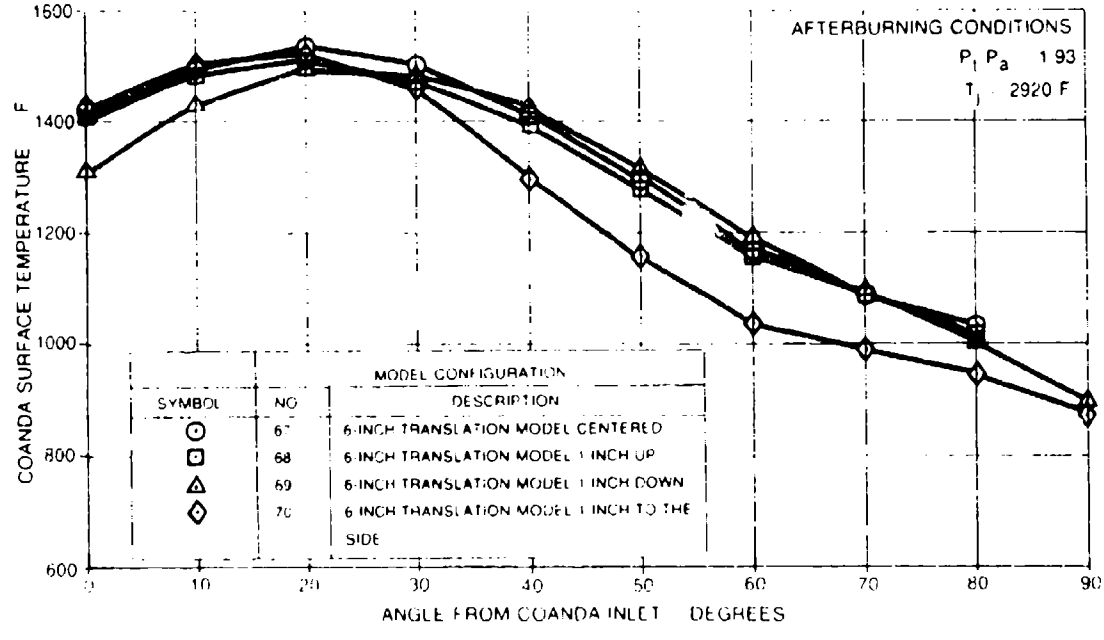

Figure 77. Coanda surface temperature distributions – 6-inch translation with misalignment (afterburning power).

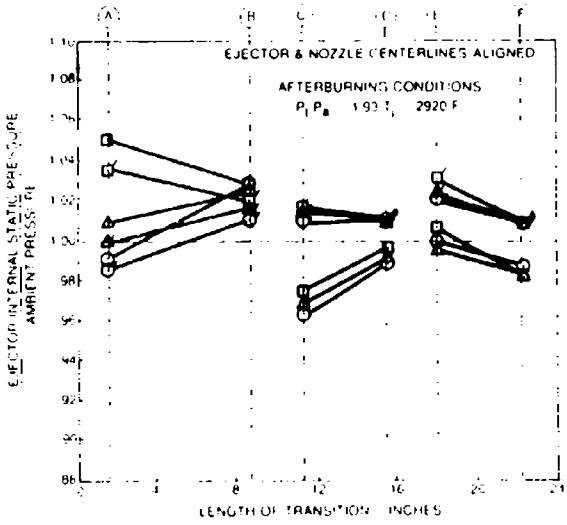

	MODEL CONFIGURATION	
SYMBOL	NO	DESCRIPTION
○ TOP ○ SIDE	63	2-INCH TRANSLATION
△ TOP △ SIDE	67	6-INCH TRANSLATION
□ TOP □ SIDE	71	12-INCH TRANSLATION

Figure 78. Transition ejector internal static pressures – translation test with model centered – (afterburning power).

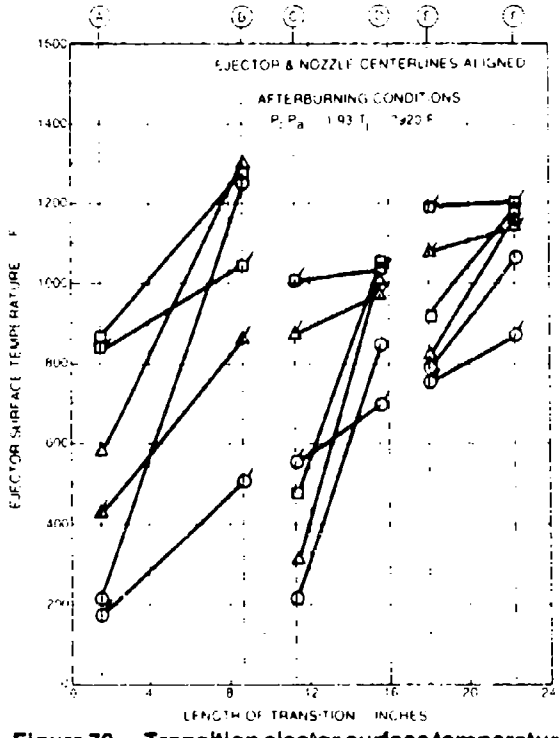

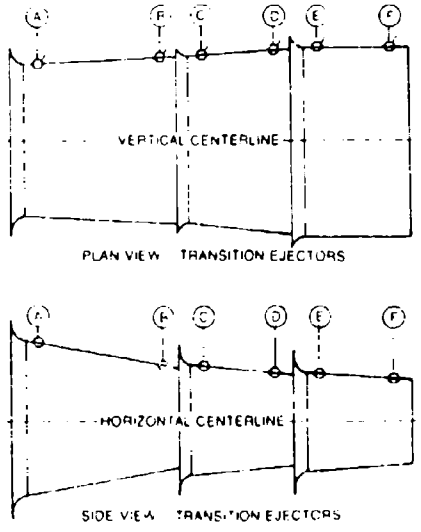

Figure 79. Transition ejector surface temperatures – translation test with model centered (afterburning power).

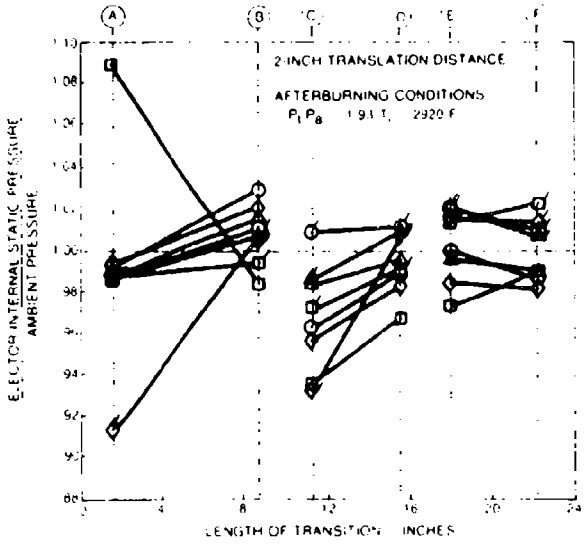

	MODEL CONFIGURATION	
SYMBOL	NO	DESCRIPTION
TOP / SIDE	63	NOZZLE & EJECTOR CENTERLINES ALIGNED
TOP / SIDE	64	EJECTOR ℄ 1-INCH ABOVE NOZZLE ℄
TOP / SIDE	65	EJECTOR ℄ 1-INCH BELOW NOZZLE ℄
TOP / SIDE	66	EJECTOR ℄ 1 INCH TO SIDE OF NOZZLE ℄

Figure 80. Transition ejector internal static pressures – 2-inch translation with misalignment – (afterburning power).

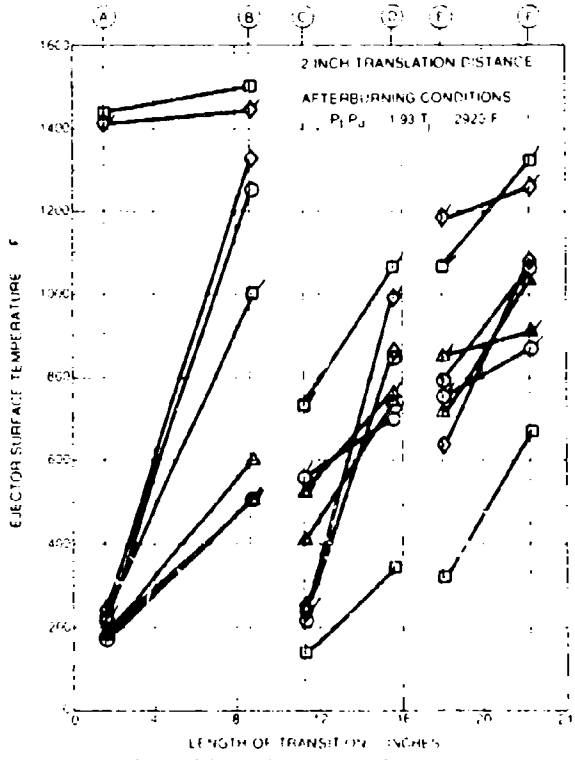

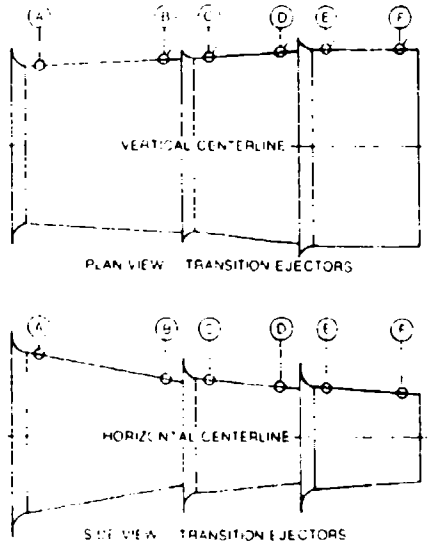

Figure 81. Transition ejector surface temperatures – 2-inch translation with misalignment – (afterburning power).

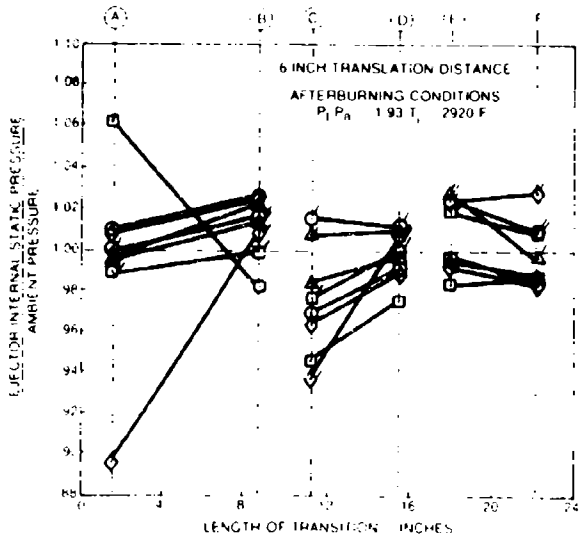

	MODEL CONFIGURATION	
SYMBOL	NO	DESCRIPTION
○ TOP ○ SIDE	67	NOZZLE & EJECTOR CENTERLINES ALIGNED
△ TOP △ SIDE	68	EJECTOR ℄ 1-INCH ABOVE NOZZLE ℄
□ TOP □ SIDE	69	EJECTOR ℄ 1-INCH BELOW NOZZLE ℄
◇ TOP ◇ SIDE	70	EJECTOR ℄ 1-INCH TO SIDE OF NOZZLE ℄

Figure 82. Transition ejector internal static pressures – 6-inch translation with misalignment (afterburning power).

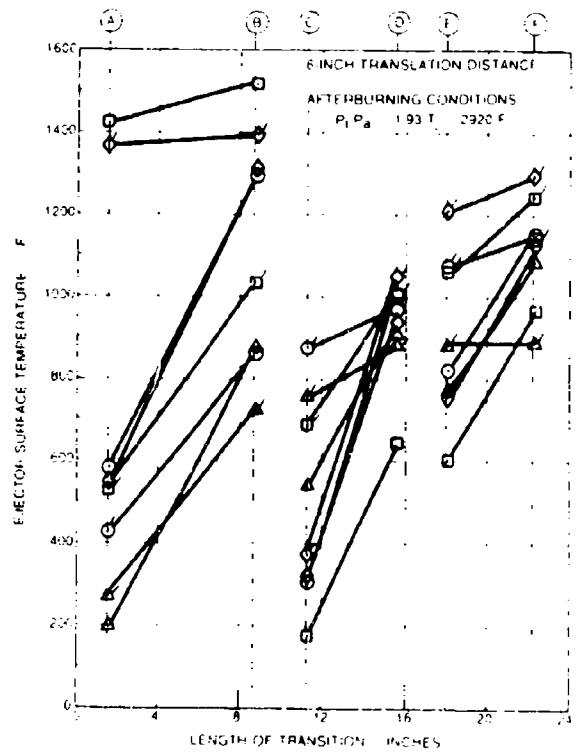

Figure 83. Transition ejector surface temperatures – 6-inch translation with misalignment (afterburning power).

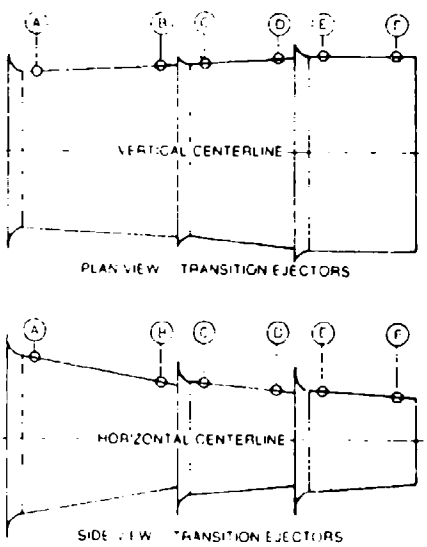

7.0 TWIN ENGINE MISALIGNMENT TEST

7.1 Objectives

The fifth model test of the series was a continuation of the development of a Coanda flow turning system for twin engine aircraft with closely spaced engines (such as F-4, F-111 and F-15 aircraft) that was begun by the Initial Twin Engine (described in Section 5.0) Model Test. The fifth and last model test of the series was a misalignment test of a twin engine model that differed from the initial twin engine suppressor model primarily in the transition ejectors. This ejector set was designed to allow more secondary entrainment between the two engine flows than in the previous twin engine model test. The purpose was to study a different (improved) model configuration for any adverse effects of concurrent jet deflection of two distinct jet flows, as well as determine if offset and/or angular misalignments create any adverse effects of concurrent jetattachment and system cooling. The model had a five ejector transition to study the feasibility of extending the transition section out in front of the suppressor to capture the flow from aircraft, such as the F-4, which have the engine exhaust forward of the airplane empennage.

7.2 Model Description and Test Apparatus

The Acoustic Arena facility described earlier in Section 2.0 was used to run this test series. The data acquisition system was the same as that outlined in that section. Facility changes were required to provide the second nozzle flow; therefore, the twin flow rig built for the Initial Twin Engine Test (Section 5.0) was reinstalled. The nozzles were placed nine inches apart which is equivalent to 54 inches full scale, simulating the distance between the F-4, F-111 and F-15 aircraft engines. The second nozzle system flow was provided with a J47 engine burner and controls to heat the air to the required temperature for exhaust simulations up to 1500°F.

A new model was fabricated for this test consisting of dual five-ejector transition sections with centerline spacing simulating the centerline distances between the F-4, F-111 and F-15 aircraft (54 inches full scale), and a double width Coanda surface with a removable center splitter. The first two ejectors of each set were cylindrical and removable. The flows of the dual engines are separated through the first three ejectors but the last two pairs are joined into units without a divider wall. Figure 84 shows a schematic of the ejector, Coanda surface and dual flow rig, along with the locations of the static pressure and surface temperature pickups.

Figure 85 presents dimensional drawings of the Coanda surface and transition ejectors. The transition section is designed to change the flow from circular to rectangular for introduction into the Coanda flow turning surface. The first ejector is convergent in area with an inlet of 44 in^2 per side and an exit of 38 in^2. The exit area ratio based on the afterburning nozzle is 1.27. The second ejector is cylindrical with an inlet and exit area of 42.9 in^2 which results in an area ratio (based on the afterburning nozzle exit area) of 1.43. The first two ejector sets were fabricated of .090 inch thick Inconel. The third ejector set starts the transition from circular to rectangular. It has a constant area of 48.3 in^2 which is an area ratio of 1.61. The fourth ejector set continues the transitioning toward a rectangular flow. The spreading of the flow in the horizontal plane causes the twin flow passages to begin to overlap at the fourth and fifth stages without a divided wall between the two flows. The overlap and resulting decrease in ejector flow area was allowed because one engine runs at idle (low flow) condition while the other is at the high airflow conditions; therefore, the total primary flow converging into one ejector is not much greater than for one engine at maximum power. If the overlap in ejectors were not allowed, the jet exhaust would have to be transitioned outward as well as reshaped to rectangular. The fourth ejector had an inlet area of 53.7 in^2 and exit area of 52.2 in^2 per side. The fifth ejector was one unit without a divider and had an inlet area of 57.1 in^2 and exit area of 54 in^2 per side. The third, fourth and fifth ejectors were fabricated of .09 thick stainless steel. The last ejector exit has an area ratio (based on the afterburning nozzle area) of 1.80 and an aspect ratio (width/height) of 1.83 per side; however, the exit is one long rectangle which results in an aspect ratio of 3.65.

The Coanda surface curvature is based on a logarithmic spiral with a six-inch straight section at each end. The Coanda surface is provided with a removable splitter and sidewalls as shown in the sketch on Figure 85. Photographs of the ejector and Coanda system in their support stand are shown on Figures 86 and 87.

Preceding Page BLANK

Figure 88 shows the twin engine Coanda model installed in the Acoustic Arena prior to testing. Figure 89 is a photograph of the Coanda model taken from upstream showing the twin flow systems.

An instrumentation list for the twin engine model is seen in Table 7. Location of the instrumentation on the model is shown on Figure 84 and can also be seen on Figures 88 and 89. Temperatures and pressure data were measured on the Coanda surface every 10 angular degrees at points directly in line with the primary nozzle centerline. The exit rake which measured pressure and temperature of the flow at 14 points across the Coanda exit was also initially located along this line. Pressure and temperature were measured on the Coanda sidewall at alternate angular positions (0°, 20°, 40°, 60°, and 80°) and temperatures were measured at corresponding positions on the Coanda splitter. Forward and aft temperatures and pressures were measured on the top and side of each ejector. Forward measurements were approximately one inch from the inlet plane and aft measurements approximately one inch from the exit plane.

In addition to the usual four primary nozzle static pressure pickups, two more were added at the 9 o'clock and 3 o'clock position (looking upstream) on the primary and secondary nozzles, respectively.

7.3 Test Plan

Table 8 presents the model configurations that were tested for evaluating the twin engine Coanda flow turning system. The configuration changes consist of varying the engine power setting, the number of transition ejectors and misalignments (both offset and angular) between exhaust nozzle and ejector inlet. Also listed are the data recorded for each configuration. The configuration numbers are listed on all data shown later in this report as an aid in identification. It should be noted in the column of Table 8 which describes the misalignment direction that the model is moved rather than the exhaust nozzle. This was necessary because of the stationary attachment of the burner and nozzle system to the facility floor.

Figures 90, 91, 92, and 93 illustrate the offset and angular misalignments described for the configurations listed in Table 8. The configuration numbers are given on these figures to aid in identification.

The flow conditions listed in Table 8 are simulated TF30-P-12A engine conditions and were defined earlier in Table 2 (Paragraph 3.3).

7.4 Test Results and Conclusions

7.4.1 Coanda Flow Turning Data

Figures 94 and 95 present Coanda exit velocity profiles computed from the exit rake total pressure and temperature data for model configurations with three, four and five ejector transitions and no misalignment at military (MRT) power and afterburning (A/B) conditions, respectively. In each case, the other engine was at idle conditions. The four ejector transition was not run at military conditions (see Table 8). These data indicate no difference in flow attachment or Coanda surface mixing because of the number of ejectors in the transition section. The Coanda surface static pressure data for these same model configurations are presented on Figures 96 and 97 for MRT and A/B flow conditions, respectively. These data also indicate very little difference in flow attachment due to the number of ejectors. Both exit velocity profiles and surface static pressure data indicate very good flow attachment at both MRT and A/B conditions.

Figures 98 and 99 show Coanda exit velocity profiles and Coanda surface static pressures, respectively, for the five ejector transition configuration with and without offset misalignments of one inch (see Figure 90) at MRT primary nozzle conditions. These data show that the only significant deterioration flow attachment occurs with sideways offsets of nozzle and ejector centerlines. The static pressure data for the sideways misalignment (Figure 99) indicates flow detachment at the 10° position which is not acceptable flow turning. It will be shown later that a sideways offset misalignment of ½ inch would probably have produced acceptable flow turning.

Figures 100 and 101 present Coanda exit velocity profiles and Coanda surface static pressures, respectively, for the five ejector transition configuration with one-half inch offset as well as angular misalignments of 3° (in the vertical plane) at MRT primary nozzle conditions. Figure 91 shows the different misalignment configuration. All configurations resulted in data that indicate good flow attachment occurred regardless of the misalignment. The configuration with the transition inlet angled upward and the nozzle offset downward (ejector centerline offset upward) shows a very slight decrease in the strength of flow attachment by the peak velocity (Figure 100) being further from the Coanda surface than for the other configurations and by the Coanda surface static pressure (Figure 101) being higher than the other configurations at the 40° to 90° positions.

Figures 102 and 103 present Coanda exit velocity profiles calculated from exit rake total pressures and temperatures for the three ejector transition configuration with offset misalignment at military rated thrust and afterburning conditions, respectively. The offset misalignments at military were one inch as before except for the sideways offset which was reduced to one-half inch where excellent flow attachment is shown. The offsets at afterburning conditions were reduced to one-half inch because the larger nozzle allowed impingement on the ejector inlet at a one inch offset. All configurations demonstrate good flow attachment and Coanda surface mixing. The Coanda surface static pressures for these same model configurations are presented on Figures 104 and 105. These data also indicate good flow attachment at all offset configurations and primary flow conditions for the three ejector transition

Figures 106 and 107 present Coanda exit velocity profiles for the three ejector transition configuration with one-half inch offset misalignments in addition to angular misalignments of 3° (in the vertical plane) at MRT and A/B primary nozzle conditions, respectively. Figure 93 shows the different misalignment configurations. All configurations resulted in data indicating good Coanda flow attachment regardless of the misalignment configuration. Only the configuration with the transition inlet angled upward and the primary nozzle offset downward at MRT indicates any decrease in flow attachment strength. This is indicated by lower velocities near the Coanda surface and peak velocity further away than for the other configurations. The Coanda surface static pressures for these configurations at military flow conditions shown on Figure 108, however, do not clearly indicate a decreased flow attachment for the configuration with inlet angled upward and nozzle offset downward. These data indicate superior attachment strength (lower static pressures) in the 10° to 30° positions for both configurations with inlet angled upward and then equivalent pressure differentials to the other configurations at the 40° to 90° positions. This may indicate that with the smaller military primary nozzle and the transition angled away from the Coanda surface, there is improved mixing and thus lower exit velocities at the Coanda 90° position. The Coanda surface static pressure data for the offset and angular misalignments and afterburning conditions are shown on Figure 109. These data support the exit velocity profile (Figure 107) data indicating good Coanda surface flow attachment for all misalignment configurations tested.

7.4.2 System Cooling Data

Coanda surface temperature data taken up the centerline of the hot side of the twin Coanda surface for the three, four and five ejector transition model configurations without misalignments are shown on Figure 110. The hot side nozzle was at afterburning conditions and the other at idle. It is obvious from these data that the three-ejector transition provides for better surface cooling than the five-ejector set, and considerably more than the four-ejector configuration. These data may produce a question as to why the velocity profiles for these configurations (shown on Figure 95) were so nearly the same,yet, the Coanda surface temperatures indicate quite different results. These seemingly incompatible data may be explained by remembering that the secondary air entrainment and mixing in the Coanda flow turning far exceeds that provided by the ejectors. Therefore, large differences in ejector pumping are not evident in the Coanda exit velocity profiles and the Coanda surface cooling (at least the first portion) is dependent on the ejector pumping capabilities. The temperatures recorded for the three ejector transition configuration are acceptable (below 1000°F).

Typical full scale Coanda surface temperature data were shown on Figure 110 to illustrate that model scale testing shows higher surface temperature data at the upper portion (above the 30° position) of the Coanda surface. These differences are due to the difficulty in scaling conduction heat transfer (i.e., the scale model Coanda surface is only

one-sixth as long as the full scale surface, therefore, it takes much less time in model scale for the temperature at the upper part of the surface to be influenced by the hotter peak temperature of the lower portion of the surface). This indicates that only peak Coanda surface temperature should be considered from the scale model data.

The Coanda surface data for model configurations with three-ejector transition and offset nozzle to ejector centerline misalignments at A/B nozzle conditions are presented on Figure 111. In general, all misalignments cause an increase in Coanda surface temperature, probably because off-center flow decreases the pumping efficiency of the ejectors. Coanda surface temperatures reached 1200°F for the sideways misalignment configuration.

Figure 112 presents the Coanda surface temperature data from the three ejector transition model with offset and angular nozzle to ejector centerline misalignments and afterburning primary nozzle conditions. Offset misalignments both up and down with the transition ejectors angled upward at the inlet cause an increase in Coanda surface temperature (up to between 1250 and 1290°F in local areas). This is because the primary flow impinges more upon the upper ejector surfaces in these configurations and effectively "shuts off" air entrainment at these upper surfaces, thus providing less cooling to the Coanda surface. The configurations with the transition inlet angled downward illustrate only slightly higher (up to 1100 F) Coanda surface temperatures than for the aligned configuration.

Figures 113, 114 and 115 present ejector surface temperature and internal static pressure data for afterburning conditions without misalignment and the five, four and three-ejector transition, respectively. Several important items are indicated by these data:

- The higher than ambient static pressures at the first ejector inlet of the five ejector set (Figure 113) indicate the first ejector area was too small to accommodate the expanding primary flow plus free jet entrainment upstream of the point at which the expanding jet meets the ejector walls.

- The high temperature at the top (and probably bottom also) of the round first ejector inlet in all configurations indicate that the primary flow is trying to attach to the convergent upper and lower surfaces of the transition ejectors.

- The higher than ambient static pressures at the inlet of the last ejector in all (three, four and five-ejector) configurations indicate a lack of secondary air pumping in the last ejector. This would be improved by enlarging the exit area of the last ejector.

Figures 116, 117 and 118 present the ejector surface temperature and internal static pressure data for the three-ejector configuration with the primary nozzle at afterburning conditions and offset upward, downward and to the side, respectively. The general trend from these data is that the first ejector inlet temperature increases dramatically on the side toward which the nozzle is offset, and then the temperature decreases at the second ejector on that side but increases on the opposite side. (Note: Data on Figures 117 and 118 are from sides opposite the direction of offset.) This trend is due to the ricochet effect discussed earlier as well as the tendency for the flow to attempt to attach to the ejector side toward which the nozzle is misaligned. The third ejector exit temperatures remain relatively constant except for the configuration (No. 127B, Figure 118) offset to the side for which the sidewall temperature opposite the offset direction increased in temperature to above 1200°F (about 400° increase from the configuration without misalignment).

Figures 119 through 122 present the ejector surface temperature and internal static pressure data for the three ejector configuration with the primary nozzle at afterburning conditions and with offset and angular misalignments. Again, the first ejector inlet temperatures were quite high (between 1500 and 1700°F) on the side toward which the nozzle was offset. Offsets of nozzle downward (see Figure 122) does not show the temperature rise because there were no thermocouples on the lower surfaces. The configurations with the transition inlet angles upward with offsets both upward and downward caused an increase (to a surface temperature between 1150 to 1300°F) in the

temperature at the side and exit of the second and third ejectors. This is probably from the spreading of the hot primary flow after it impinged on the ejector upper surfaces.

7.4.3 Conclusions

The following conclusions may be made from the results of the twin engine misalignment test:

- The Coanda suppressor system will operate with offset and/or angular misalignments between nozzle and ejector centerlines. However, as was seen in previous single engine misalignment tests the sideways or horizontal misalignment is limited to about half (three inches full scale) that for vertical misalignments (six inches full scale).

- The ejector system used could be improved by slight changes in areas. The five ejector transition needs to have the first ejector area increased (or its length decreased). Both five and three ejector transitions need to have the exit area of the last ejector increased. These changes would help the system cooling problems.

- Coanda surface cooling is more acceptable with the three-ejector transition than with the five-ejector configuration used in this test because of more efficient ejector pumping. This conclusion, however, would not be true if the five-ejector set had been sized correctly. Generally offset and/or angular misalignments cause increased Coanda surface temperatures but not to a level that would create serious problems.

- Offset and/or angular misalignments create first ejector inlet temperatures that are undesirable (1500° to 1700 F) for low carbon steel. If such misalignments are to be encountered in actual suppressor operation it is recommended that at least the first ejector be fabricated from a high temperature material such as Inconel.

TABLE 7. TWIN ENGINE INSTRUMENTATION REQUIREMENTS

TYPE AND LOCATION	UNITS	QUANTITY	RANGE	ACCURACY
STATIC PRESSURE AT NOZZLE	psia	8	0 - 20	± .05 psi
STATIC PRESSURE EJECTOR WALLS	psia	12	10 - 16	± .02 psi
STATIC PRESSURE COANDA SURFACE	psia	10	10 - AMB	± .02 psi
TOTAL PRESSURE COANDA EXIT RAKE	psia	14	AMB - 20	± 1%
SURFACE TEMPERATURE THERMOCOUPLE EJECTOR WALLS	°F	12	AMB - 1500°	± 2%
SURFACE TEMPERATURE THERMOCOUPLE COANDA SURFACE	°F	10	AMB - 1300°	± 2%
SURFACE TEMPERATURE THERMOCOUPLE COANDA SPLITTER	°F	5	AMB - 1500°	± 2%
TOTAL TEMPERATURE COANDA EXIT RAKE	°F	14	AMB - 1300°	± 2%
GENERAL INSTRUMENTATION REQUIREMENTS				
TOTAL PRESSURE JET EXHAUST	psia	①	0 - 35	± ½%
TOTAL TEMPERATURE JET EXHAUST	°F ②	①	0 - 1600° ②	± 2%
AIRFLOW - PRIMARY JET	LBS SEC ③	1	0 - 8.0	± 1%
AIRFLOW - COANNULAR OR 2ND NOZZLE	LBS SEC ③	1	0 - 10.0	± 1%
FUEL FLOW - PRIMARY JET	gpm	1	0 - 3.5	± 1%
FUEL FLOW - COANNULAR OR 2ND NOZZLE	gpm	1	0 - 0.7	± 1%
AMBIENT PRESSURE	psia	1	—	± ½%
AMBIENT TEMPERATURE	°F	1	—	± 2%

① ONE EXHAUST PRESSURE AND TEMPERATURE REQUIRED FOR MISALIGNMENT TEST AND TWC EACH FOR COANNULAR AND TWIN ENGINE TESTS

② FOR AFTERBURNING CONDITIONS (≈3000°F) SET UP ON A PREDETERMINED FUEL AND AIRFLOW RATE. FOR NONAFTERBURNING CONDITIONS MEASURE TEMPERATURE DIRECTLY

③ MEASURE AND RECORD STANDARD FLOW NOZZLE. P, ΔP, AND TEMPERATURE, AND CALCULATE MASS FLOW IN A COMPUTER PROGRAM

TABLE 8
TWIN ENGINE MISALIGNMENT TEST CONFIGURATIONS

CONFIGURATION NUMBER	PRIMARY NOZZLE DIA. INCHES		PRIMARY FLOW CONDITION		EJECTOR CONFIGURATION	NOZZLE/EJECTOR MISALIGNMENT	DATA		
	LEFT HAND	RIGHT HAND	LEFT HAND	RIGHT HAND			SURFACE P_s & T_m	EXIT P_t & T_t	TEST RUN NUMBER
84	4.31	4.31	IDLE	IDLE	SET OF 5	NO OFFSET, NO ANGULAR	X	X	56-1
85	4.31	4.31	MILITARY	IDLE	SET OF 5	NO OFFSET, NO ANGULAR	X	X	56-2
86	4.31	4.31	IDLE	IDLE	SET OF 5	MODEL 1" DOWN NO ANGULAR	X	X	57-1
87	4.31	4.31	MILITARY	IDLE	SET OF 5	MODEL 1" DOWN NO ANGULAR	X	X	57-2
88	4.31	4.31	IDLE	IDLE	SET OF 5	MODEL 1" UP NO ANGULAR	X	X	59-1
89	4.31	4.31	MILITARY	IDLE	SET OF 5	MODEL 1" UP NO ANGULAR	X	X	59-2
90	4.31	4.31	IDLE	IDLE	SET OF 5	MODEL 1" TO SIDE NO ANGULAR	X	X	60-1
91	4.31	4.31	MILITARY	IDLE	SET OF 5	MODEL 1" TO SIDE NO ANGULAR	X	X	60-2
92	4.31	4.31	IDLE	IDLE	SET OF 5	MODEL OFFSET, 1/2" DOWN, INLET 3° DOWN	X	X	61-1
93	4.31	4.31	MILITARY	IDLE	SET OF 5	MODEL OFFSET, 1/2" DOWN, INLET 3° DOWN	X	X	61-2
94	4.31	4.31	IDLE	IDLE	SET OF 5	MODEL OFFSET, 1/2" UP, INLET 3° UP	X	X	63-1
95	4.31	4.31	MILITARY	IDLE	SET OF 5	MODEL OFFSET 1/2" UP, INLET 3° UP	X	X	63-2
96	4.31	4.31	IDLE	IDLE	SET OF 5	MODEL 1/2" DOWN INLET 3° UP	X	X	64-1
97	4.31	4.31	MILITARY	IDLE	SET OF 5	MODEL 1/2" DOWN INLET 3° UP	X	X	64-2
98	4.31	4.31	IDLE	IDLE	SET OF 5	MODEL 1/2" UP INLET 3° DOWN	X	X	62-1
99	4.31	4.31	MILITARY	IDLE	SET OF 5	MODEL 1/2" UP INLET 3° DOWN	X	X	62-2
100	6.18	4.31	AFTER-BURNING	IDLE	SET OF 5	NO OFFSET NO ANGULAR	X	X	65
100A	6.18	4.31	AFTER-BURNING	IDLE	SET OF 4	NO OFFSET NO ANGULAR	X	X	67
101	6.18	4.31	AFTER-BURNING	IDLE	SET OF 5	MODEL 1" DOWN NO ANGULAR	X	X	66
102	6.18	4.31	AFTER BURNING	IDLE	SET OF 5	MODEL 1" UP NO ANGULAR	X	X	NOT RUN
103	6.18	4.31	AFTER-BURNING	IDLE	SET OF 5	MODEL 1" TO SIDE NO ANGULAR	X	X	NOT RUN
104	6.18	4.31	AFTER-BURNING	IDLE	SET OF 5	MODEL OFFSET 1/2" DOWN, INLET 3° DOWN	X	X	NOT RUN
105	6.18	4.31	AFTER BURNING	IDLE	SET OF 5	MODEL OFFSET 1/2" UP, INLET 3° UP	X	X	NOT RUN
106	6.18	4.31	AFTER BURNING	IDLE	SET OF 5	MODEL 1/2" DOWN INLET 3° UP	X	X	NOT RUN
107	6.18	4.31	AFTER-BURNING	IDLE	SET OF 5	MODEL 1/2" UP INLET 3° DOWN	X	X	NOT RUN

TABLE 8
TWIN ENGINE MISALIGNMENT TEST CONFIGURATIONS (CONT'D)

CONFIGURATION NUMBER	PRIMARY NOZZLE DIA INCHES		PRIMARY FLOW CONDITION		EJECTOR CONFIGURATION	NOZZLE/EJECTOR MISALIGNMENT	DATA		
	LEFT HAND	RIGHT HAND	LEFT HAND	RIGHT HAND			SURFACE P_s & T_m	EXIT P_t & T_t	TEST RUN NUMBER
108	4.31	4.31	IDLE	IDLE	SET OF 3	NO OFFSET NO ANGULAR	X	X	85-1
109	4.31	4.31	MILITARY	IDLE	SET OF 3	NO OFFSET NO ANGULAR	X	X	85-2
110	4.31	4.31	IDLE	IDLE	SET OF 3	MODEL 1" DOWN NO ANGULAR	X	X	84-1
111	4.31	4.31	MILITARY	IDLE	SET OF 3	MODEL 1" DOWN NO ANGULAR	X	X	84-2
112	4.31	4.31	IDLE	IDLE	SET OF 3	MODEL 1" UP NO ANGULAR	X	X	88-1
113	4.31	4.31	MILITARY	IDLE	SET OF 3	MODEL 1" UP NO ANGULAR	X	X	88-2
114A	4.31	4.31	IDLE	IDLE	SET OF 3	MODEL 1/2" TO SIDE, NO ANGULAR ①	X	X	86-1
114B	4.31	4.31	IDLE	IDLE	SET OF 3	MODEL 1/2" TO SIDE, NO ANGULAR ②	X	X	87-1
115A	4.31	4.31	MILITARY	IDLE	SET OF 3	MODEL 1/2" TO SIDE, NO ANGULAR ①	X	X	86-2
115B	4.31	4.31	MILITARY	IDLE	SET OF 3	MODEL 1/2" TO SIDE, NO ANGULAR ②	X	X	87-2
116	4.31	4.31	IDLE	IDLE	SET OF 3	MODEL OFFSET, 1/2" DOWN, INLET 3° DOWN	X	X	81-1
117	4.31	4.31	MILITARY	IDLE	SET OF 3	MODEL OFFSET, 1/2" DOWN, INLET 3° DOWN	X	X	81-2
118	4.31	4.31	IDLE	IDLE	SET OF 3	MODEL OFFSET, 1/2" UP, INLET 3° UP	X	X	82-1
119	4.31	4.31	MILITARY	IDLE	SET OF 3	MODEL OFFSET, 1/2" UP, INLET 3° UP	X	X	82-2
120	4.31	4.31	IDLE	IDLE	SET OF 3	MODEL 1/2" DOWN INLET 3° UP	X	X	83-1
121	4.31	4.31	MILITARY	IDLE	SET OF 3	MODEL 1/2" DOWN INLET 3° UP	X	X	83-2
122	4.31	4.31	IDLE	IDLE	SET OF 3	MODEL 1/2" UP INLET 3° DOWN	X	X	80-1
123	4.31	4.31	MILITARY	IDLE	SET OF 3	MODEL 1/2" UP INLET 3° DOWN	X	X	80-2
124	6.18	4.31	AFTER BURNING	IDLE	SET OF 3	NO OFFSET NO ANGULAR	X	X	74
125	6.18	4.31	AFTER BURNING	IDLE	SET OF 3	MODEL 1/2" DOWN NO ANGULAR	X	X	70
126	6.18	4.31	AFTER BURNING	IDLE	SET OF 3	MODEL 1/2" UP NO ANGULAR	X	X	71
127A	6.18	4.31	AFTER BURNING	IDLE	SET OF 3	MODEL 1/2" TO SIDE NO ANGULAR ①	X	X	72

TABLE 8
TWIN ENGINE MISALIGNMENT TEST CONFIGURATIONS (CONT'D)

CONFIGURATION NUMBER	PRIMARY NOZZLE DIA INCHES LEFT HAND	PRIMARY NOZZLE DIA INCHES RIGHT HAND	PRIMARY FLOW CONDITION LEFT HAND	PRIMARY FLOW CONDITION RIGHT HAND	EJECTOR CONFIGURATION	NOZZLE/EJECTOR MISALIGNMENT	DATA SURFACE P_s & T_m	DATA EXIT P_t & T_t	DATA TEST RUN NUMBER
127B	6.18	4.31	AFTER BURNING	IDLE	SET OF 3	MODEL 1/2" TO SIDE, NO ANGULAR ②	X	X	73
128	6.18	4.31	AFTER BURNING	IDLE	SET OF 3	MODEL OFFSET, 1/2" DOWN, INLET 3° DOWN	X	X	77
129	6.18	4.31	AFTER BURNING	IDLE	SET OF 3	MODEL OFFSET, 1/2" UP, INLET 3° UP	X	X	75
130	6.18	4.31	AFTER BURNING	IDLE	SET OF 3	MODEL 1/2" DOWN INLET 3° UP	X	X	76
131	6.18	4.31	AFTER BURNING	IDLE	SET OF 3	MODEL 1/2" UP INLET 3° DOWN	X	X	78

① PRIMARY FLOW NEARER SIDEWALL

② PRIMARY FLOW NEARER SPLITTER

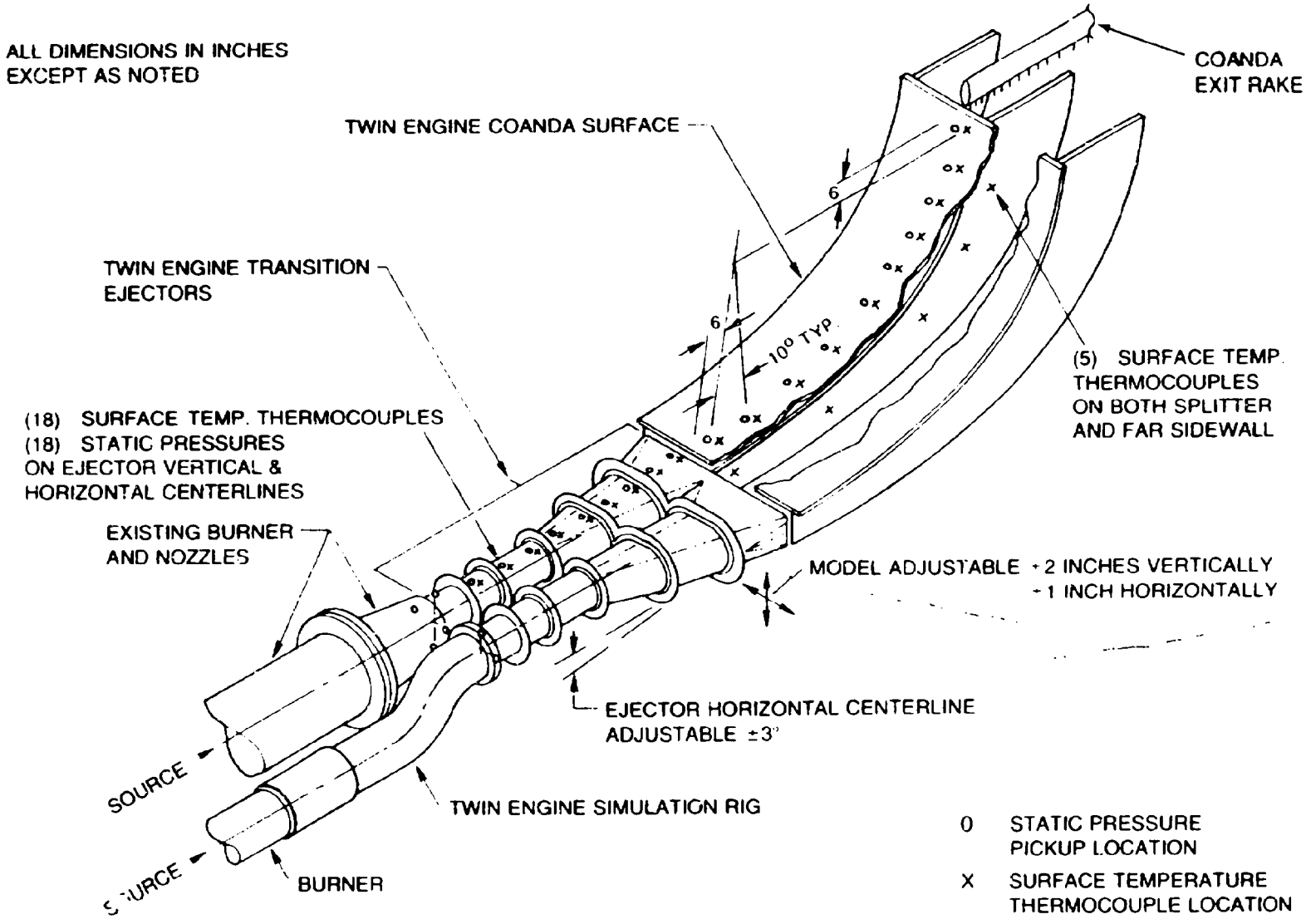

Figure 84. Twin engine Coanda and ejectors misalignment test setup.

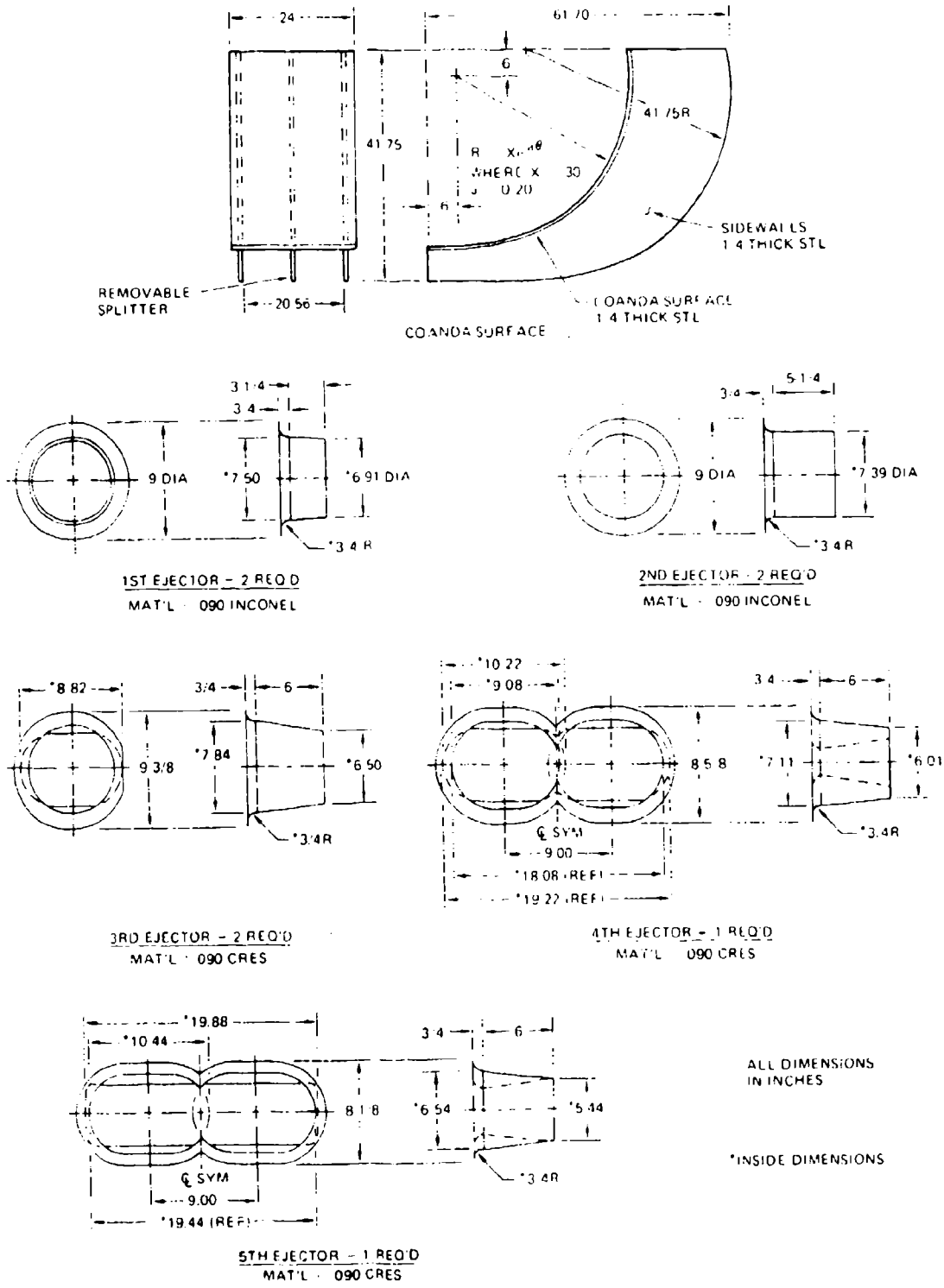

Figure 85. Dimensional drawings of Coanda surface and ejectors for twin engine misalignment test.

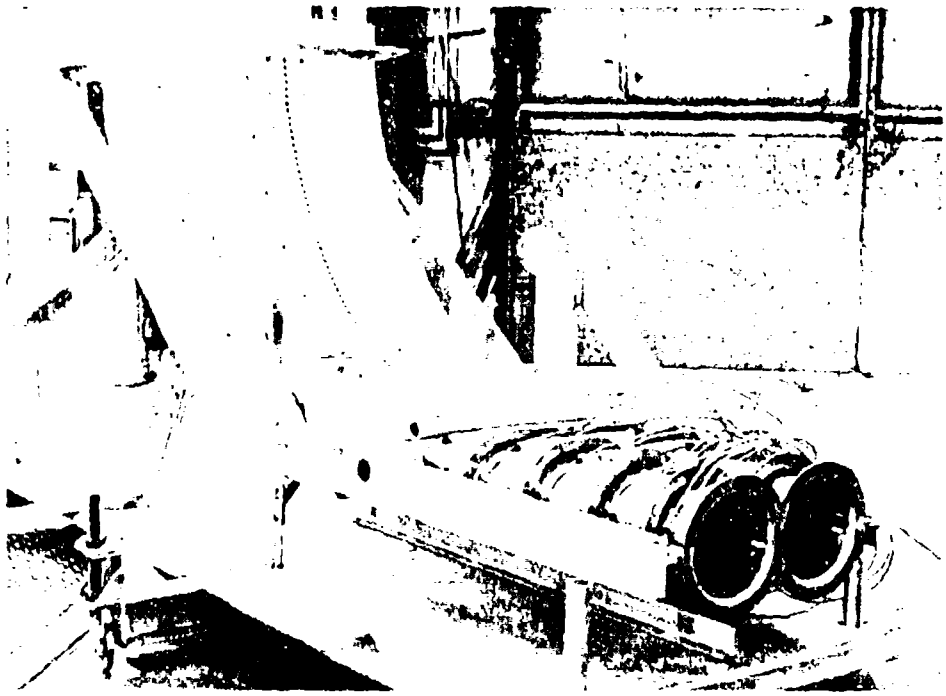

Figure 86. Twin-engine Coanda misalignment test model.

Figure 87. Rear view of twin-engine Coanda misalignment test model.

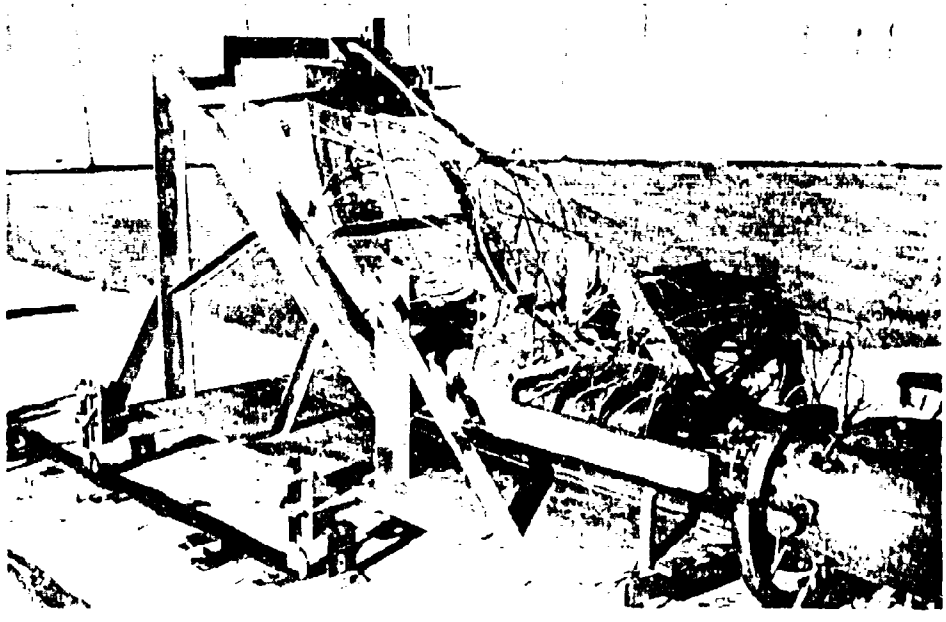

Figure 88. Twin-engine Coanda misalignment test model setup in Acoustic Arena.

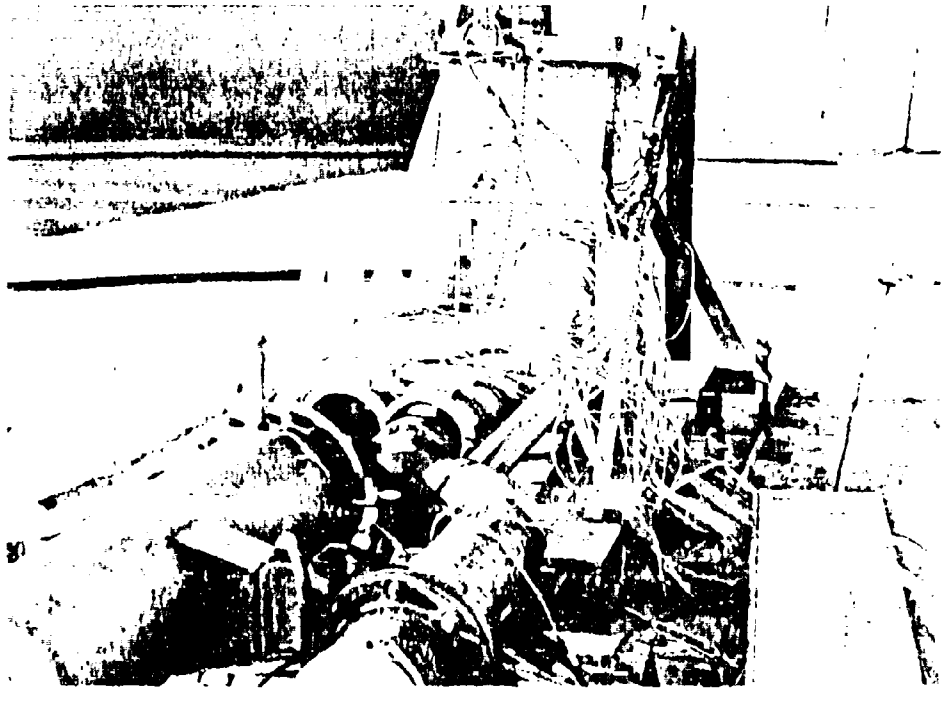

Figure 89. Dual flow nozzles and twin-engine Coanda test model in Acoustic Arena.

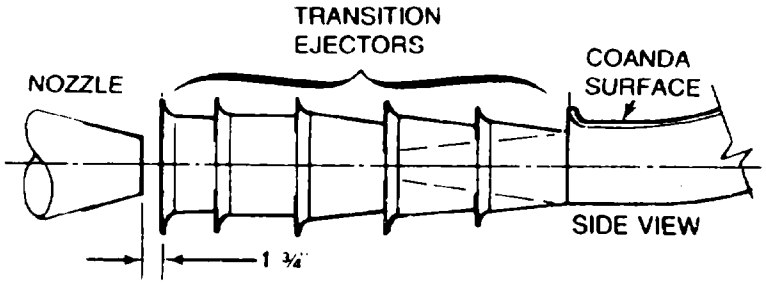

Configuration Numbers 84, 85 & 100 (Ref. Table 8)

(a) No offset, no angular misalignments

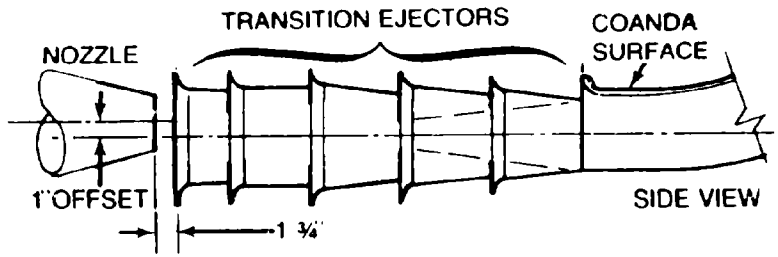

Confifiguration Numbers 86, 87 & 101 (Ref. Table 8)

(b) Model offset 1"down, no angular misalignment

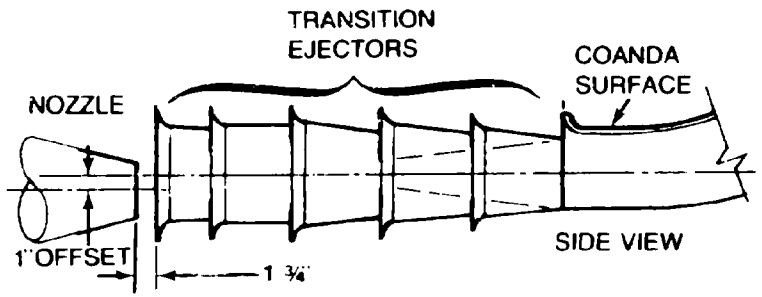

Configuration Numbers 88, 89 & 102 (Ref. Table 8)

(c) Model offset 1"up, no angular misalignment

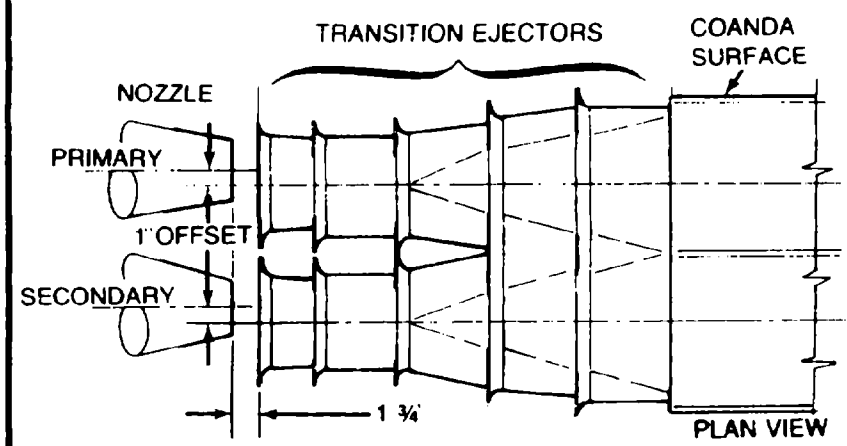

Configuration Numbers 90, 91 & 103 (Ref. Table 8)

(d) Model offset 1"to side, no angular misalignment

Figure 90. Explanation of offset misalignments – five ejector transition.

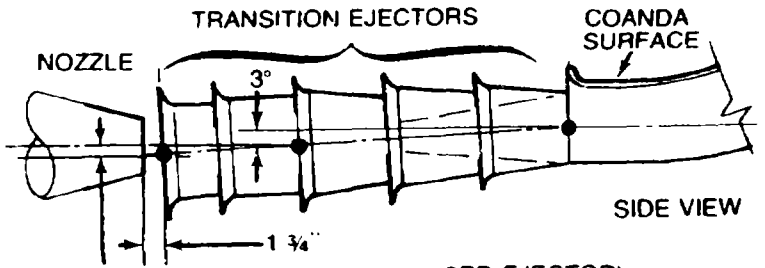

½" OFFSET (MODEL CENTERED ON 3RD EJECTOR)

Configuration Numbers 92, 93 & 104 (Ref. Table 8)

(a) Model offset ½" down, transition inlet 3° down

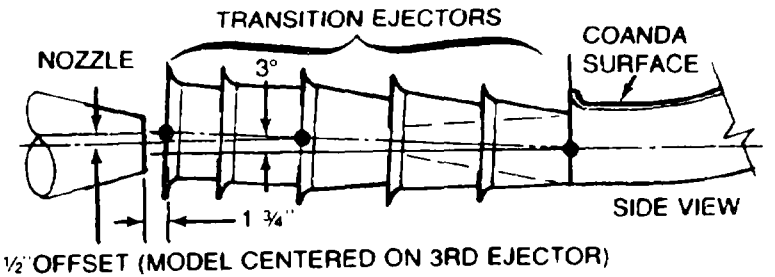

½" OFFSET (MODEL CENTERED ON 3RD EJECTOR)

Configuration Numbers 94, 95 & 105 (Ref. Table 8)

(b) Model offset ½" up, transition inlet 3° up

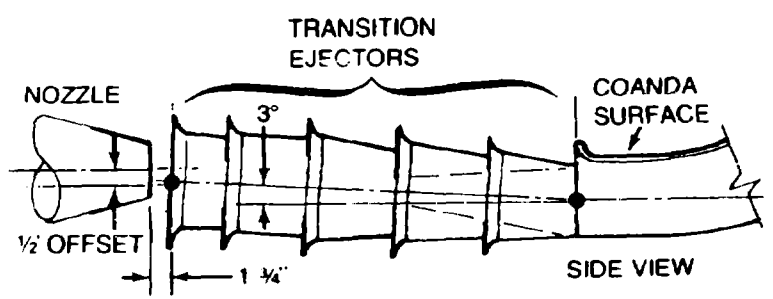

Configuration Numbers 96, 97 & 106 (Ref. Table 8)

(c) Model offset ½" down, transition inlet 3° up

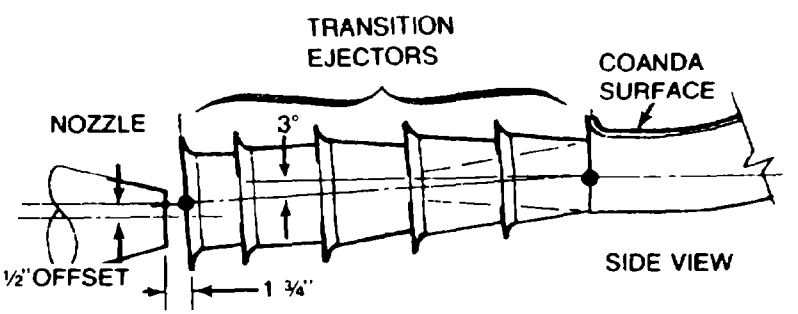

Configuration Numbers 98, 99 & 107 (Ref. Table 8)

(d) Model offset ½" up, transition inlet 3° down

Figure 91. Explanation of offset and angular misalignments – five ejector transition.

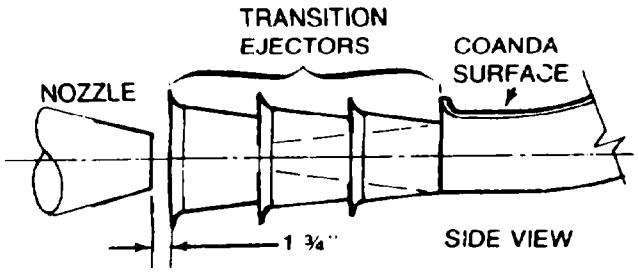

Configuration Numbers 108, 109 & 124 (Ref. Table 8)

(a) No offset, no angular misalignments.

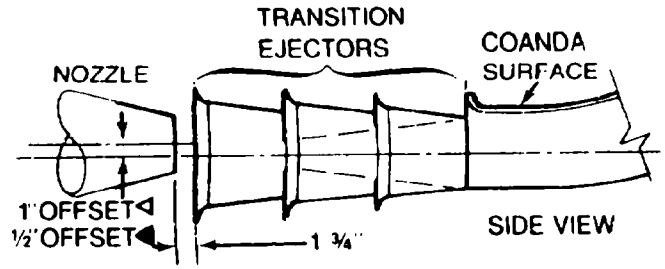

◁Configuration numbers 110 & 111 (Ref. Table 8)

◀Configuration Number 125 (Ref. Table 8)

(b) Model offset 1" and ½" down, no angular misalignments.

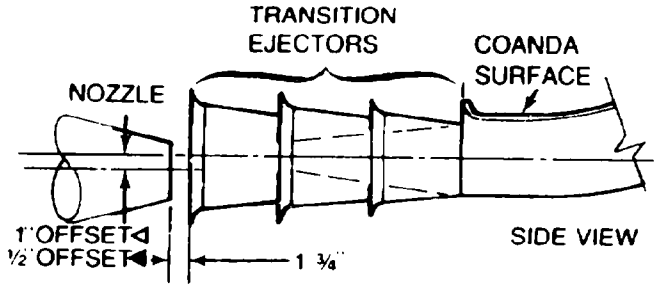

◁Configuration Numbers 112 & 113 (Ref. Table 8)

◀Configuration Number 126 (Ref. Table 8)

(c) Model offset 1" and ½" up, no angular misalignments

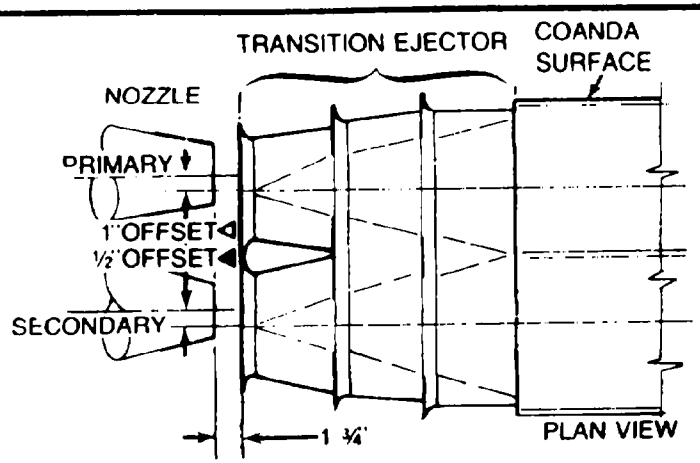

◁Configuration Numbers 114A & 115A (Ref. Table 8)
◀Configuration Number 127A (Ref. Table 8)
(Configuration Number 127B offset ½" in opposite direction)

(d) Model offset 1" and ½" to side, no angular misalignments

Figure 92. Explanation of offset misalignments – three ejector transition.

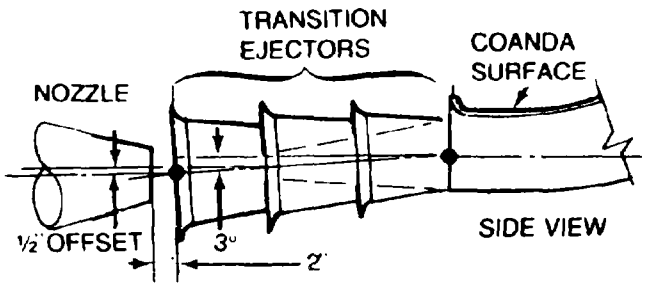

Configuration Numbers 116, 117 & 128 (Ref. Table 8)

(a) Model offset ½" down, transition inlet 3° down

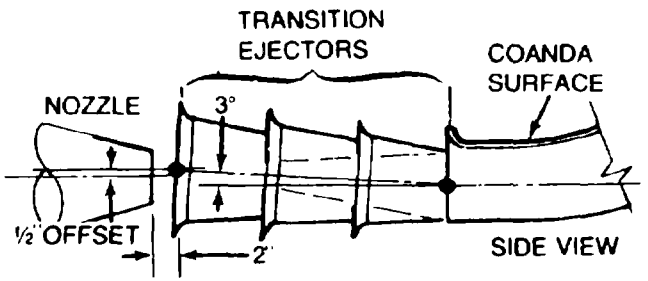

Configuration Numbers 118, 119 & 129 (Ref. Table 8)

(b) Model offset ½" up, transition inlet 3° up

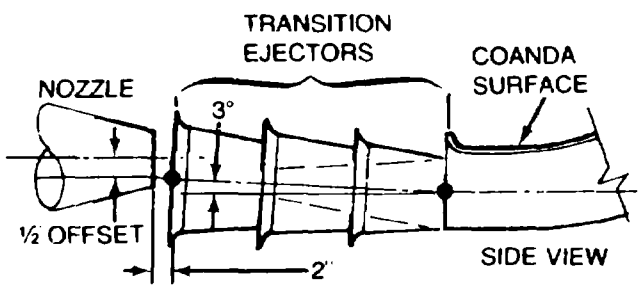

Configuration Numbers 120, 121 & 130 (Ref. Table 8)

(c) Model offset ½" down, transition inlet 3° up

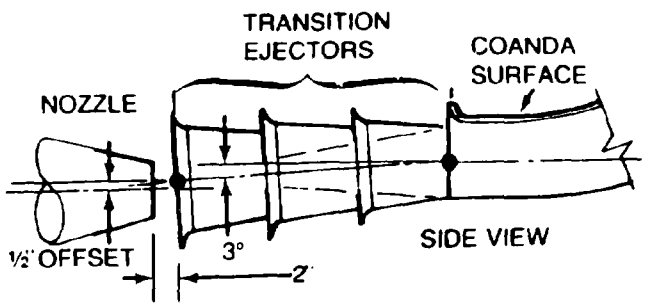

Configuration Numbers 122, 123 & 131 (Ref. Table 8)

(d) Model offset ½" up, transition inlet 3° down

Figure 93. Explanation of offset and angular misalignments – *three ejector transition*

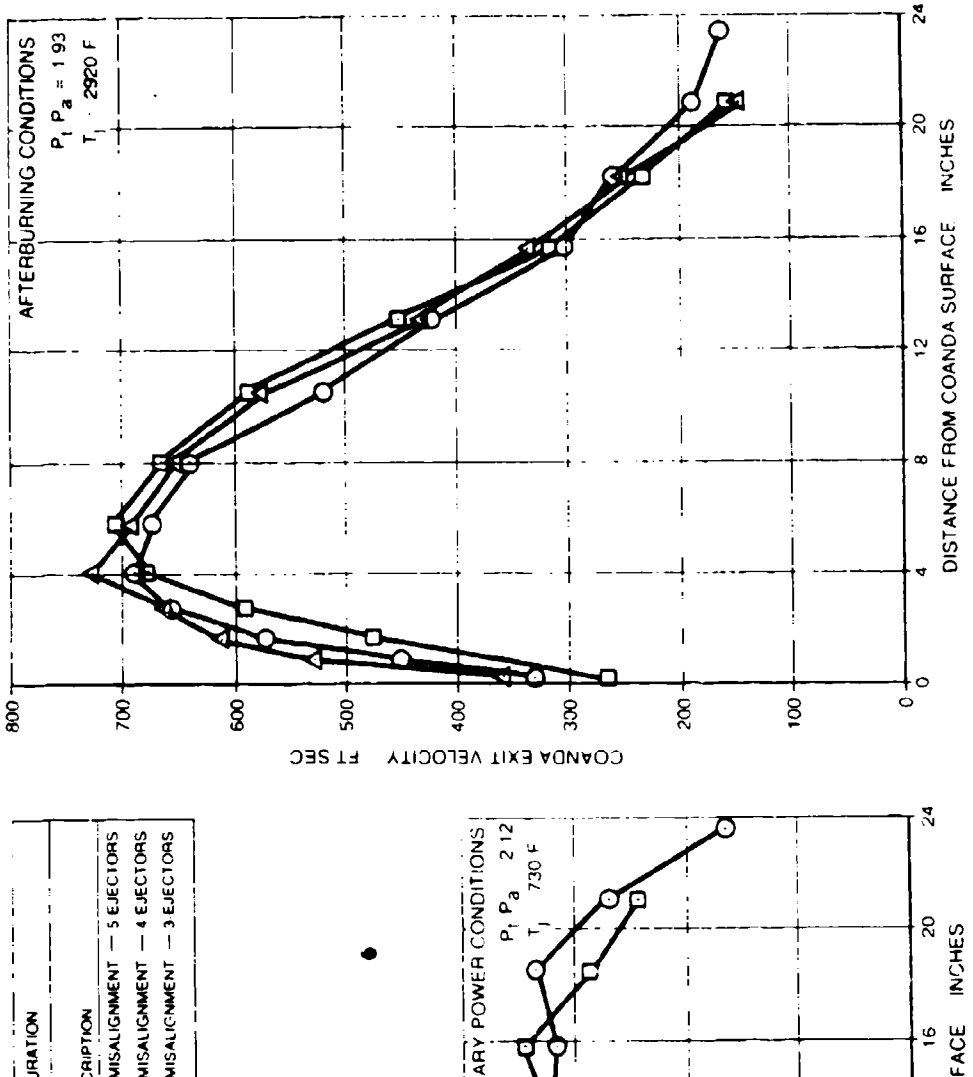

Figure 95. Coanda exit velocity profiles – three, four and five ejector transitions without misalignment (one engine at A/B and one engine at idle).

Figure 94. Coanda exit velocity profiles – three and five ejector transitions without misalignment (one engine at military and one engine at idle)

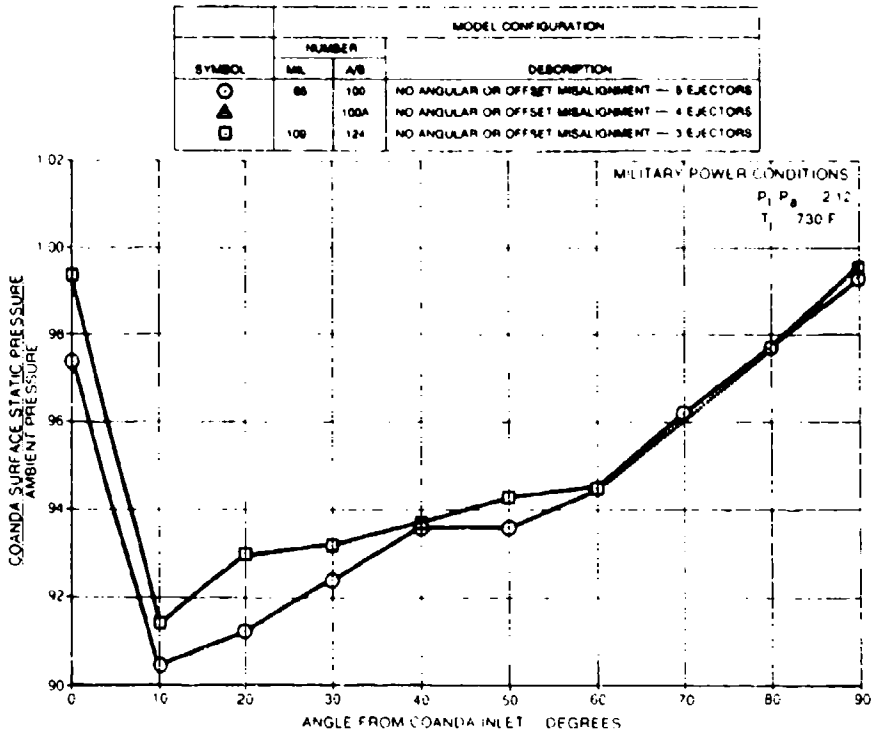

Figure 96. Coanda surface static pressures – three and five ejector transitions without misalignment (one engine at military and one engine at idle).

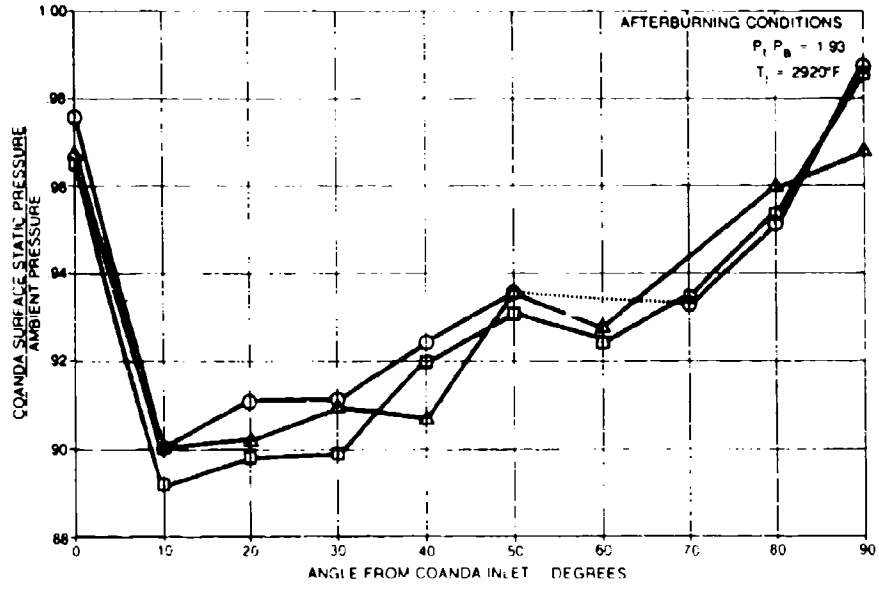

Figure 97. Coanda surface static pressures – three, four and five ejector transitions without misalignment (one engine at A/B and one engine at idle).

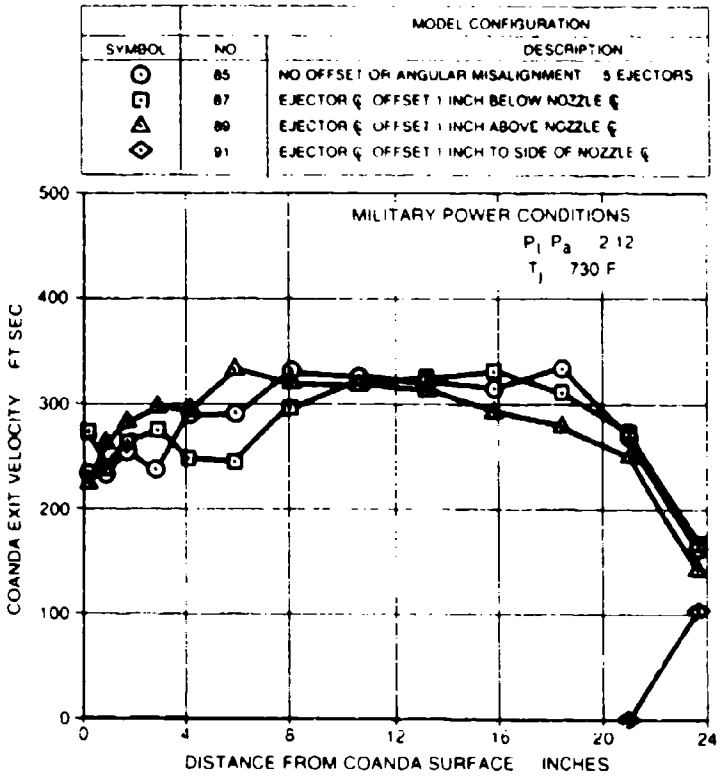

Figure 98. Coanda exit velocity profiles – five ejector transition with offset misalignments (one engine at military one engine at idle).

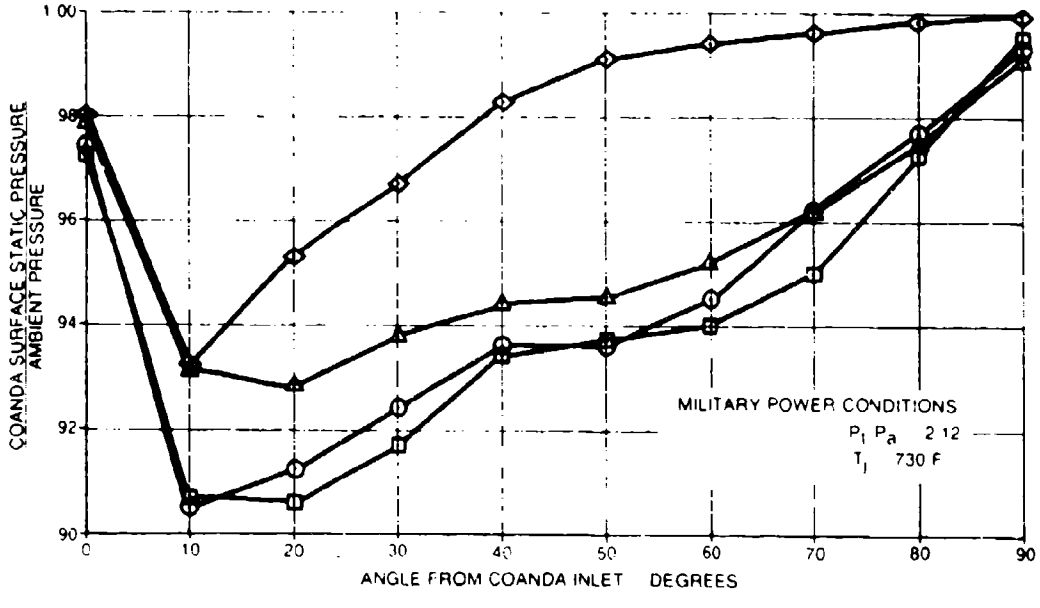

Figure 99. Coanda surface static pressures – five ejector transition with offset misalignments (one engine at military, one engine at idle).

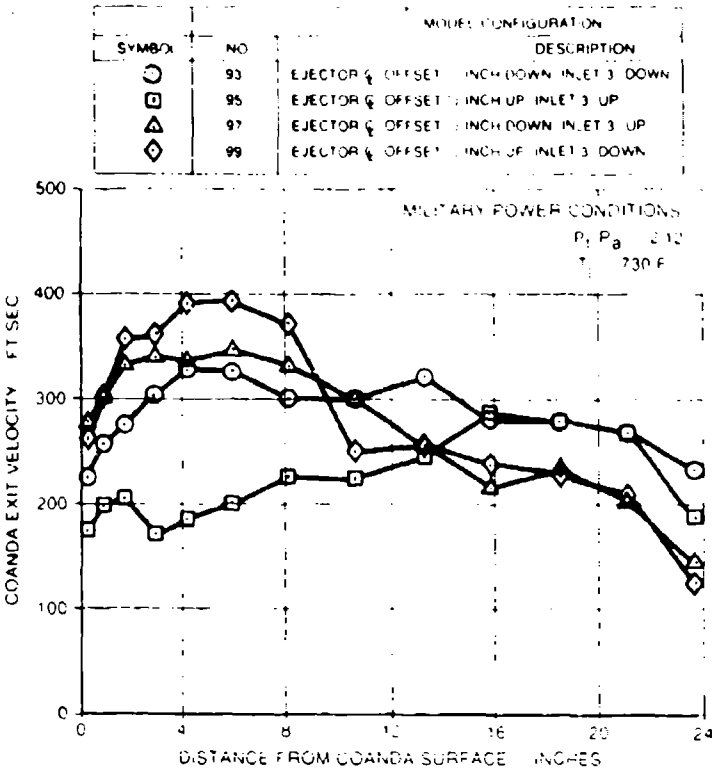

Figure 100. Coanda exit velocity profiles – five ejector transition with offset and angular misalignments (one engine at military, one engine at idle).

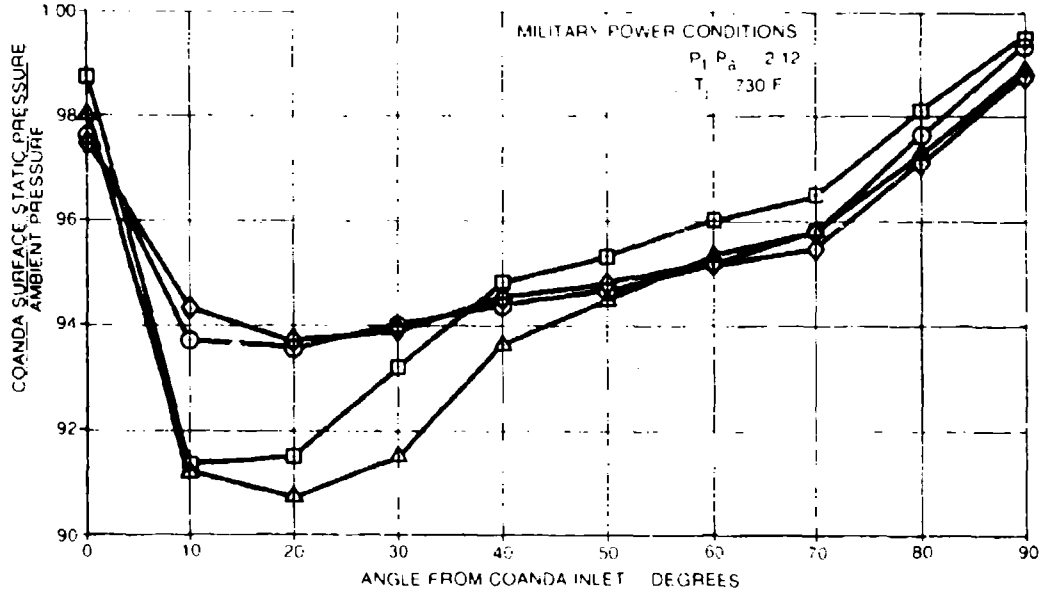

Figure 101. Coanda surface static pressures – five ejector transitions with offset and angular misalignments (one engine at military, one engine at idle).

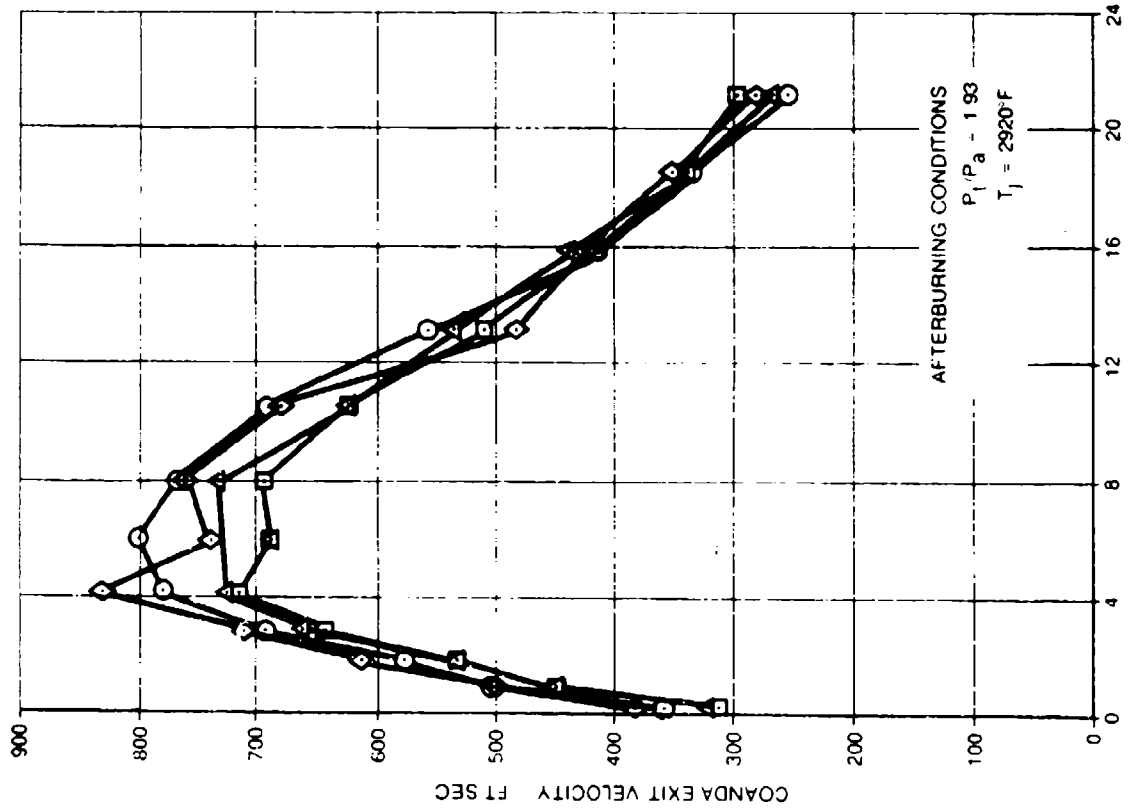

Figure 103. Coanda exit velocity profiles – three ejectors with offset misalignment (one engine at A/B and one engine at idle).

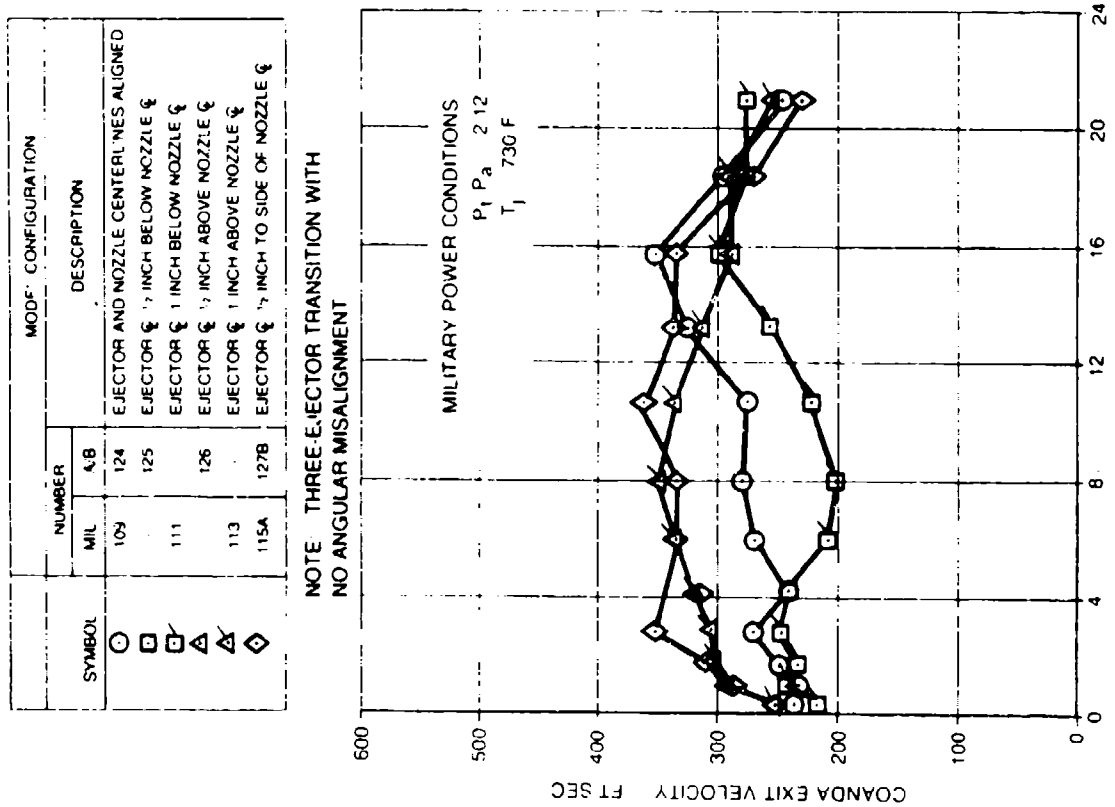

Figure 102. Coanda exit velocity profiles – three ejectors with offset misalignment (one engine at military and one engine at idle).

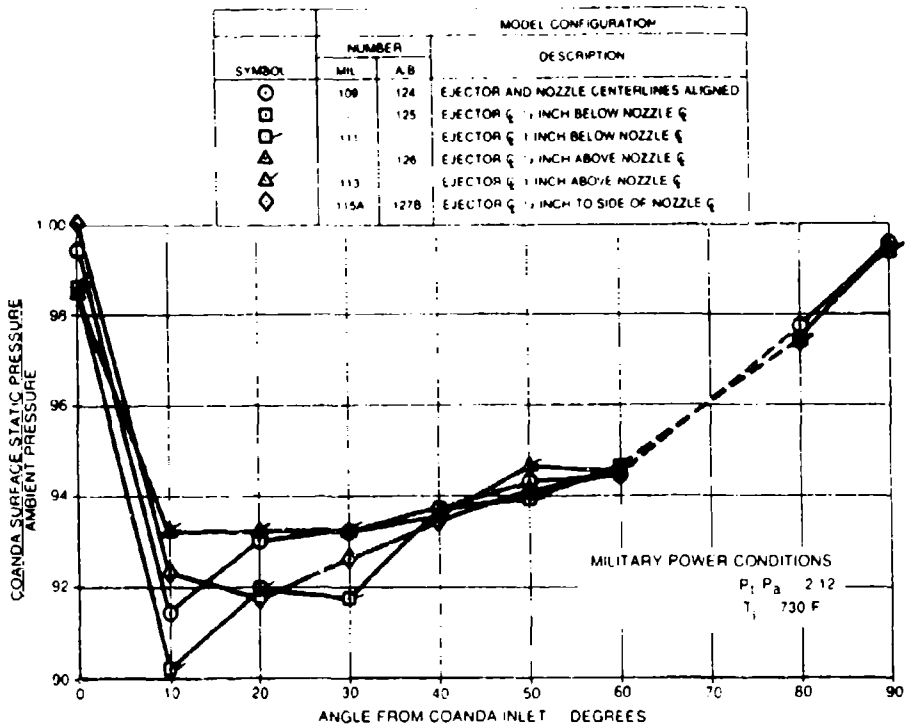

Figure 104. Coanda surface static pressures – three ejector transition with offset misalignments (one engine at military and one engine at idle).

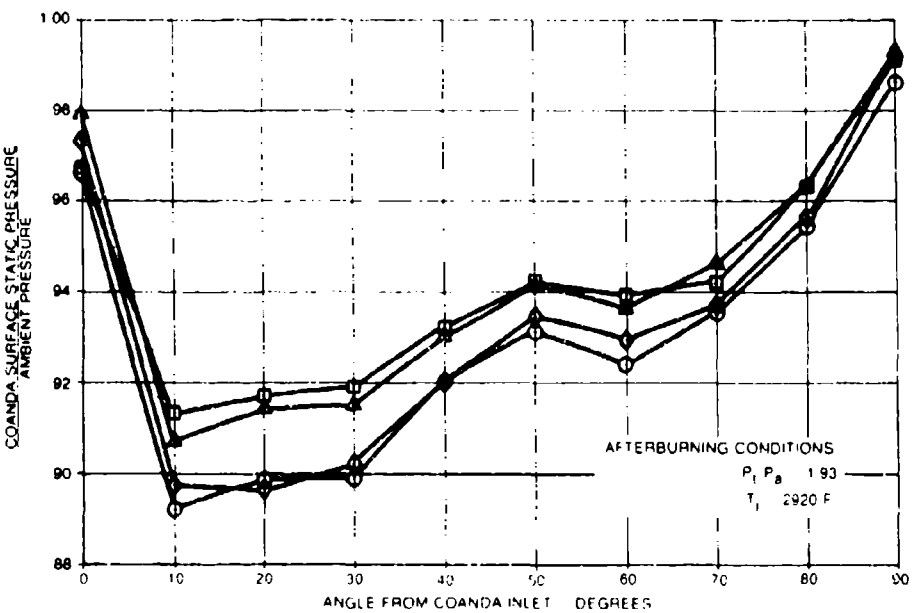

Figure 105. Coanda surface static pressures – three ejector transition with offset misalignments (one engine at A/B and one engine at idle).

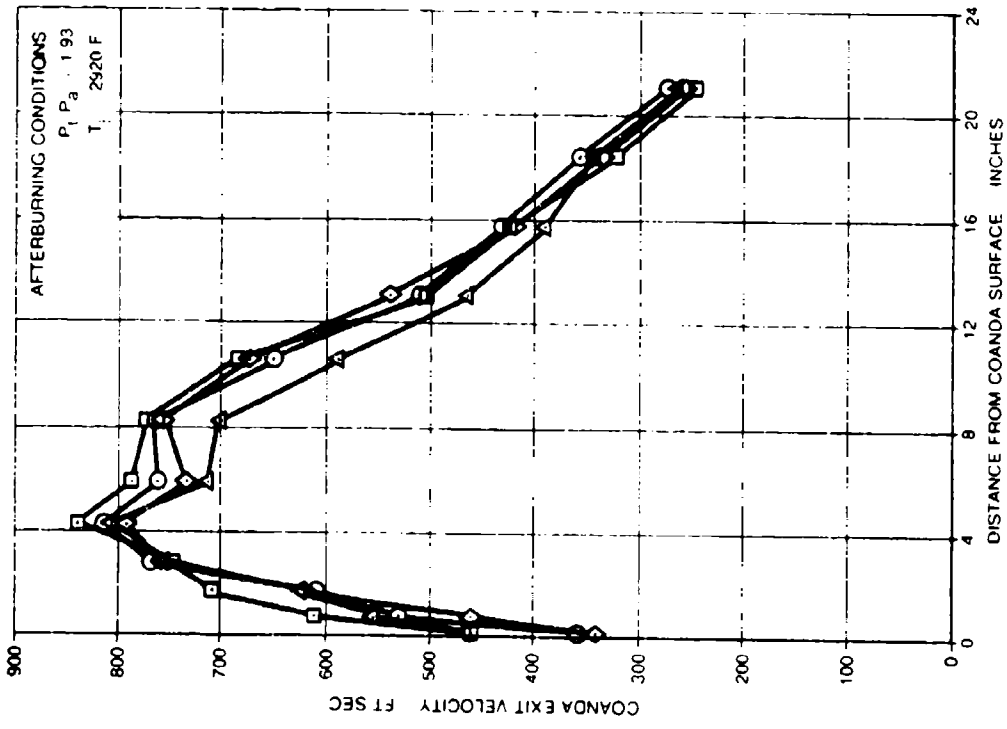

Figure 107. Coanda exit velocity profiles – three ejector transition with offset and angular misalignments (one engine at A/B and one engine at idle).

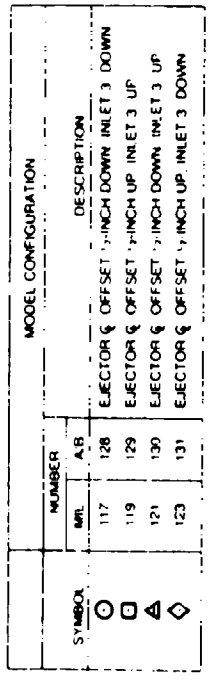

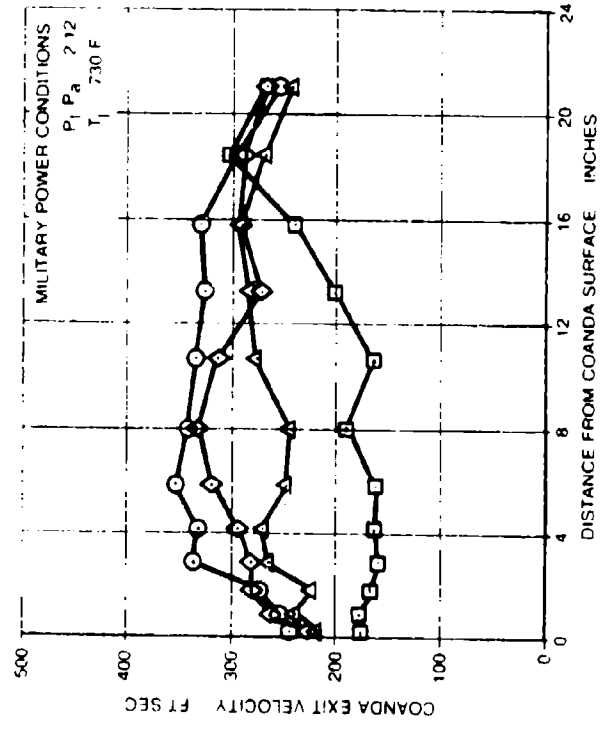

Figure 106. Coanda exit velocity profiles – three ejector transition with offset and angular misalignments (one engine at military and one engine at idle).

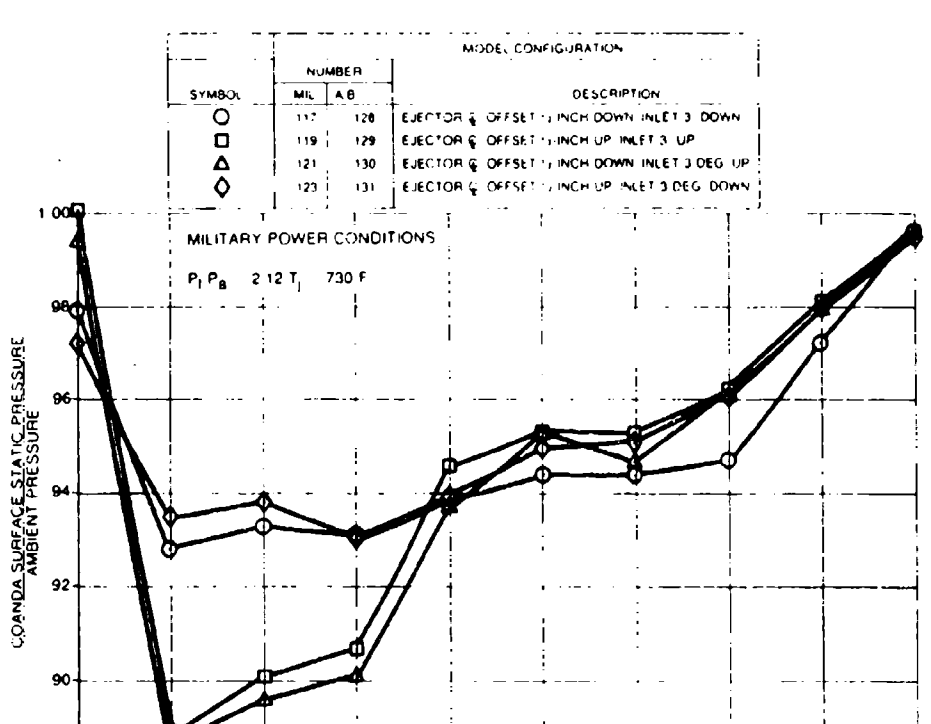

Figure 108. Coanda surface static pressures – three ejector transition with offset and angular misalignments (one engine at military and one engine at idle).

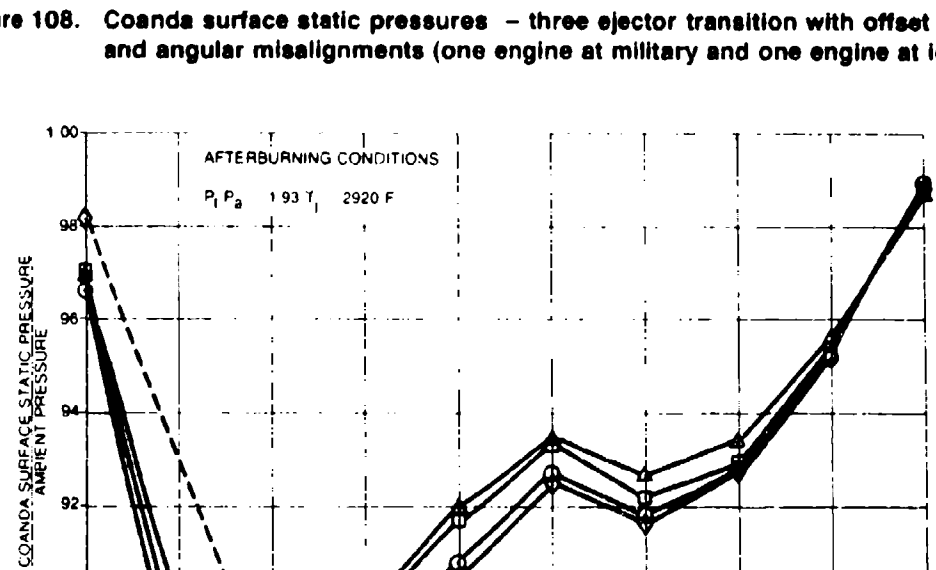

Figure 109. Coanda surface static pressures – three ejector transition with offset and angular misalignments (one engine at A/B and one engine at idle).

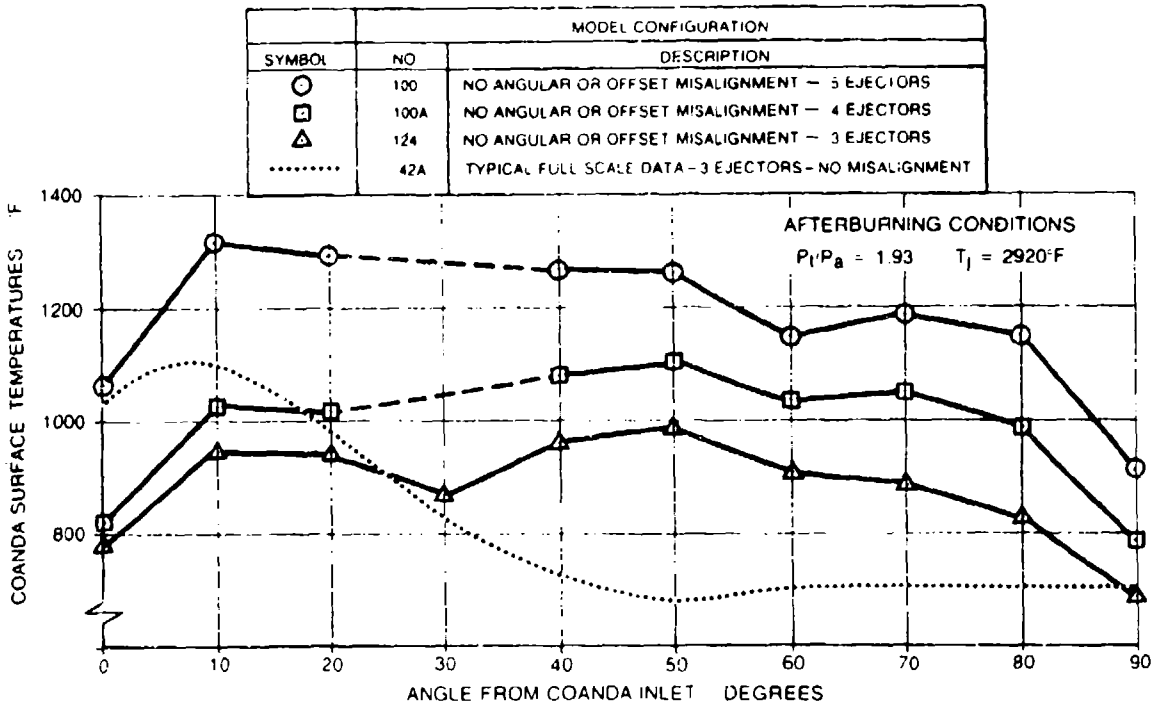

Figure 110. Coanda surface temperatures – three, four and five ejector transitions – no misalignment (one engine at A/B and one engine at idle).

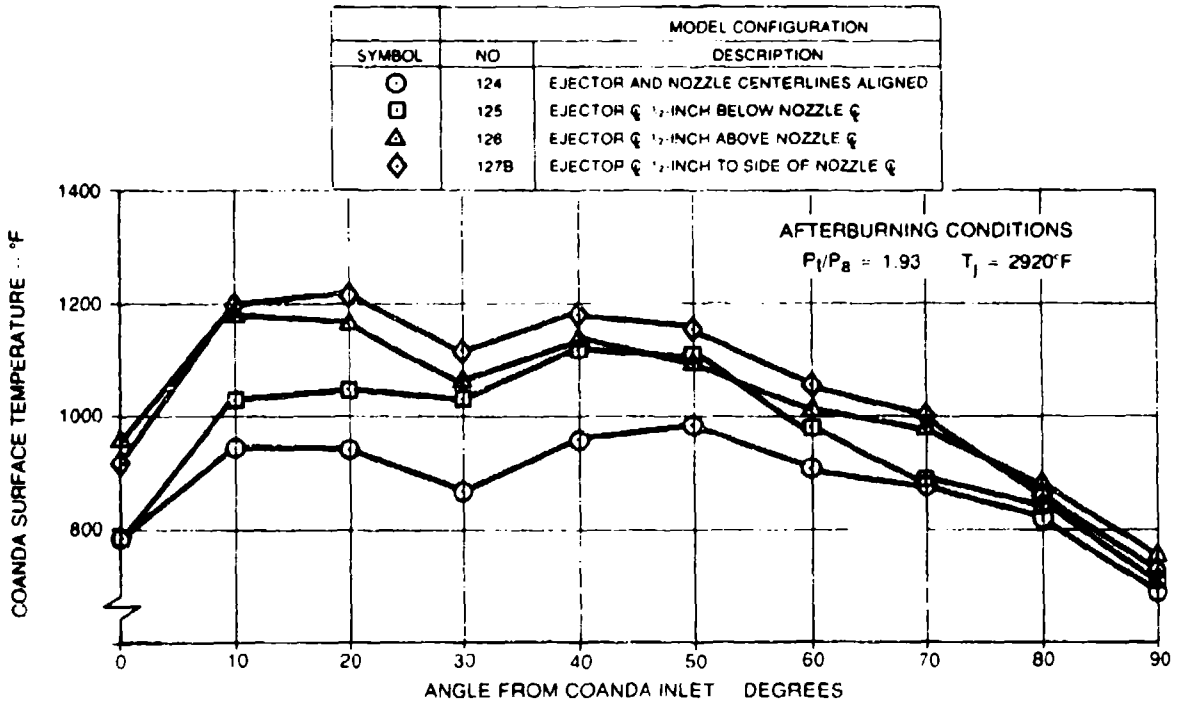

Figure 111. Coanda surface temperatures – three ejectors with offset misalignment (one engine at A/B and one engine at idle)

SYMBOL	MODEL CONFIGURATION NO	DESCRIPTION
⊙	128	EJECTOR ℄ OFFSET ½-INCH DOWN, INLET 3° DOWN
⊡	129	EJECTOR ℄ OFFSET ½-INCH UP, INLET 3° UP
△	130	EJECTOR ℄ OFFSET ½-INCH DOWN, INLET 3° UP
◇	131	EJECTOR ℄ OFFSET ½-INCH UP, INLET 3° DOWN

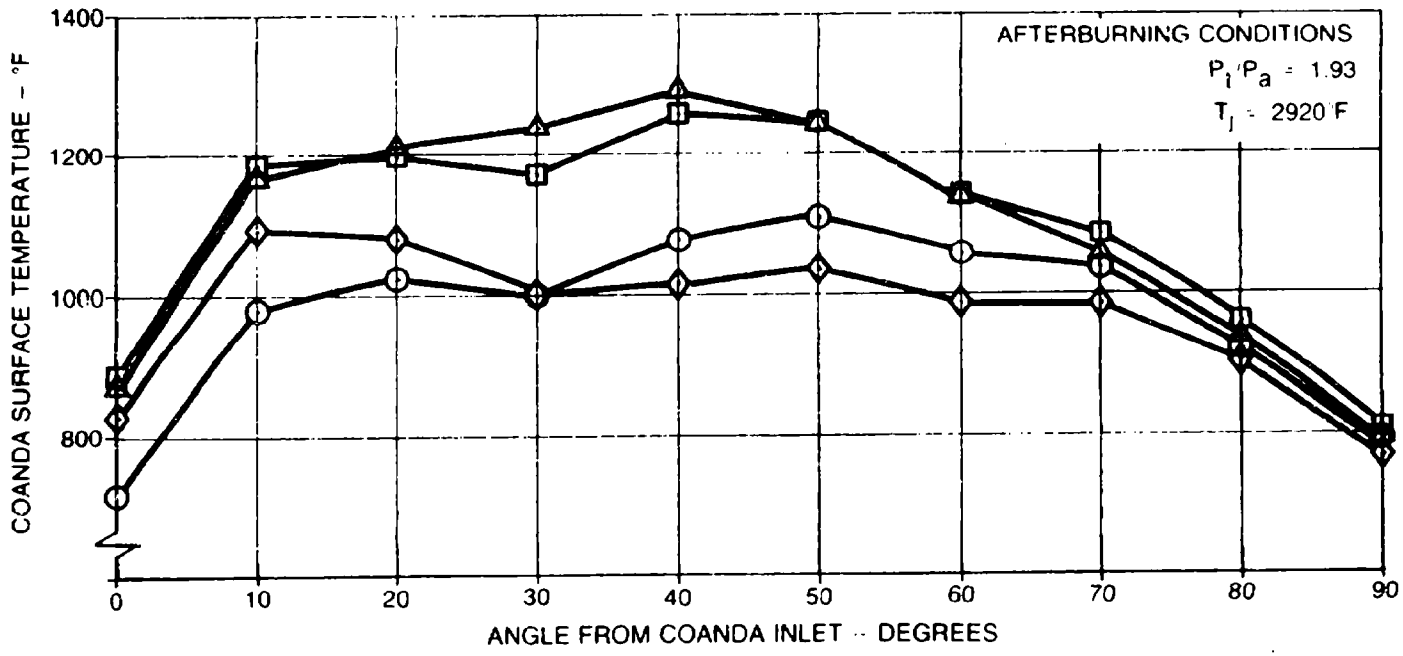

Figure 112. Coanda surface temperatures – three ejector transition with offset and angular misalignments (one engine at A/B and one engine at idle)

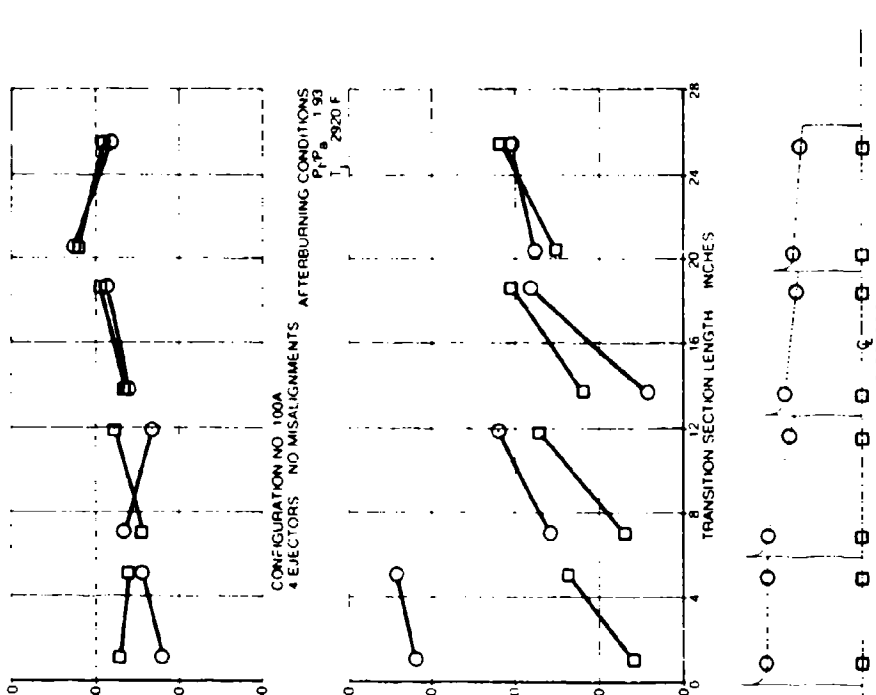

Figure 114. Ejector surface temperature and internal static pressure data – four ejector transition without misalignments (one engine at A/B and one engine at idle).

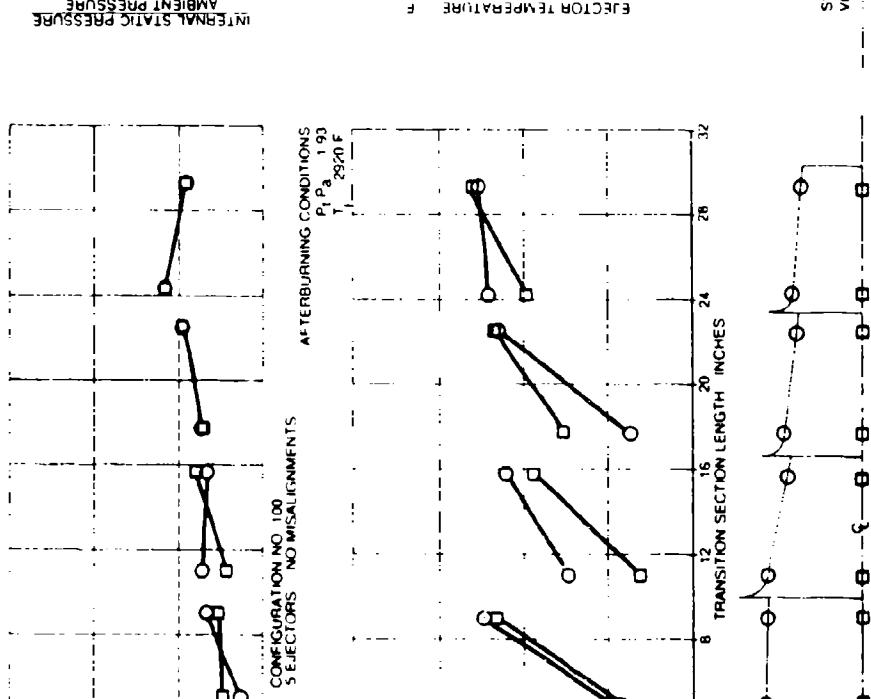

Figure 113. Ejector surface temperature and internal static pressure data – five ejector transition without misalignments (one engine at A/B and one engine at idle).

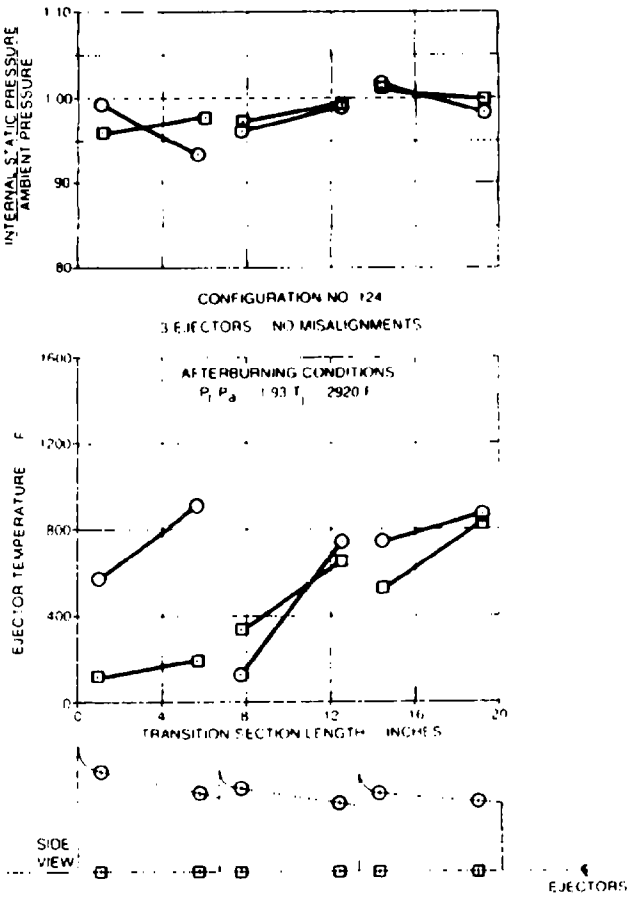

Figure 115. Ejector surface temperature and internal static pressure data – three ejector transition without misalignments (one engine at A/B and one engine at idle).

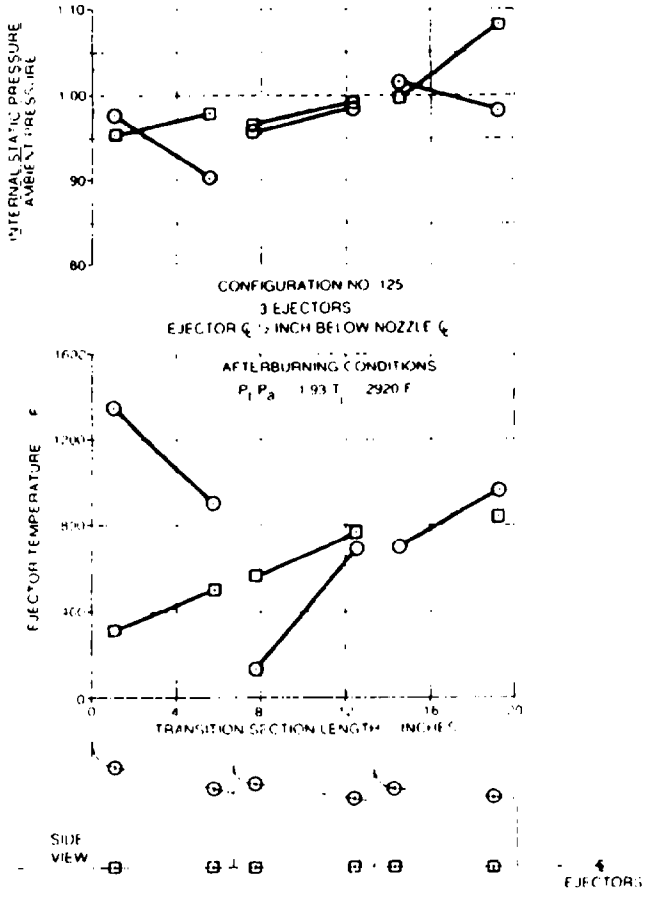

Figure 116. Ejector surface temperature and internal static pressure data – three ejector transition with nozzle offset upward (one engine at A/B and one engine at idle).

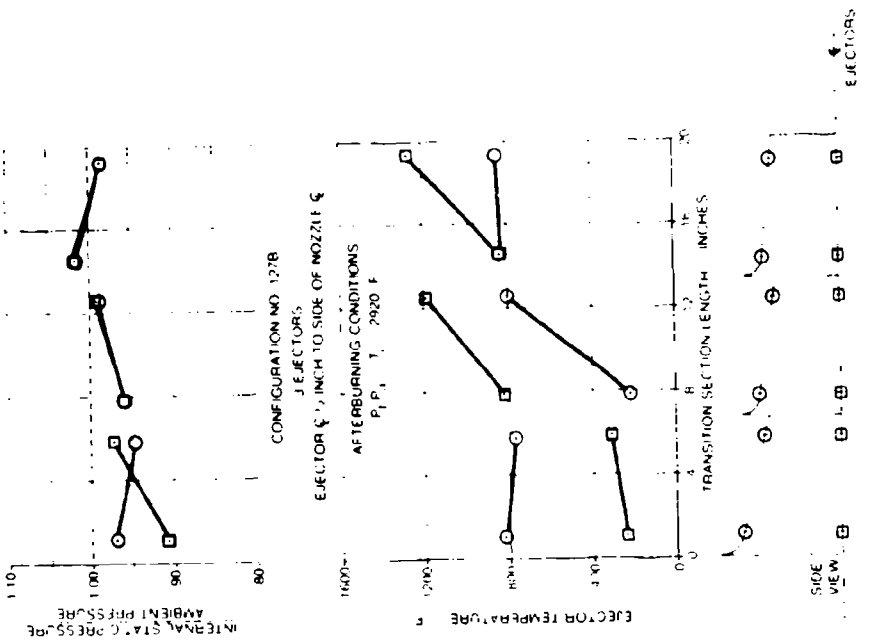

Figure 118. Ejector surface temperature and internal static pressure data – three ejector transition with nozzle offset to side (one engine at A/B and one engine at idle).

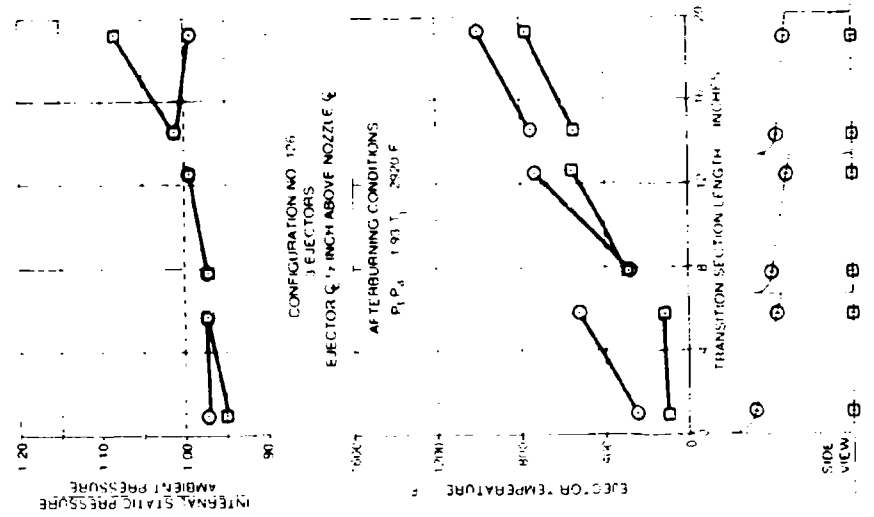

Figure 117. Ejector surface temperature and internal static pressure data – three ejector transition with nozzle offset downward (one engine at A/B and one engine at idle).

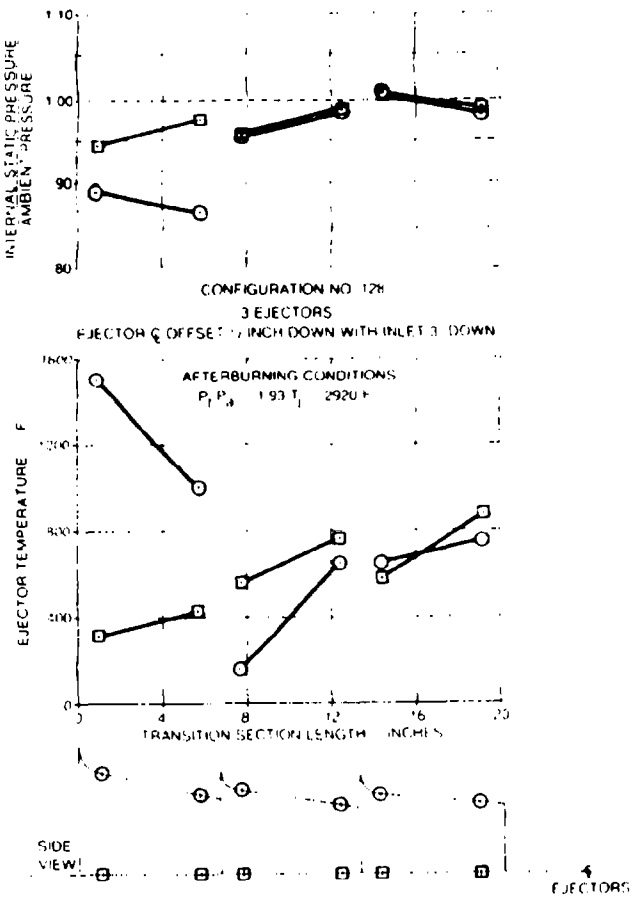

Figure 119. Ejector surface temperature and internal static pressure data – three ejector transition with nozzle offset upward and ejector inlet angled downward (one engine at A/B and one engine at idle).

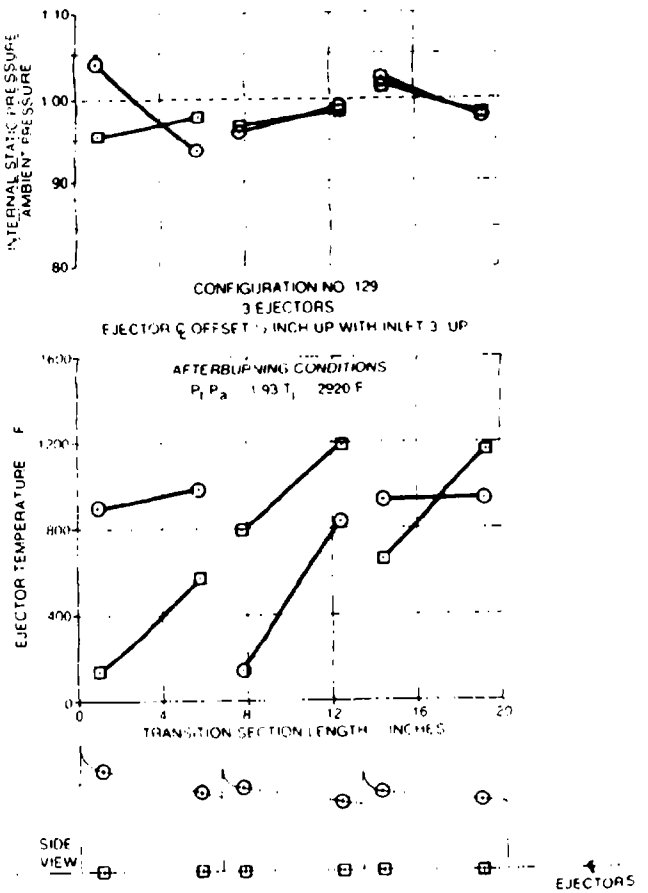

Figure 120. Ejector surface temperature and internal static pressure data – three ejector transition with nozzle offset downward and ejector inlet angled upward (one engine at A/B and one engine at idle)

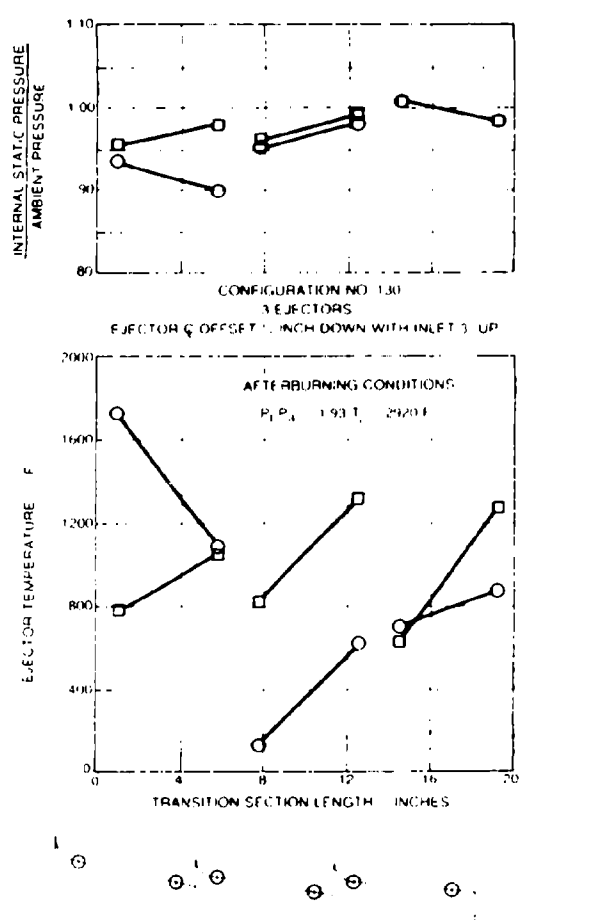

Figure 121. Ejector surface temperature and internal static pressure data – three ejector transition with nozzle offset upward and ejector inlet angled upward (one engine at A/B and one engine at idle).

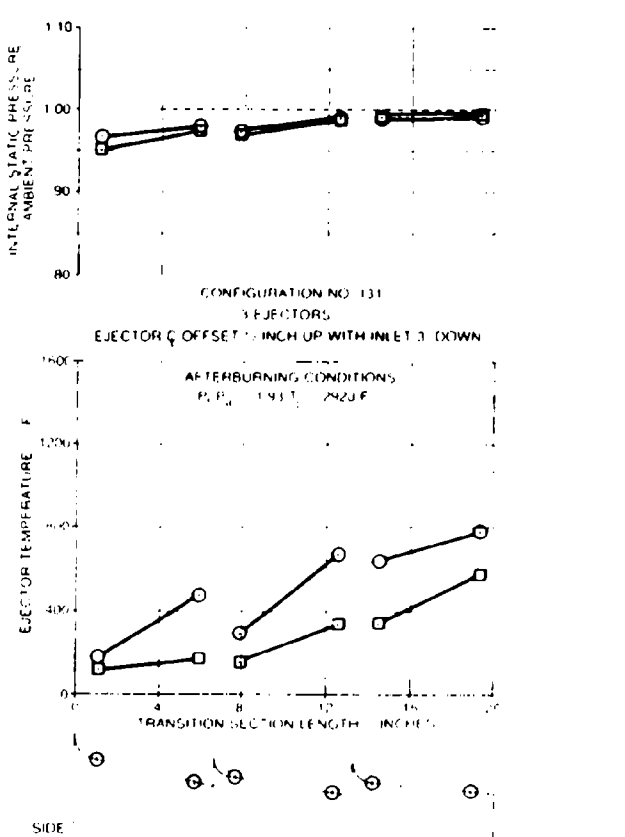

Figure 122. Ejector surface temperature and internal static pressure data – three ejector transition with nozzle offset downward and ejector inlet angled downward (one engine at A/B and one engine at idle).

REFERENCES

1. "Test Cell Experimental Program Coanda/Refraction Noise Suppression Concept - Advanced Development," Final Technical Report for Navy Contract N00156-74-C-1710, Navy Document Number NAEC-GSED-97, The Boeing Company, Wichita, Kansas, March 1976.

2. Ballard, R. E., Brees, D. W., and Sawdy, D. T., "Feasibility and Initial Model Studies of a Coanda/Refraction Type Noise Suppressor System," The Boeing Company, Wichita, Kansas, D3-9068, January 1973

3. Ballard, R. E., and Armstrong, D. L., "Configuration Scale Model Studies of a Coanda/Refraction Type Noise Suppressor System," The Boeing Company, Wichita, Kansas, D3-9258, October 1973.

4. Contract N00156-74-C-1710, "Coanda/Refraction Noise Suppressor System," Naval Air Engineering Center and The Boeing Company, July 1974.

5. Ballard, R. E. and Burton, L. L., "Navy Coanda-Refraction Ground Noise Suppressor Program Plan," The Boeing Company, Wichita, Kansas, D3-9574-1, August 1975.

LIST OF ABBREVIATIONS, ACRONYMS AND SYMBOLS

A	Area
A/B	Afterburner, afterburning
A/D	Analog to digital
Amb.	Ambient
A.R.	Area ratio
Conf.	Configuration
CPU	Central processing unit
CRES	Corrosion reresistant steel
CRT	Cathode ray tube
℄	Centerline
DIA., dia	Diameter
EGT	Engine exhaust gas total temperature
EPR	Engine pressure ratio; i.e., P_{t7}/P_{t2} for nonafterburning and P_{t10}/P_{t2} for afterburning engines
°F	Degrees Fahrenheit
FGT	Fan exhaust gas total temperature
FPR	Fan pressure ratio; i.e., $P_{t2.5}/P_{t2}$
FT., ft.	Feet
$FT.^2$, $ft.^2$	Square feet
$FT.^3$, $ft.^3$	Cubic feet
GPM, gpm	Gallons per minute
GSED	Ground Support Equipment Department
IN., in.	Inch
$IN.^2$, $in.^2$	Square inches
K	Kilo (thousand)
lbs.	Pounds

LIST OF ABBREVIATIONS, ACRONYMS AND SYMBOLS (CONT'D)

M	Mach number
MAT'L	Material
MAX.	Maximum
MIN.	Minimum
MRT	Military rated thrust
NAEC	Naval Air Engineering Center
OASPL	Overall sound pressure level
PNL	Perceived noise level
PSI, psi	Pounds per square inch
PSIA, psia	Pounds per square inch, absolute
PSID, psid	Pounds per square inch, differential
P_a, P_{amb}	Ambient pressure
P_s	Internal static pressure
P_t	Total pressure
P_{tp}	Primary total pressure
P_{t1}	Free stream total pressure
P_{t2}	Low pressure compressor inlet total pressure
$P_{t2.5}$	Fan exhaust total pressure
P_{t7}	Primary nozzle total pressure
P_{t10}	Afterburning nozzle total pressure
R	Radius
°R	Degrees Rankine
SEC., sec.	Second
S.F.	Scale Factor
SPL	Sound pressure level
SQ., sq.	Square
STL	Steel

LIST OF ABBREVIATIONS, ACRONYMS AND SYMBOLS (CONT'D)

T_a, T_{amb}	Ambient temperature
T_j	Jet temperature
T_m	Metal surface temperature
T_t	Total temperature
T_{tp}	Primary total temperature
$T_{t2.5}$	Fan exhaust gas total temperature
T_{t7}	Primary exhaust gas total temperature
T_{t10}	Afterburner exhaust gas total temperature
TYP	Typical
$\dot{W}_a$	Airflow rate
$\dot{W}_p$	Primary airflow rate
$\dot{W}_s$	Secondary airflow rate
W/O	Without
Δ	Differential

AIRCRAFT SYSTEM ONE-SIXTH SCALE MODEL STUDIES
Coanda/Refraction Noise Suppression Concept – Advanced Development

NAEC-GSED-98
Contract N00156-74-C-1710

The proven Coanda/refraction concept is applied to the Navy requirement for effective exhaust noise suppression of aircraft (installed engines) ground run up tests. The technical approach is comprised of analytic studies and one-sixth scale model tests using simulated sources for single and twin-engine aircraft. The results of previous exploratory studies, using simulated static sources, are applied to the more complex situation with the engine tailpipe centerline displaced horizontally, vertically, longitudinally and angularly from the model suppressor inlet. Test runs at varied simulated engine power settings and varied model geometric orientations were conducted to determine the effects on jet attachment to the Coanda surface and on cooling air eduction. The extensive recorded test data were analyzed to identify aero/thermodynamic trends related to suppressor internal components, ejector geometry and material cooling properties. Results present operational limits and configurations for further development as exhaust systems for aircraft test enclosures and aircraft run up suppressors.

AIRCRAFT SYSTEM ONE-SIXTH SCALE MODEL STUDIES
Coanda/Refraction Noise Suppression Concept – Advanced Development

NAEC-GSED-98
Contract N00156-74-C-1710

The proven Coanda/refraction concept is applied to the Navy requirement for effective exhaust noise suppression of aircraft (installed engines) ground run up tests. The technical approach is comprised of analytic studies and one-sixth scale model tests using simulated sources for single and twin-engine aircraft. The results of previous exploratory studies, using simulated static sources, are applied to the more complex situation with the engine tailpipe centerline displaced horizontally, vertically, longitudinally and angularly from the model suppressor inlet. Test runs at varied simulated engine power settings and varied model geometric orientations were conducted to determine the effects on jet attachment to the Coanda surface and on cooling air eduction. The extensive recorded test data were analyzed to identify aero/thermodynamic trends related to suppressor internal components, ejector geometry and material cooling properties. Results present operational limits and configurations for further development as exhaust systems for aircraft test enclosures and aircraft run up suppressors.

AIRCRAFT SYSTEM ONE-SIXTH SCALE MODEL STUDIES
Coanda/Refraction Noise Suppression Concept – Advanced Development

NAEC-GSED-98
Contract N00156-74-C-1710

The proven Coanda/refraction concept is applied to the Navy requirement for effective exhaust noise suppression of aircraft (installed engines) ground run up tests. The technical approach is comprised of analytic studies and one-sixth scale model tests using simulated sources for single and twin-engine aircraft. The results of previous exploratory studies, using simulated static sources, are applied to the more complex situation with the engine tailpipe centerline displaced horizontally, vertically, longitudinally and angularly from the model suppressor inlet. Test runs at varied simulated engine power settings and varied model geometric orientations were conducted to determine the effects on jet attachment to the Coanda surface and on cooling air eduction. The extensive recorded test data were analyzed to identify aero/thermodynamic trends related to suppressor internal components, ejector geometry and material cooling properties. Results present operational limits and configurations for further development as exhaust systems for aircraft test enclosures and aircraft run up suppressors.

AIRCRAFT SYSTEM ONE-SIXTH SCALE MODEL STUDIES
Coanda/Refraction Noise Suppression Concept – Advanced Development

NAEC-GSED-98
Contract N00156-74-C-1710

The proven Coanda/refraction concept is applied to the Navy requirement for effective exhaust noise suppression of aircraft (installed engines) ground run up tests. The technical approach is comprised of analytic studies and one-sixth scale model tests using simulated sources for single and twin-engine aircraft. The results of previous exploratory studies, using simulated static sources, are applied to the more complex situation with the engine tailpipe centerline displaced horizontally, vertically, longitudinally and angularly from the model suppressor inlet. Test runs at varied simulated engine power settings and varied model geometric orientations were conducted to determine the effects on jet attachment to the Coanda surface and on cooling air eduction. The extensive recorded test data were analyzed to identify aero/thermodynamic trends related to suppressor internal components, ejector geometry and material cooling properties. Results present operational limits and configurations for further development as exhaust systems for aircraft test enclosures and aircraft run up suppressors.